UNIVERSITY OF PUNE

A PROJECT REPORT

ON

AN INNOVATIVE MULTI-DOF ROBOTIC ARM ASSEMBLY FOR PRESS SHOPS

SUBMITTED BY

MANDAR HARSHE	B3320815
COLIN MENEZES	B3320828
BHUSHAN WALZADE	B3320850

UNDER GUIDANCE OF

PROF. L. G. NAVALE

DEPARTMENT OF MECHANICAL ENGINEERING

MODERN EDUCATION SOCIETY'S

COLLEGE OF ENGINEERING

PUNE- 411001

YEAR 2006-2007

Modern Education Society's College Of Engineering
Pune – 411001

CERTIFICATE

THIS IS TO CERTIFY THAT THE PROJECT REPORT

ENTITLED

AN INNOVATIVE MULTI-DOF ROBOTIC ARM ASSEMBLY FOR PRESS SHOPS

SUBMITTED BY

MANDAR HARSHE	B3320815
COLIN MENEZES	B3320828
BHUSHAN WALZADE	B3320850

IN PARTIAL FULFILLMENT FOR THE AWARD OF DEGREE OF B.E. (MECHANICAL ENGINEERING) OF THE UNIVERSITY OF PUNE, PUNE IS APPROVED.

PROF. L. G. NAVALE	PROF. V. N. CHOUGULE	DR. L. G. NAVALE
Project Guide	H.O.D.	Principal
Mech. Engg. Dept.	Mech.Engg. Dept	MESCOE, Pune.

EXAMINER

Acknowledgements

We would like to express our sincere thanks to Mr. Hemachandra Shrotri, M.D. of Nirmiti Stampings Pvt Ltd, for giving us an opportunity to work on this project. His vast experience and guidance have been especially valuable to us. We are also grateful to Prof. L. G. Navale for his inspiration and guidance. Prof. K. H. Munde helped us in the initial stages of the work, and his inputs resulted in the publication of a paper in the International Conference on Advances in Machine Design and Industry Automation 2007. We are extremely grateful for his help.

We would like to thank Prof. V. N Chougule, the head of the Mechanical Department, for allowing us to undertake this project and provide us the necessary help. We received valuable help on the electrical and electronics aspects of the project from Prof. Aasma Shaikh of the Electronics & Telecommunication Department, Prof. Mrs. Dharmadhikari and Prof. B. H. Deshmukh of the Electrical Department. Prof. V. Sugur and Prof A. Mitra of the Mechanical Department helped us in matters concerning their specializations.

Details and technical support on the various products available in the market are especially hard to come by. In this regard, we thank the technical staff of Srijan Control Drives Ltd, Festo Controls Pvt. Ltd, Albro

Engineers and Armatech Pvt. Ltd for their help and patience in explaining the various products available and helping us select those suitable for our application requirements. We would like to thank Mr. Satish Nikam of Nirmiti Stampings Pvt. Ltd, who was in charge of the manufacturing works of the project.

A project of such a wide spectrum requires inputs from numerous fields. We are thankful to the faculty of our department and also to all our colleagues who helped us with their inputs at various stages of the project. Finally, we would like to thank our colleagues Mr. Parikshit Dhodapkar, Mr. Gaurav Kakati and Mr. Paresh Panditrao,of the E&TC Department, who worked on the electronic controls of the robot and Mr. Nitant Harani of the Mechanical Department for helping us in Finite Element Analysis of the manipulator.

Mandar Harshe Colin Menezes Bhushan Walzade

Contents

List of Figures

List of Tables

Abstract

Repetitive tasks and high accuracy have become the two contradictory needs of any industrial process. By introducing autonomous robotic applications, simple repetitive tasks can be accomplished keeping the demands of the accuracy and speed in mind. However, developing these applications for industries specific to countries like India, where cheap labour is available, becomes a major problem to be tackled in terms of cost.

This project deals with the design, fabrication and control of a robotic arm used to load metal sheets into a press. Two stepper motors control the motion of the arm while one controls the orientation of the wrist. The arm works in tandem with other arms, to be used to lift the sheets and finally unload them. The sheet size is expected to vary and the arm must cope up to these differing sizes. The original position of sheet will vary as per the sheet size while the arm will be programmed to place it at the die center. Robot motion is controlled using proximity sensors placed at suitable locations on the machine press itself. The motor control is achieved using a microcontroller. The end effector of the transferring and unloading arm will be magnetic, while that of the lifting arm will use vacuum cups.

Thus we have designed an assembly of three arms – 1 DOF Lifting Arm; 3 DOF Transfering Arm; 2 DOF Unloading Arm.

Part I

Company Profile

Nirmiti Stampings Pvt. Ltd

Nitmiti Stamplings Pvt. Ltd is an ISO/TS 16949 Certified company which is a manufacturer of Sheet Metal Components, Assemblies and Press Tools. It is located in a prime industrial area of Pune, which is the automotive hub of India. The company was incorporated in the year 1995. What started as a small enterprise with only one staff member, 6 workers and with a turnover of Rs 3.3 million (US $ 0.07 million) has today grown into an organization with a total strength of 70 members and a turnover of Rs 80 million (US $1.77 Million) servicing both national and international clients. The company is certified for TS 16949 by BVQI.

Company Statement

- Vision
  - Leadership in our respective product range
  - Move up the value chain and provide our customers ready to use products
  - Be the preferred supplier in our product range
  - Be a global player in our product range
  - Maintain a growth rate of atleast 30%
- Mission

- To supply our products at the
  - right time
  - right price
  - right quality
- Train and motivate our employees to achieve our vision
- Delight the customer-internal and external always

- Values
  - Respect your customers, associates and employees
  - Promote the highest ethical standards
  - Promote teamwork and increase participation of all employees
  - Be accountable
  - Create an excitement and satisfaction for all
    Customers, Suppliers & Employees
  - Honour our commitments to the society

Product Range

- *Press Tools*
  - Compound, Progressive
  - Upto 1000 x 1200 mm
  - For all metals, hylam, plastics, gaskets
- *Sheet Metal Components*
  - Automotive

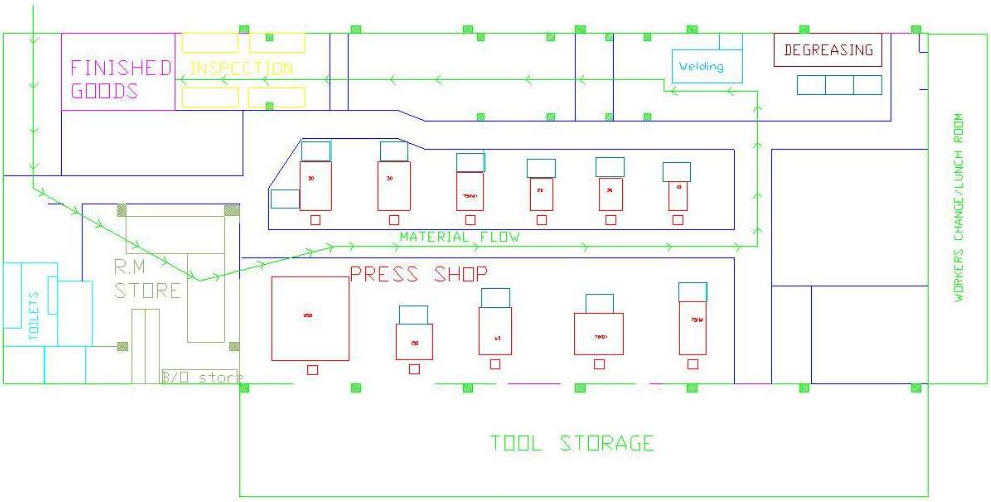

Figure 1: Shop Floor Layout

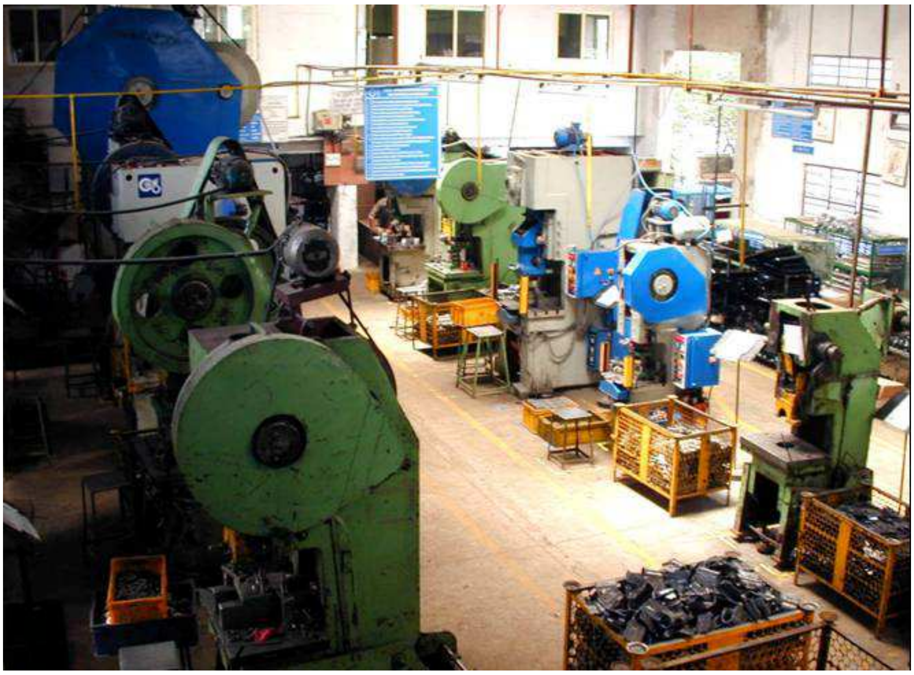

Figure 2: Shop Floor

        * Ride control
        * Parking brake system
        * Gear shifters
        * Cable clamps
        * Radiator Supports
    - Electronic/White Goods
        * Speaker Baskets, Bottom & Top Plates, Hylam Parts, Audio Panels/Refrigerator parts
    - Others
        * Meters, Padlocks, Night latches,
        * Petrochemical components
- *Assemblies*
    - Gear shift lever
    - Ride control
    - Gas Lamps

Machinery

- Presses
    - 250 Ton Pneumatic with die cushion (Bed Size 1500 x 1200)
    - 150 Ton Mechanical
    - 75 Ton Mechanical (3 Nos)
    - 63 Ton Pneumatic with die cushion
    - 50 Ton Pneumatic with die cushion

Figure 3: Company Products

Figure 4: 250 Ton Pneumatic Press

Figure 5: Tooling used for the Pneumatic Press

  - 50 Ton Mechanical
  - 35 Ton Mechanical
  - 20 Ton Pneumatic
  - 20 Ton Mechanical
- Welding
  - Mig Welding 1 No
  - Capacitance Discharge Welding 25 KVA 1 No

Major Customers

- Gabriel India Ltd.
- LG Electronics Ltd.
- Tata Ficosa Automotive Systems Ltd.
- Tata Toyo Radiators Ltd.
- Fleetguard Filters Pvt.Ltd.
- Renowned Auto Mfgrs Ltd.
- Spicer India Ltd.
- Behr India Ltd (E O U).
- Piaggio Vehicles Pvt. Ltd.

Part II

Problem Analysis

Problem Description

A press shop which manufactures components for automobiles is expected to deal in large volumes. Most components are small in size and are precision jobs. Hence, loading the raw material into the press becomes critical, and the rate of production depends entirely on the loading and unloading speed. An operator designated for this job will frequently experience boredom and exhaustion, each of which affects the productivity of the plant. This menial job is best left to an automated process and the operator can be assigned to more fitful jobs where his skills are best utilized.

Thus, the task at hand was to design a robotic arm to perform the necessary pick and place actions for loading the raw material (metal sheets) and unloading the finished components. The task entails analysis, design and fabrication of the robot. We will install the robot at Nirmiti Stampings Pvt. Ltd, Bhosari.

Robot Features

For the purposes listed previously, integrating a standard manipulator for pick-and-place tasks is quite impractical. This is essentially due to the constraints imposed by the press and die on which the job is to be placed. In most cases, the vertical space (i.e. the distance between punch and die mounted in the press) available is limited (to the order of about 150 mm), and this puts a constraint on the end-effector to be compact. This prevents the final joints from being prismatic. The mechanism to be used must be such that it does not take up additional space or cause any hinderance to already installed machines. The metal sheets (used as raw material) are generally stacked vertically and hence, a pick-and-place mechanism cannot be just a planar mechanism. The guideposts on the die and features on the press also put in constraints on the path that can be traced while loading and unloading of sheets.

The robot arm assembly that has to be developed must be designed as a stand-alone machine and must be integrated into an existing press. Since sheet size and the component manufactured on the press change, the robot must be programmable. This is mainly to accommodate for the changes in absolute locations where the sheets or components may be held. The machine has to be developed to be extremely simple to control and program as the robot will not be operated by skilled technicians.

Thus, the robot must take in a minimum number of inputs from the operator, plan a path based on this data and perform the loading and unloading operations. This control and path planning has to be done by the robot itself, in the sense that no external interfacing to computers is possible. This need arises from the fact that it would be extremely impractical in terms of cost to equip a shop floor with a computer dedicated to controlling a single robot. The robot thus needs to perform simple motions in order to allow easy control by a simple micro-controller based system.

Chapter 1

Literature Survey

1.1 Robotics [5]

Automation is defined as a technology that is concerned with the use of mechanical, electronic, and computer-based systems in the operation and control of production. This technology includes transfer lines, mechanized assembly machines, feedback control systems, and robots. There are three broad classes of industrial automation: fixed automation, programmable automation, and flexible automation.

Of these three types, robotics coincides most closely with programmable automation. The robot can be programmed to move its arm through a sequence of motions in order to perform some useful task. It will repeat that motion pattern over and over again until reprogrammed to perform some other task. Hence the programming feature allows robots to be used for a variety of different industrial operations, many of which involve the robot working together with other pieces of automated or semiautomated equipment. These operations include machine loading and unloading, spot welding, and spray painting.

The official definition of an industrial robot as provided by the Robotics Industries Association (RIA) is :

> An industrial robot is a reprogrammable, multifunctional manipulator designed to move materials, parts, tools, or special devices through variable programmed motions for performance of a variety of tasks.

1.1.1 Robot Anatomy

Common Robot Configurations

The vast majority of today's commercially available robots possess one of the four basic configurations:

- Polar configuration
- Cylindrical configuration
- Cartesian coordinate configuration
- Jointed-arm configuration

These basic configurations are illustrated in Fig. 1.1

1.1.2 Robot Motions

The robots movement can be divided into two general categories: arm and body motions, and wrist motions. The individual joint motions associated with these two categories are sometimes referred to by the term "degrees of freedom", and a typical industrial robot is equipped with 4 to 6 degrees of freedom.

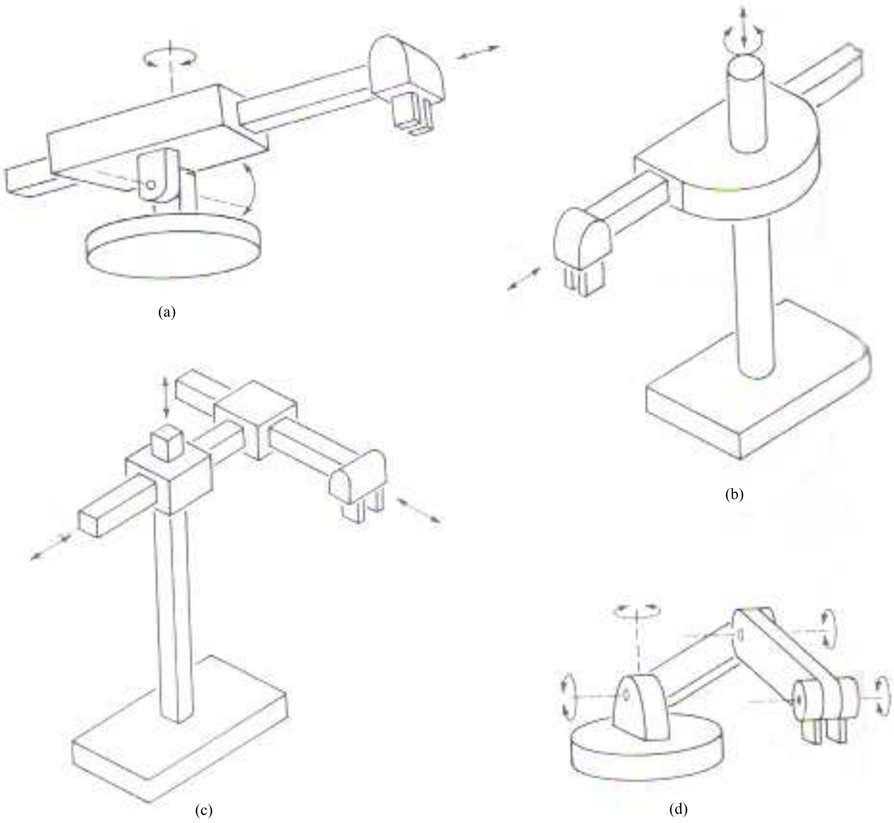

Figure 1.1: The four basic robot anatomies: (a) polar, (b) cylindrical, (c) cartesian, (d) jointed arm

The robot motions are accomplished by means of powered joints. Connecting the various manipulator joints together are rigid members that are called links. The joints used in the design of industrial robots typically involve a relative motion of the adjoining links that is either linear or rotational. Linear joints involve a sliding or translational motion of the connecting links. This motion can be achieved in a number of ways (e.g., by a piston, a telescoping mechanism, and relative motion along a linear track or rail).

There are at least three types of rotating joint that can be distinguished in robot manipulators. The three types are shown in Fig. 1.2.
The arm and body joints are designed to enable the robot to move its end effector to a desired position within the limits of the robots size and joint movements. For robots of polar, cylindrical, or jointed-arm configuration, the 3 degrees of freedom associated with the arm and body motions are (Fig. 1.3):

1. Vertical traverse : This is the capability to move the wrist up or down to provide the desired vertical attitude.
2. Radial traverse : This involves the extension or retraction (in or out movement) of the arm from the vertical center of the robot.
3. Rotational traverse : This is the rotation of the arm about the vertical axis.

The wrist movement is designed to enable the robot to orient the end effector properly with respect to the task to be performed. To solve the orientation problem, the wrist is normally provided with up to 3 degrees of freedom. (Fig. 1.4)

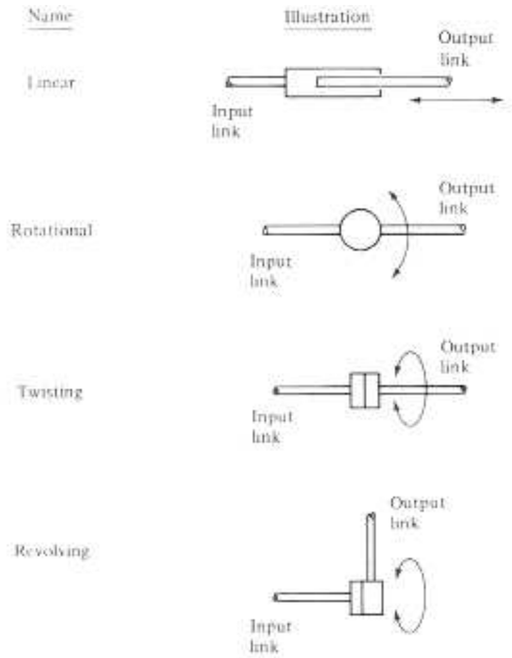

Figure 1.2: Several types of joints used in robots: (a) rotational joint with rotation along an axis perpendicular to arm member axis, (b) rotational joint with twisting action, (c) linear motion joint, usually achieved by a sliding action

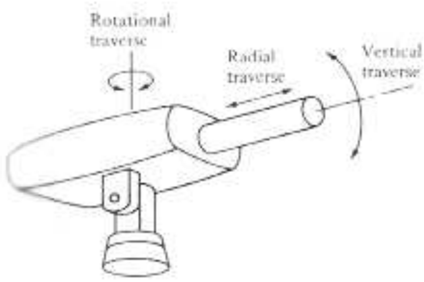

Figure 1.3: Three degree of freedoms associated with arm and body of a polar coordinate robot.

1. Wrist roll : Also called wrist swivel, this involves rotation of the wrist mechanism about the arm axis.
2. Wrist pitch : Given that the wrist roll is in its center position, the pitch would involve the up or down rotation of the wrist.
3. Wrist yaw : Again, given that the swivel is in the center position of its range, wrist yaw would involve the right or left rotation of the wrist.

1.1.3 Work Volume

Work volume is the term that refers to the space within which the robot can manipulate its wrist end. The work volume is determined by the following physical characteristics of the robot:

1. The robots physical configuration
2. The sizes of the body, arm, and wrist components
3. The limits of the robots joint movements.

The influence of the physical configuration on the shape of the work volume is shown in Fig 1.5. The size of each work volume shape is influenced by the dimensions of the arm components and by the limits of its joint movements.

1.1.4 Robot Drive System

The drive system determines the speed of the arm movements, the strength of the robot, and its dynamic performance. To some extent, the drive system determines the kinds of applications that the robot can accomplish. Commercially available industrial robots are powered by one of three types of drive systems. These three systems are :

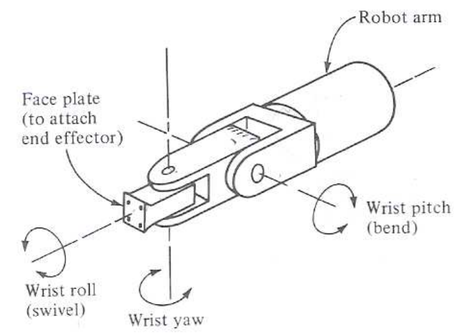

Figure 1.4: Three degree of freedoms associated with the robot wrist.

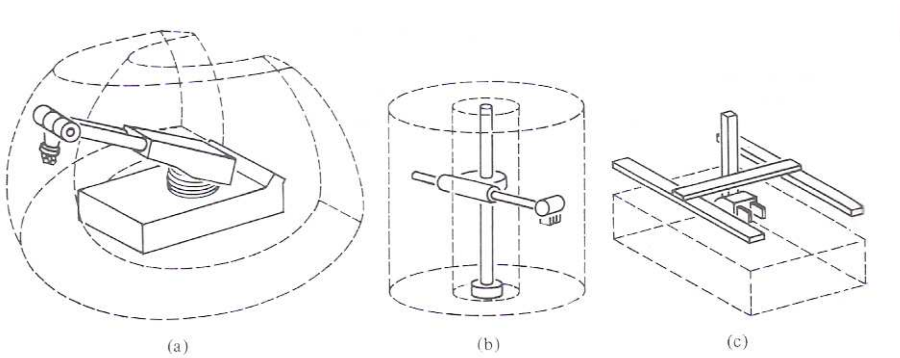

Figure 1.5: Work volumes for various robot anatomies: (a) polar, (b) cylindrical; and (c) cartesian

1. Hydraulic drive
2. Electric drive
3. Pneumatic drive

The three systems are compared in Table 1.1

1.1.5 Control Systems

In order to operate, a robot must have a means of controlling its drive system to properly regulate its motion. Commercially available industrial robots can be classified into four categories according to their control systems. The four categories are:

1. Limited-sequence robots
2. Playback robots with point-to-point control
3. Playback robots with continuous path control
4. Intelligent robots

1.1.6 End Effectors

In robotics, the term end effectors is used to describe the hand or tool that is attached to the wrist. The end effector represents the special tooling that permits the general-purpose robot to perform a particular application. This special tooling must be designed specifically for the application.

End effectors can be divided into two categories: grippers and tools. Grippers could be utilized to grasp an object, usually a workpart, and hold it during the robot work cycle. There are a variety of holding methods

Electrical Actuators	**Hydraulic Actuators**	**Pneumatic Actuators**
Moderate payload capacity	High Payload capacity	Low Payload capacity
High Power to weight ratio	Moderate Power to weight ratio	Low Power to weight ratio
Highly accurate and precise	Moderate accuracy and precision	Low accuracy and precision
Highly reliable and requires low maintenance	Low reliability and requires high maintenance	Moderate reliability and requires moderate maintenance
Low cost	High Cost	Moderate cost
Can work in narrow speed range	Moderate range of speed	Wide speed range

Table 1.1: Comparison of different drive systems

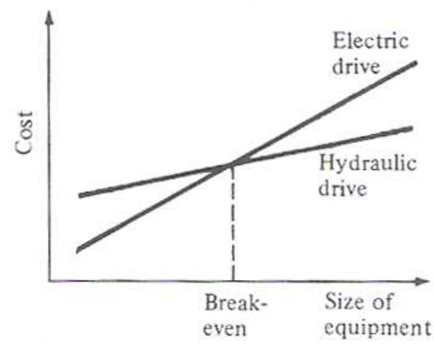

Figure 1.6: Cost vs. size for electric drive and hydraulic drive

that can be used in addition to the obvious mechanical means of grasping the part between two or more fingers. These additional methods include the use of suction cups, magnets, hooks, and scoops. A tool would be used as an end effector in applications where the robot is required to perform some operation on the workpart. These applications include spot welding, arc welding, spray welding, and drilling. In each case, the particular tool is attached to the robots wrist to accomplish the application.

1.1.7 Grippers

Grippers are end effectors used to grasp and hold objects. The objects are generally work parts that are to be moved by the robot. These part handling applications include machine loading and unloading, picking parts from a conveyor, and arranging parts into a pallet.

Depending on the mechanism used for the purpose of gripping they can be classified as:

1. Mechanical Grippers
2. Adhesive Grippers
3. Hooks, Scoops etc
4. Vacuum Cups
5. Magnetic Grippers

Magnetic Grippers

Electromagnetic grippers are easier to control, but require a source of dc power and an appropriate controller unit. As with any other robotic-gripping device, the part must be released at the end of the handling cycle.

This is easier to accomplish with an electromagnet than with a permanent magnet. When the part is to be released, the controller unit reverses the polarity at a reduced power leave before switching off the electromagnet. This procedure acts to cancel the residual magnetism in the work piece and ensure a positive release of the part.

The advantages of magnetic grippers in material handling applications are:

- Pickup times are faster
- Variations in part size can be tolerated. The gripper does not have to be designed for one particular work part.
- They have the ability to handle metal parts with holes (not possible with vacuum grippers.)
- They require only one surface for gripping.

A disadvantage of magnetic grippers is the problem of picking up only one sheet from a stack. The magnetic attraction tends to penetrate beyond the top sheet in the stack resulting in the possibility that more than a single sheet will be lifted by the magnet. This problem can be confronted in several ways:

- The magnetic grippers can be designed to limit the effective penetration to the desired depth, which would correspond to the thickness of the top sheet
- The stacking device used to hold the sheets can be designed to separate the sheets for pickup by the robot. One such type of stacking device is called a “fanner”. It makes use of a magnetic field to induce a charge in the ferrous sheets in the stack. Each sheet towards the

top of the stack is given a magnetic charge, causing them to possess the same polarity and repel each other. The sheet at the top of the stack tends to rise above the remainder of the stack, thus facilitating pickup by the robot gripper.

Suction Cups

Suction cups are flexible pick up devices designed for use with vacuum generator. They are made in various sizes and shapes and are used in different handling applications. Suction cups are typically made of elastic material such as soft rubber or soft plastic a vacuum is created between the cup and the part surface with the help of a vacuum pump or a venturi.

The principle of operation either involves either creation of a vacuum by a vacuum generator or use of an air ejector called a venturi. For easier control and operation reasons, the technique based on the venturi effect is used. It consists of an air ejector and suction cups. As illustrated in the Fig 1.7, a restrictor inside the ejector causes acceleration in the flow of air towards port R which pulls in the ambient air through port A. This causes a vacuum. The devices made on the venturi effect, enables 85 to 90% vacuum using 4 to 5 bar compressed air.

1.1.8 Robotic Sensors

Sensors used as peripheral devices in robotics include both simple types such as limit switches and sophisticated types such as machine vision systems. Sensors are also used as integral components of the robots position feedback control system. Their function as peripheral devices in a robotic work cell is to permit the robots activities to be coordinated with

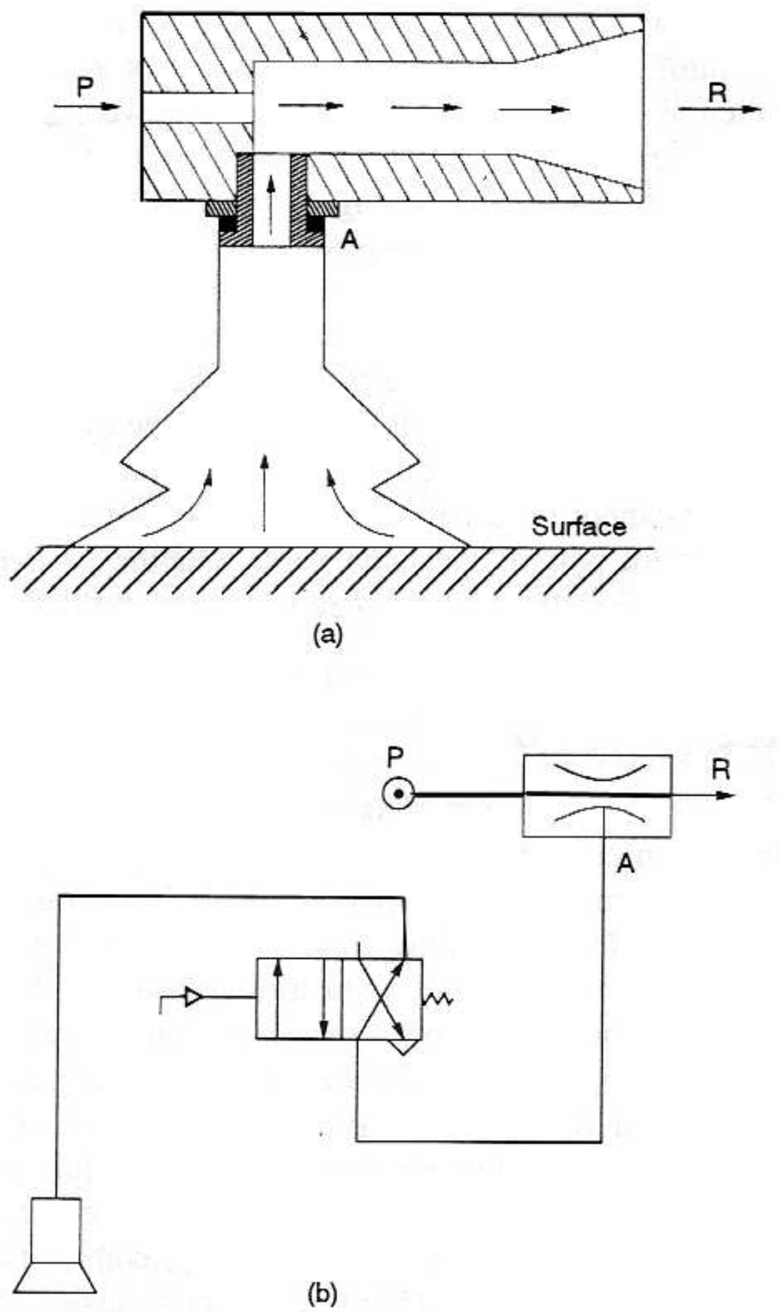

Figure 1.7: (a) Schematic view of a venturi (b) Application of venturi

other activities in the cell. The sensors used in robotics include the following general categories:

1. *Tactile sensors:* These are sensors which respond to contact forces with another object. Some of these devices are capable of measuring the level of force involved.

2. *Proximity and range sensors:* A proximity sensor is a device that indicates when an object is close to another object but before contact has been made. When the distance between the objects can be sensed, the device is called as range sensor.

3. *Miscellaneous types:* The miscellaneous category includes the remaining kinds of sensors that are used in robotics. These include sensors for temperature, pressure, and other variables.

4. *Machine vision:* A machine vision system is capable of viewing the workspace and interpreting what it sees.

These systems are used in robotics to perform inspection, parts recognition, and other similar tasks. Sensors are an important component in work cell control and in safety monitoring systems.

1.2 Stepper Motors [1]

1.2.1 Definition of a Stepper Motor

The definition of stepper motor given in British Standard Specification is

> "A stepper motor is a brushless DC motor whose rotor rotates in discrete angular increments when its stator winding are energized in a programmed manner. Rotation occurs because

> of magnetic interaction between rotor poles and poles of the sequentially energized stator windings. The rotor has no electrical windings , but has salient and/or magnetized poles."

A stepper motor is a digital actuator whose input is in the form of programmed energization of the stator windings and whose output is in the form of discrete angular rotation. It is, therefore, ideally suited for use as an actuator in computer control systems, digital control systems, etc. Control systems employing stepper motors as actuators are known as incremental motion control systems (IMCS).

1.2.2 Step Angle θ_s:

This is the angle through which an unloaded stepper motor rotates for every step of the energisation sequence. It is determined by the number of teeth on the rotor and stator, as well as the number of steps in the energisation sequence.

1.2.3 Steps/Revolution (Z):

It is given by

$$Z = 360°/\theta_s \tag{1.1}$$

For permanent magnet hybrid (PMH) step motors,

$$\theta_s = 360°/(N_r \times K_{ws}) = 360°/Z \tag{1.2}$$

Where N_r = no. of teeth on rotor discs

& K_{ws} = 4 for 4-step sequence (i.e. 1 phase on amd 2 phase on)

= 8 for 8-step (i.e.1-2 or hybrid) sequence of energisation of stator windings.

Motor Type	**Advantages**	**Disadvantages**
Stepper Motors	Can be driven open loop without feedback	Fixed step angle; no flexibilty in step resulotion
	No accumulative position error	Low efficiency with ordinary controller
	Responds directly to digital control signals; so stepper motors are natural choice for digital computer control	high overshoot and oscillation in step response
	Mechanically simple; requires little or no maintenance	Limited ability to handle high inertia load
	Free from contamination	Friction load increases position error, but error is not accumulative
	Can be repeatedly stalled without damage	Limited output and sizes available
	Relatively rugged and durable	
Variable Reluctance Stepper Motors	High torque to inertia ratio	No detente torque available with windings de-energized
	Low rotor interia	Exhibits mid-range resonance at some stepping rates under some drive conditions
	Capable of high stepping rate; high speed slewing capability	Normally available in 3.6 to 30 deg. step angles
	Ability to freewheel	Low efficiencies at low voltages and stepping rates

	Light weight	
	3,4 and 5 phase, single and multi-stack models available	
Permanent Magnet Hybrid Motors	Provides detente torque with windings de-energized	Higher inertia and weight due to presence of rotor magnet
	Less tendency to resonate	Performance affected by change in magnet strength
	Higher holding torque capabilty	
	Better damping due to presence of rotor magnet	
	High stepping rate capability	
	High efficiency at lower speeds and lower stepping rates	
Electro-hydraulic Motor	Very high holding toque capability	Requires high pressure hydraulic supply in addition to electric supply
	Very high torque-to-inertia ratio	More complex construction and operation
	Can handle high inertia load well	
	Capable of high stepping rates	
	Less tendency to oscillate and resonate	

Table 1.2: Comparison of Stepper Motors

1.2.4 Step Angle Accuracy:

Is usually $\pm 5\%$ of θ_s ; in a few cases, we can get accuracy of 3%. In certain exceptional cases, it is possible to get an accuracy of ± 1

Typical accuracy curve for a stepper motor is shown in Fig 1.8. Observe that the positioning error is non-cumulative. Consequently positioning error at that end of N step will be the same as that for a single step, viz. $\pm 5\%$ of θ_s. Further as the motor is loaded, the positioning error increases.

1.2.5 Static Characteristics:

Torque-Angle Curve: It is shown in Fig. 1.9 . It is seen that the torque increases, almost sinusoidally, with angle θ from the equilibrium position.

Holding Torque (T_h): It is the maximum load torque which the energized stepper motor can withstand without slipping from equilibrium position. If the holding is exceeded, the motor suddenly slips from the present equilibrium position and goes to the next stable equilibrium position.

Detente Torque (T_d): It is the maximum load torque which is unenergized stepper motor can withstand without slipping. Detente torque is due to residual magnetism, and is, therefore, available only in PM and hybrid stepper motor. It is about 5 – 10 $\%$ of holding torque. It is typically a fourth harmonic torque as shown in Fig. 1.10. It is also known as *cogging torque*.

Torque Current Curve: A typical torque current for a stepper motor is shown in Fig 1.11 . It is seen that the curve is initially linear but, later on, its slope progressively decreases as the magnetic circuit of the motor saturates.

Torque Constant (K_t): Torque constant of a stepper motor is defined as the initial slope of the torque-current (T-I) curve of the stepper motor. It is

N_r	$K_{ws} = 4$		$K_{ws} = 8$	
	Z	$\theta_s(°)$	Z	$\theta_s(°)$
6	24	15.0	48	7.5
9	36	10.0	72	5.0
12	48	7.5	96	3.75
15	60	6.0	120	3.0
25	100	3.6	200	1.8
30	120	3.0	240	1.5
50	200	1.8	400	0.9
75	300	1.2	600	0.6

Table 1.3: Relation between θ_s and N_r for PMH stepper motor

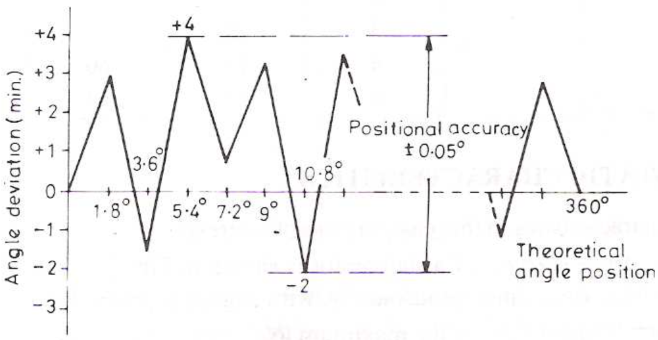

Figure 1.8: Positional Accuracy

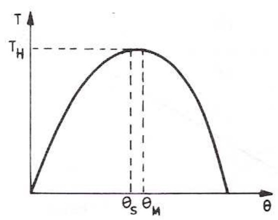

Figure 1.9: Torque Angle Curve

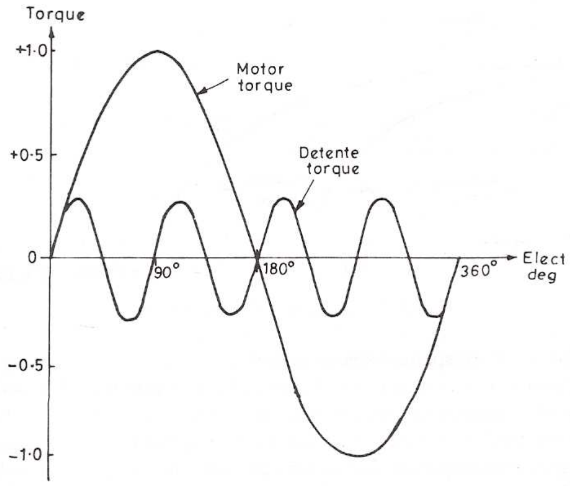

Figure 1.10: PM Hybrid Motor Torque and Detente Torque Profiles

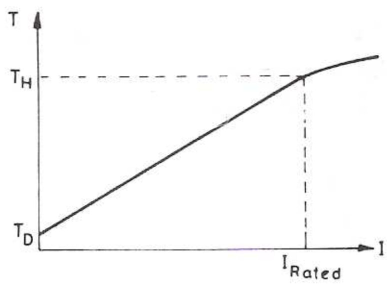

Figure 1.11: Torque-Current Curve

also known as torque sensitivity.

1.2.6 Dynamic Characteristics:

These are presented by torque-stepping rate curves for the motor as shown in Fig 1.12. The two torque-stepping rate curves shown in fig are pull-in and pull-out curves. Their significance is as follows:

Pull-in Curve: Corresponds to the so-called start-stop or single stepping mode of stepper motor operation as shown in Fig. 1.13(a). In this mode, the rotor comes to rest after moving through one step. Consequently, the rotor will not move any further as soon as you stop energizing the motor winding in the given programmed sequence. The motor can, therefore, start or stop with each individual pulse i.e. respond to each individual pulse.

Pull-out Curve: Corresponds to slewing mode of stepper motor operation as shown in Fig. 1.13(b). In this mode, the rotor is still moving in response to the previous pulse when the next pulse comes. Consequently, the motor can run at a much faster rate in slewing mode than in start-atop mode. However, the motor cannot start slewing from rest; nor can it stop immediately when you stop applying pulses. The motor will over-run by several steps before it comes to rest.

1.3 Pneumatics [7]

1.3.1 Features of Pneumatics

The following features are notable:

1. Wide availability of air.

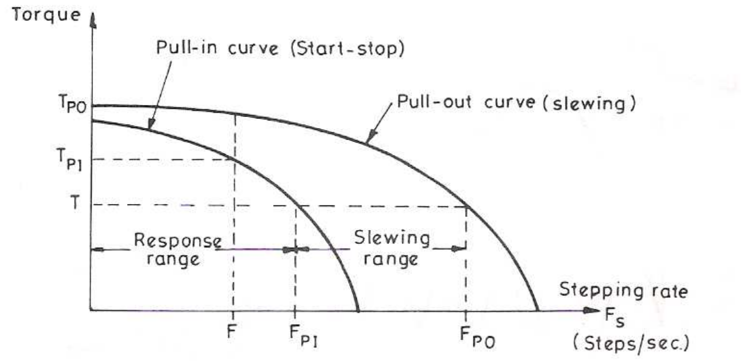

Figure 1.12: Torque-Speed Characteristics

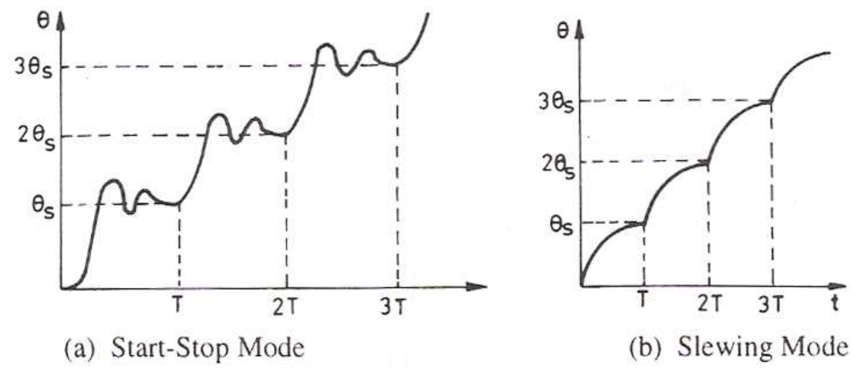

Figure 1.13: Modes of Operation

2. Compressibility of air.

3. Easy transportability of compressed air in pressure vessels, containers, and in long pipes.

4. Fire-proof characteristics of the medium.

5. Simple construction of pneumatic elements and easy handling.

6. High degree of controllability of pressure, speed and force.

7. Easier maintenance.

Compared to hydraulic system, pneumatic system has better operational advantages but it cannot replace hydraulic system so far as power requirement and accuracy of operations is concerned.

1.3.2 Basic Pnuematic System

The basic system requirements for introducing pneumatics in one's plant is listed below:

1. Compressor Plant : The production plant using pneumatic tools, etc. should be equipped with the compressed air plant of appropriate capacity to meet the compressed air needs of the systems.

2. Pipeline : A well-laid compressed air pipeline system should be drawn from the compressor plant to the consumption point of pneumatic energy in various sections of the plant where pneumatic gadgets and systems are to be introduced.

3. Control Valves : Various types of control valves are used to regulate, control, and monitor the air energy, for control of direction, pressure, flow, etc.

4. Air Actuator : Various types of air cylinders or air motors are used to perform the useful work for which the pneumatic system is designed like using cylinders for linear movement of jigs, fixtures, raw materials feeding, etc.

5. Auxiliary Appliances : Various types of auxiliary equipment may have to be used in pneumatic system for effecting better performance, easy controllability and higher reliability.

1.3.3 Pipe Materials

If the system pressure is quite high, materials of pipes and their physical and metallurgical properties become an important parameter and for their correct selection. But as pneumatic system usually works at a much lower pressure in comparison to hydraulic system, one may not need super high strength material for pneumatic pipelines and fittings. Materials which are mostly used for pneumatic pipes and tubes are listed below :

1. Galvanised iron pipes.
2. Cast iron pipes.
3. Copper tubes.
4. Aluminium tubes.
5. Rubber hose.
6. Plastic and nylon hose.
7. High strength steel pipe.
8. Brass tube.
9. Reinforced rubber or plastic hose, etc.

1.3.4 Air Compressor

Though not directly connected to the pneumatic system, the air compressor plays a vital role in the overall system performance. Various types of air compressors are used in the industry. But positive displacement compressors are more popular. Positive displacement compressors are classified as rotary type, e.g. screw, lobe, vane compressors and reciprocating type, e.g. piston type air compressor.

1.3.5 FRL Unit

The air that is sucked by the air compressor is not clean because of the presence of various types of contaminants in the atmosphere. Moreover, the air that is supplied to the system from the compressor is further contaminated by virtue of generation of contaminants downstream. The pressure of the air does not remain stable due to the possibility of line fluctuations. Hence to enable supply of clean, pure and contamination free compressed air, the air requires to be filtered. The system performance and accuracy depends much on the pressure-stability of the air supply. An air line filter and a pressure regulator, therefore, are indispensible along with a third component — an airline lubricator. The main function of the lubricator is to provide the air with a lubricating film of oil. These three units together are called service unit of FRL unit.

Air-Filter

Air-filters are used in pneumatic systems to perform the following main functions:

- To prevent entrance of solid contaminants to the system.

S. No	Pipe Material	Maximum pressure (bar)
1	Copper	250
2	Aluminium	125
3	Brass	200
4	Stainless steel	2500–4500
5	Polythene at 80°C	12-15
6	Nylon 100°C	7–10
7	Vinyl at 25°C	8–10
8	Rubber at 80°C	3–7

Table 1.4: Pressure rating of pipe materials

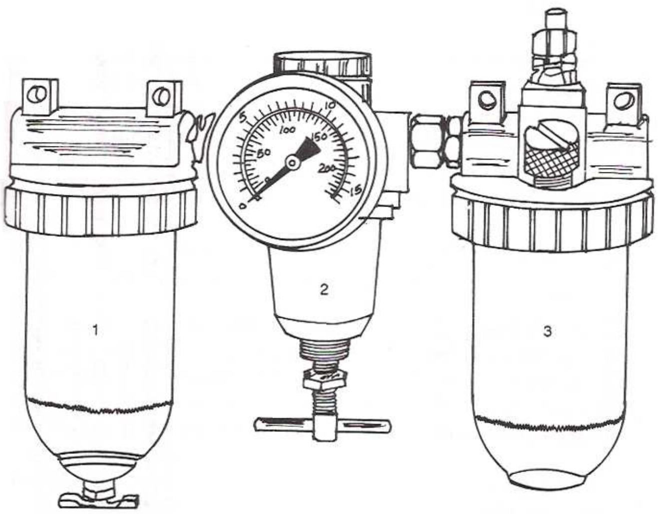

Figure 1.14: FRL unit in combination: 1. Filter 2. Regulator 3. Lubricator

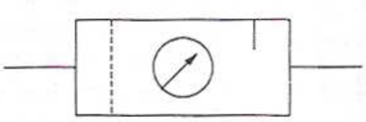

Figure 1.15: FRL unit: Symbol

- To condense and remove the water vapour that is present in the air passing through it.
- To arrest any submicron particles that may pose a problem in the system components.

The main component of the filter is the filter cartridge, which is made mostly of sintered brass, or bronze but other materials are also used.

Pressure Regulator

The main function of the pressure regulator is to regulate the incoming pressure to the system so that the desired air pressure is capable of flowing at steady condition. It is done by using various valves and spring force.

Lubricator

The compressed air is first filtered and then regulated to the specific pressure and made to pass through a lubricator in order to form a mist of oil and air for the sole purpose of providing lubrication to the mating components of the valves, cylinders etc. All lubricators follow the principle of venturimeter.

1.3.6 Pneumatic Cylinders

The pneumatic power is converted to straight line reciprocating motion by pneumatic cylinders. The various industrial applications for which air cylinders are used can be divided dutywise into three groups — light duty, medium duty and heavy duty. But according to the operating principle, air cylinders can be sub-divided as single acting and double acting cylinders.

Single Acting Cylinder In a single acting cylinder, the compressed air is fed only in one side. Hence, this cylinder can produce work only in one direction. The return movement of the piston is effected by a built-in spring or by application of an external force.

Double Acting Cylinder In a double acting cylinder, the force exerted by the compressed air moves the piston in either of the two directions. They are used particularly when the piston is required to perform work not only on the advance movement but also on the return. In principle, the stroke length is unlimited, although buckling and bending must be considered before we select a particular size of piston diameter, rod length and stroke length.

1.3.7 Direction Control Valve

In certain designs of direction control valves, 5 openings are preferred instead of 4 openings. This ensures easy exhausting of the valve. The Fig. 1.17 shows a 5/2 direction control valve - spool type design. The spool slides inside the main bore and according to the spool position, the ports gets connected or disconnected. The working peinciple is as follows:

Position 1 When the spools is actuated towards outer direction, port P gets connected to ‘B’ and ‘S’ remains closed while A gets connected to ‘R’.

Position 2 When the spool is pushed in the inner direction, port ‘P’ and ‘A’ get connected to each other and ‘B’ to ‘S’ while port ‘R’ remains closed.

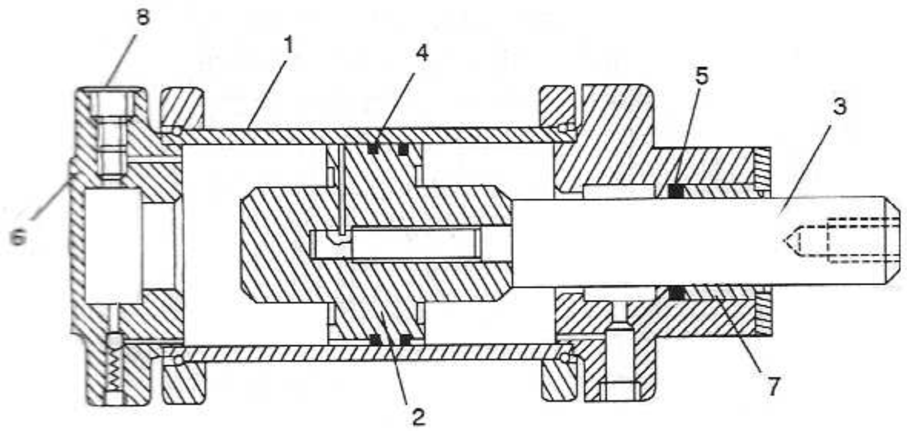

Figure 1.16: Double Acting Cylinder: 1. Tube 2. Piston 3. Piston Rod 4. Double O-ring packing on piston 5. O-ring for piston rod 6. End cover 7. Bush 8. Cushion Assembly

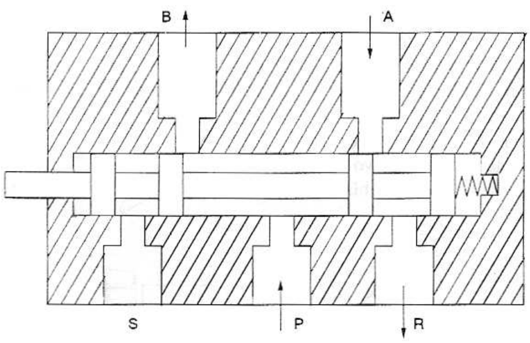

Figure 1.17: 5/2 D.C. valve

Chapter 2

Initial Ideas - Alternate Designs

The problems faced in implementing any standard available robots have already been discussed. Initially we proposed some ideas for the mechanism, but which had to be discarded. The ideas, along with their drawbacksm are discussed in this chapter.

2.1 Cartesian Configuration

The idea of using pneumatic cylinders in a configuration similar to that of a cylindrical configuration was initially considered. There would be a base cylinder which would provide for the vertical motion for the lifting that was required. Another cylinder perpendicular to that would give the necessary horizontal motion for receiving the sheets and loading them into the press. There would be another cylinder mounted to provide the third linear motion (Fig 2.1).

In this case we had the advantage of the fact that we were working on a pneumatic press and that the necessary air supply was readily available. There would have been no need for a separate compressor unit, as in the case of the third arm that has been implemented.

The problem faced with this was that pneumatic cylinders are very bulky. For a given stroke length the total length of the cylinder is at least twice of this. The restriction of the ram in its downward stroke leaves only 450 mm gap between the bed and the ram. The pneumatic cylinder would have to work as cantilever with heavy loads attached or a separate supporting frame would have to be made to guide the piston rod, all making the assembly very complicated. This full arrangement would have had to be mounted on the bed and the surrounding area fenced out to avoid any mishaps. Stacking a fresh bunch of sheets will be quite difficult too. Hence, this idea was discarded.

2.2 Spherical Configuration

Another idea was to use a motor at the shoulder joint as in a spherical configuration. In this, we would have one base motor for rotation of the entire assembly. A separate motor at the shoulder, for lifting, and a pneumatic cylinder, for the necessary linear motion for collecting and placing the sheet in the die would be used (Fig 2.2).

The major drawback of this was that since the weight of the entire assembly is more than 25 kg, the base motor would have to be very large. The motor at the shoulder had to pick up the sheet against gravity with the load of the arm and the pneumatic cylinder, all of which calls for another big motor. The precise control of a D.C. or A.C. induction motor is not quite possible and the cost of a stepper motor or servo motors of a large

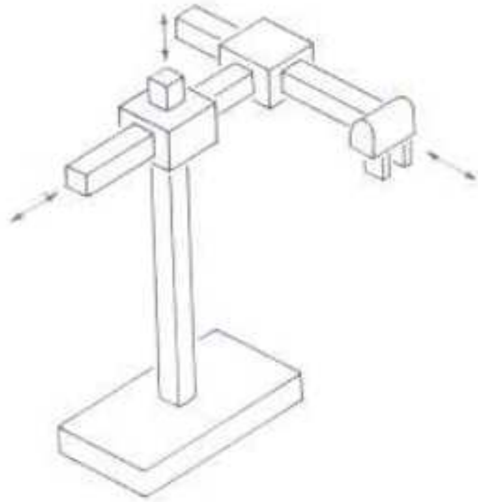

Figure 2.1: Cartesian configuration

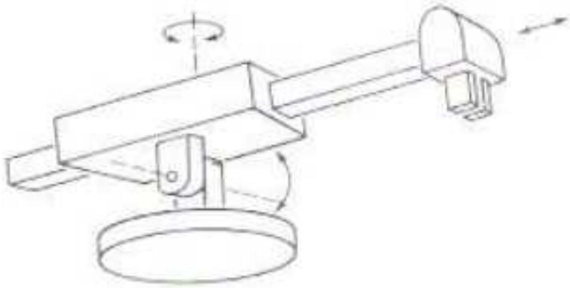

Figure 2.2: Spherical configuration

torque capacity is very high. As a result, this idea too was discarded.

2.3 Planar Configuration with Pulleys for lifting

The third attempt at trying to find a solution saw us trying to use a pulley arrangement instead of the motor at the shoulder as in the previous case. The arrangement would be quite similar, with the base motor to rotate the assembly and the pneumatic cylinder for transferring. The shoulder motor would be replaced by telescopic chutes at the end. With the help of steel cord running all along the robot from the base, the three chutes would be lowered or raised. There would be a motor at the base which would wind the cords on pulleys.

The problem encountered in this arrangement was that this would make the assembly quite bulky requiring a lot of tubing. Apart from that there was also a possibility of the cords not being wound on the pulleys evenly causing angular tilt of the sheet or sudden seizure in the motion.

2.4 End Effectors

In all of the above designs the possibility of using suction cups or electro magnets was thought of. Suction cups had an advantage that the pneumatic power required for it was easily available. However the sheets have to be greased with a particular liquid before loading, which is done manually. This would call for additional filtering units for the cups, which increased costs considerably.

The sheets which were to be loaded are always M.S. or of an EN series. Hence using electromagnets was a cheaper and favorable alternative. The only problem with these is that it is difficult to lift only one sheet from the stack using electromagnets. Thus, it is only for this application that we must use suction gripper, and use electromagnets for other tasks.

Chapter 3

Final Mechanism Description

After considering all the ideas that we had initially proposed, we arrived at a final set of mechanisms that would work in tandem to perform the required tasks of loading and unloading the press. The robot consists of 3 separate arms - each for performing a different role. The different tasks to be performed will be: (Fig. 3.1)

1. Lifting the sheet
2. Planar transfer of sheet up to the die
3. Unloading of finished product

The first arm to come in contact with the plates (raw material) is the lifting arm. The lifter arm, driven by a DC motor, uses suction cups to grasp the sheets and a lead screw type arrangement to lift them to desired height. As the screw rotates, the nut is displaced either up or down depending on the direction of rotation of the screw. This lifter is equipped with proximity switches that sense the height at which the next sheet is and also fix the height of vertical travel. This travel limit is set by the operator.

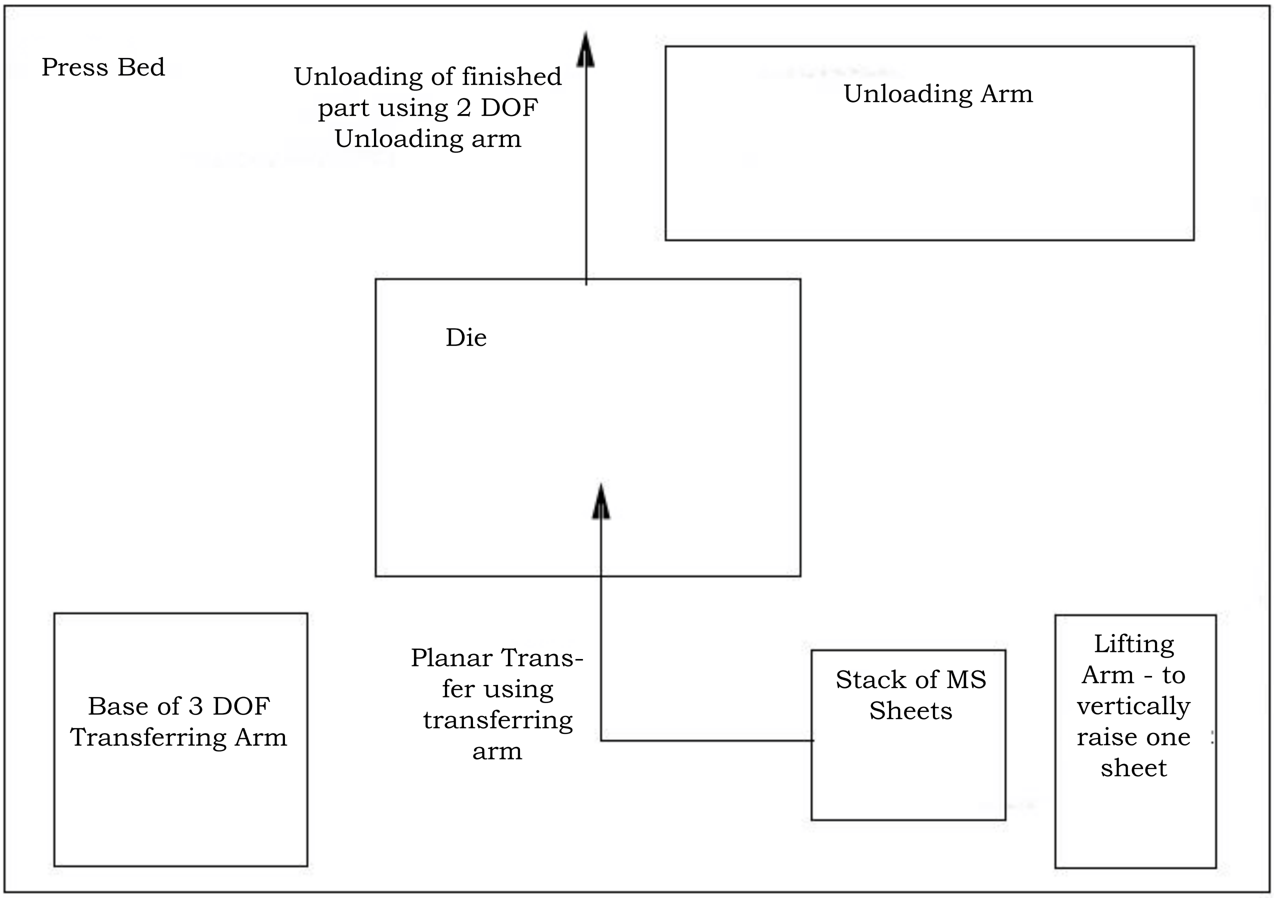

Figure 3.1: Block Diagram of robotic assembly

When the lifting arm reaches the topmost position with the plate, it waits at the position until a second arm, the transferring arm, takes over. The transferring arm is a 3 DOF planar arm, which transfers the plate along a plane parallel to the horizontal. The end effector is electromagnetic. This arm moves along a fixed path, set by the operator during the programming mode. The start point coincides with the topmost position of the lifting arm and the final position is the die center. The electromagnets of the arm switch on, gripping the plate, following which the lifting arm releases the plate. As a result, the plate is now manipulated by the transferring arm. It transfers the plate to the die center, and upon reaching this location, switches off the electromagnets. The height of the two arms are so set that the plate is around 5 mm above the die when the magnets are switched off. This height difference is sufficient to allow for the plates to fall onto the die without any misalignment.

After the sheet has been loaded, the robot sends a signal to the press and the punch starts its descent. Once the sheet has been worked upon, a signal is sent to the robot controller which activates the unloading mechanism. The unloading mechanism is a 2 DOF arm with one linear actuator — a pneumatic piston-cylinder, and one motor, driving a rack. The height of arm from the bed is manually adjustable. The pneumatic cylinder pushes the piston out and positions the electromagnet over the finished product. The motor then drives the rack vertically downwards, to get the electromagnets in contact with the job. The arm picks up the job, and each motion is reversed in opposite sequence and the job is dropped into a container by switching off the magnets.

This entire assembly is thus a set of 3 arms — a 1 DOF lifting arm, a 3 DOF transferring arm and a 2 DOF unloading arm.

Part III

Robot Design

Chapter 4

First Arm

4.1 Prototype 1

4.1.1 Features

The design of this arm, as described earlier, uses a lead screw mechanism to achieve vertical lifting of the metal sheet. This lead screw is driven by a motor, coupled by a gear drive. In this design, the motor selected was a 1-Phase AC motor. The motor was coupled using a spur gear pair with a gear ratio of 1:1. As direction reversal of 1- Phase AC motors is not possible, the motor was connected to an Electromagnetic Double Clutch - Brake system. The end of travel in upward direction was specified by adjusting the height of the sensor plate, on which the proximity switches would be mounted. (Fig 4.1)

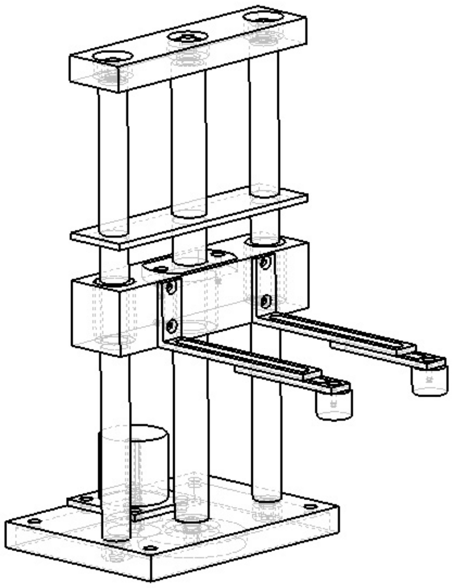

Figure 4.1: Lifting arm: First Design

Components	**Specifications**
Actuator	Permanent Magnet DC Motor 2000rpm; 100Watt ;6Kg-cm
Transmission Drive	Spur Gears (m=2; z=58; G 1:1) Lead Screw (Acme Thread; M22; P=5)
End Effector	2 Electormagnets (ϕ 50$\times$20mm)
Degree of Freedom	only 1 D.o.f.
Lifter Beam	50$\times$50$\times$200mm
Brackets	5$\times$10$\times$150mm
Sensor Mount	Horizontal above lifter beam
Sensing Elements	2 Proximity Sensors

Table 4.1: Lifting Arm - Specifications of first prototype

4.1.2 Component Design

Lead Screw

The lead screw used to lift the central beam needs to lift a total weight of about 5 kg. Thus the minimum allowable core diameter is given by

$$W = \sigma \cdot \frac{\pi}{4} \cdot d_c^2 \tag{4.1}$$

Thus we get minimum $d_c = 0.79$ mm.

As we need a pitch of 5 mm, we choose trapezoidal threads having

d_c	=	16.5 mm
d_o	=	22 mm
Area of core A_c	=	214 mm^2

Calculation of driving torque

$d = \frac{22 + 16.5}{2} = 19.25$

$$tan(\alpha) = \frac{nP}{\pi d} \tag{4.2}$$

$\therefore \alpha = 4.726°$

$$\mu_1 = \frac{\mu_c}{\cos\beta} = 0.1242 \tag{4.3}$$

$$\phi = \tan^{-1}(\mu_1) = 7.08° \tag{4.4}$$

Torque required to rotate screw in nut

$$T_1 = W\tan(\alpha + \phi) \cdot \frac{d}{2} = 98.55\mathrm{N-mm} \tag{4.5}$$

Torque required to overcome collar friction at base

$$T_2 = \frac{2}{3}\mu W(\frac{R_o^3 - R_i^3}{R_o^2 - R_i^2}) = 59.1543\mathrm{N-mm} \tag{4.6}$$

$T = T_1 + T_2 = 157.7$ N-mm

However, an AC motor with speed reversal is not available and additional components like Electromagnetic Double Clutch -Brake is needed. This increases the costs and complication of the part considerably. Hence, this design was discarded.

4.2 Prototype 2

4.2.1 Features

As in the previous design we continue to use a lead screw but the drawbacks of the A.C. motor concerning direction reversal are overcome by using a stepper motor. This gives us a slower speed of about 100rpm with reasonably high torque. Thus, to achieve the required motion of 320mm in 2 sec we change the gear ratio of 1:1 to 5:1. The speed is further increased by using a lead screw with a pitch of 5mm and four starts and an overall lead of 20mm. The need of any breaking system was not felt due to the ability of precise braking of the stepper motor when driven at 100 rpm. A proximity sensor is mounted on side sensor mount instead of a top sensor mount. This change was done as the central beam might collide with the top sensor plate. On sensing the beam, it sends a signal to the stepper motor which switches off. (Fig 4.2)
The pneumatic circuit for this arm is shown in Fig 4.3.

Figure 4.2: Lifting Arm: Final Design

Components	**Specifications**
Actuator	DC Stepper Motor 500rpm; 17Kg-cm
Transmission Drive	Spur Gears (G 1:1; m=2; z_p =30; z_g =150) Lead Screw (Trapizoidal Thread; M22; P=5; Lead=20mm)
End Effector	2 Vacuum Grippers (ϕ 50mm)
Degree of Freedom	only 1 D.o.f.
Lifter Beam	25×60×200mm
Brackets	6×12×150mm
Sensor Mount	Vertical parallel to lifter beam
Sensing Elements	2 Proximity Sensors

Table 4.2: Lifting arm - Specifications of prototype 2

4.2.2 Component Design

(a) Lead Screw

The lead screw used to lift the central beam needs to lift a total weight of about 5 kg. Thus the minimum allowable core diameter is given by

$d_c = 0.79mm$.

As we need a pitch of 5 mm and 4 starts, we choose trapezoidal threads having

d_c	=	16.5 mm
d_o	=	22 mm
Area of core A_c	=	214 mm^2

Calculation of driving torque

$$d = \frac{22 + 16.5}{2} = 19.25$$

$$\tan(\alpha) = \frac{nP}{\pi d}$$

$$\therefore \alpha = 18.299°$$

$$\mu_1 = \frac{\mu_c}{\cos\beta} = 0.1242$$

$$\phi = \tan^{-1}(\mu_1) = 7.08°$$

Torque required to rotate screw in nut

$$T_1 = W\tan(\alpha + \phi) \cdot \frac{d}{2} = 223.71\text{N-mm}$$

Torque required to overcome collar friction at base

$$T_2 = \frac{2}{3}\mu W(\frac{R_o^3 - R_i^3}{R_o^2 - R_i^2}) = 59.1543 \text{ N-mm}$$

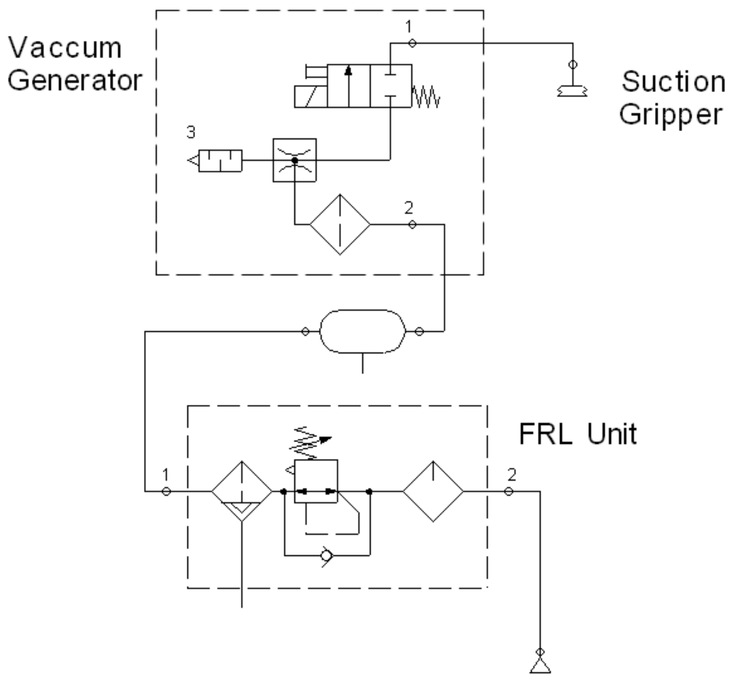

Figure 4.3: Pneumatic Circuit for Gripper

$T = T_1 + T_2 = 282.87$ N-mm

Design of nut

The bearing pressure is:

$$P_b = \frac{W}{(\pi/4)(d_o^2 - d_c^2)Z} \tag{4.7}$$

For high rubbing speed with steel screw and PB nut, P_b = 1 to 1.5 N/mm^2. Setting P_b = 1 gives,

$Z = \frac{h}{p} = 0.2949$

$\therefore h = 1.47$ mm

We select a screw with height h = 30 mm.

(b) Gear Design

We require a gear ratio of 1:5. Thus, we use standard gears from Albro Engineers available for this gear ratio.

The pinion is with dimensions

$d_p = 150mm$, $Z_p = 75mm$ and $m = 2$

and the gear with

$d_g = 30mm$, $Z_g = 15mm$ and $m = 2$

The face width of these is $b = 15mm$

The material used for these gears is EN8D with tensile strength

S_{ut} = 700 N/mm^2

and hardness of 460BHN (case hardened)

We check these gears for their strength and evaluate the factor of safety.

Beam Strength

$$\sigma_{bg} = \sigma_{bp} = \frac{S_{ut}}{3} = \frac{700}{3} = 233.33 N/mm^2 \tag{4.8}$$

Assuming a 20° full depth involute tooth system,

$$Y_g = 0.484 - \frac{2.87}{Z_g} = 0.2926 \tag{4.9}$$

$$Y_p = 0.484 - \frac{2.87}{Z_p} = 0.4457 \tag{4.10}$$

where Y_g is the Lewis form factor.

$$\therefore \sigma_{bg} \cdot Y_g < \sigma_{bp} \cdot Y_p \tag{4.11}$$

Thus, we check only the gear for safety.

The Lewis equation for beam strength of spur gear tooth is

$$\begin{aligned} F_b &= \sigma_{yg} \cdot b \cdot m \cdot Y_g \\ &= 2048.17 \text{ N} \end{aligned} \tag{4.12}$$

Wear Strength

Ratio factor,

$$\begin{aligned} Q &= \frac{2Z_g}{Z_g + Z_p} \\ &= 1.667 \end{aligned} \tag{4.13}$$

Load stress factor,

$$\begin{aligned} K &= 0.16 \, (\frac{BHN}{100})^2 \\ &= 3.3856 \end{aligned} \tag{4.14}$$

The Buckingham's equation for wear strength of a gear tooth is

$$\begin{aligned} F_w &= d_p \cdot b \cdot Q \cdot K \\ &= 2544.27 \text{ N} \end{aligned} \tag{4.15}$$

As $F_b < F_w$, the gear pair is weaker in bending and hence it should be checked for safety against failure in bending.

Precise Estimation of Dynamic Load by Buckigham's Equation

The Buckigham's equation for the dynamic load in the tangential direction is given by

$$F_d = \frac{21V(bc + F_{t_{max}})}{21V + \sqrt{bc + F_{t_{max}}}} \tag{4.16}$$

where $F_{t_{max}}$ = max. tangential force

= $K_a \cdot K_m \cdot F_t$

Taking $K_a = 1.5$ (application factor for electric motor with moderate shock) & $K_m = 2.2$ (load distribution factor for non-precise gear)

Theoretical tangential force

$$\begin{aligned} F_t &= \frac{p}{v} = \frac{T_g}{d_g/2} \\ &= 26.16 \text{ N} \end{aligned} \tag{4.17}$$

$\therefore F_{t_{max}} = 86.295N$

$$\begin{aligned} V &= \text{pitch line velocity in m/s} \\ &= \frac{\pi \cdot d_g \cdot N}{60 \times 1000} \\ &= 0.785 \end{aligned} \tag{4.18}$$

$$c = 11500\,e \ \text{N/mm} \tag{4.19}$$

deformation factor for steel pinion and steel gear.
$e = 21.31 \times 10^{-3} mm$ for given gear pair.

$\therefore c = 245.075 N/mm$

$\therefore F_d = 796.97N$

Estimating Factor of Safety

$$\begin{aligned} \mathrm{F}_{eff} &= K_a \,.\, K_m \,.\, F_t + F_d \\ &= 883.27 \text{ N} \end{aligned} \tag{4.20}$$

$$\therefore \begin{aligned} \mathrm{N}_{eff} &= \frac{F_b}{F_{eff}} \\ &= 2.31 \end{aligned} \tag{4.21}$$

Thus, the gears used are safe against failure.

(c) Bracket

The brackets on which the suction cups are attached is held only at one end and the entire load of the plates is borne by it. We designed a bracket and checked it by loading each bracket of the arm by a load of 20 N. This is almost twice the load that will be experienced by each bracket.

The analysis was done on the software CosmosExpress, the results of which are given in Table 4.3, Table 4.4 and Fig 4.4.

(d) Vacuum Generator

Together with the corresponding suction grippers and suction cups, vacuum generators are capable of picking up and retaining workpieces with smooth, impervious surfaces. Workpieces can be picked up in any position. The air supply of these vacuum generators is controlled by the built-in solenoid valve. After switching supply power on, the valve shifts and the flow of compressed air generates a vacuum by means of the ejector principle. Suction stops when the supply power to the valve is switched off. The integrated silencer reduces exhaust noise to a minimum. The selection of pneumatic components was done using the manufacturer's catalogues [4].

Mesh Type:	Solid mesh
Mesher Used:	Standard
Automatic Transition:	Off
Smooth Surface:	On
Jacobian Check:	4 Points
Element Size:	2.6347 mm
Tolerance:	0.13173 mm
Quality:	High
Number of elements:	6080
Number of nodes:	12347

Table 4.3: Mesh Information for Bracket

Stress Type	**Max.**	**Location**
Von Mises Stress	121.659 N/mm^2	(5 mm , 10 mm, 9.2858 mm)

Table 4.4: Stress Results

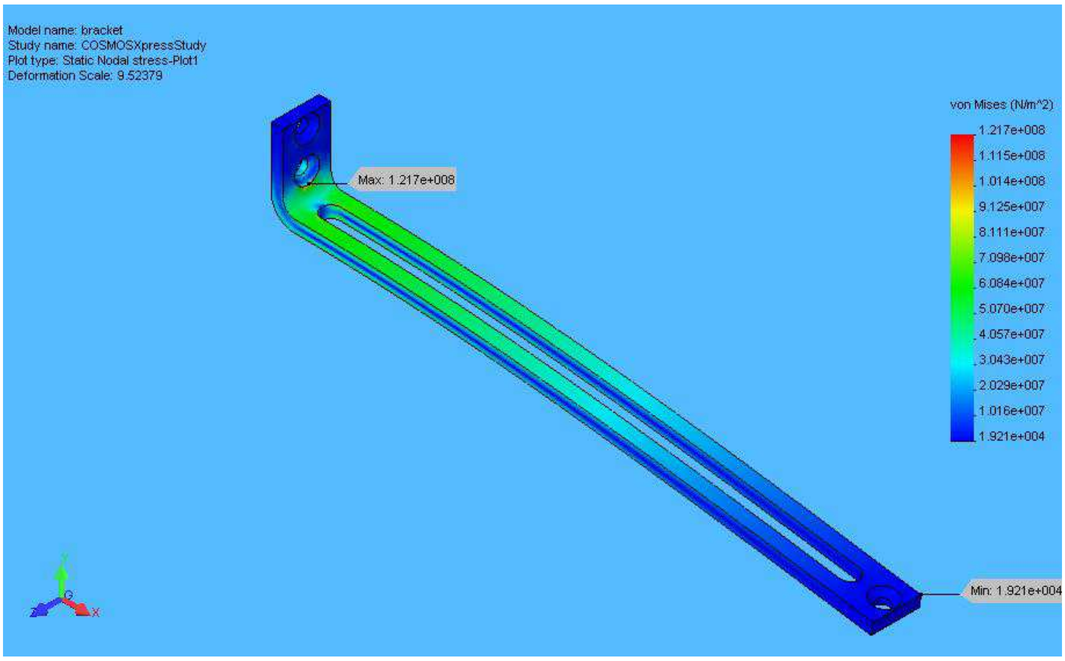

Figure 4.4: Stress Results

Figure 4.5: Vacuum generator

Feature	Data/description
Nominal size, Laval nozzle	0.95 mm
Assembly position	Any
Ejector characteristic	High vacuum
Design structure	T-shaped
Operating pressure	1.5 - 8 bar
Max. vacuum	85 %
Duty cycle	100 %
Nominal operating voltage DC	24 V
Operating medium	Filtered, unlubricated compressed air, 40 μm filtration
Medium temperature	0 - 60 °C
Protection class	IP65
Ambient temperature	0 - 60 °C
Authorisation	c UL us - Recognized (OL)
Product weight	210 g
Electrical connection	Plug
Mounting type	Optional with through hole with internal (female) thread
Pneumatic connection, port 1	G1/8
Pneumatic connection, port 3	Non-ducted
Vacuum connection	G1/8
Materials note	Copper and Teflon-free
Materials information, housing	Aluminium

Table 4.5: Vacuum Generator: Datasheet

(e) Suction Gripper

The modular design of the suction grippers (ESG) results in more than 2000 possible variants. The gripper comes in 6 different suction cup materials: perbunan, polyurethane, vulkollan, silicone, viton and anti-static perbunan. It includes angle compensation with ball joint and filter. The selection of gripper is done using the software ProPneu (Version 4.2.10.2004) provided by Festo Controls Ltd. The load (Fig. 4.7) acting on the gripper depends upon the acceleration and jerk characteristics (Fig. 4.6). We note that the gripper selected shows satisfactory performance under the given conditions.

(f) Push-in Y connector

The Quick Star connector series offers a reliable solution for connection. The stainless steel retaining ring inside the fitting holds the tubing securely without damaging its surface. Vibration and pressure surges are safely absorbed. The tubing can be detached easily by pressing down the blue release ring. An NBR rubber sealing ring guarantees a perfect seal between standard OD tubing and the body of the fitting. Standard tubing is suitable for use with compressed air and vacuum. All of the brass components are nickel plated, and are thus highly resistant to corrosion.

(g) Socket Connector Cable

With these plug sockets, the stranded wires are pressed into the insulation displacement contact when the screw is tightened. The plug socket remains closed, only the outer sleeve is removed and the wire insulation remains intact. No additional assembly tools are required.

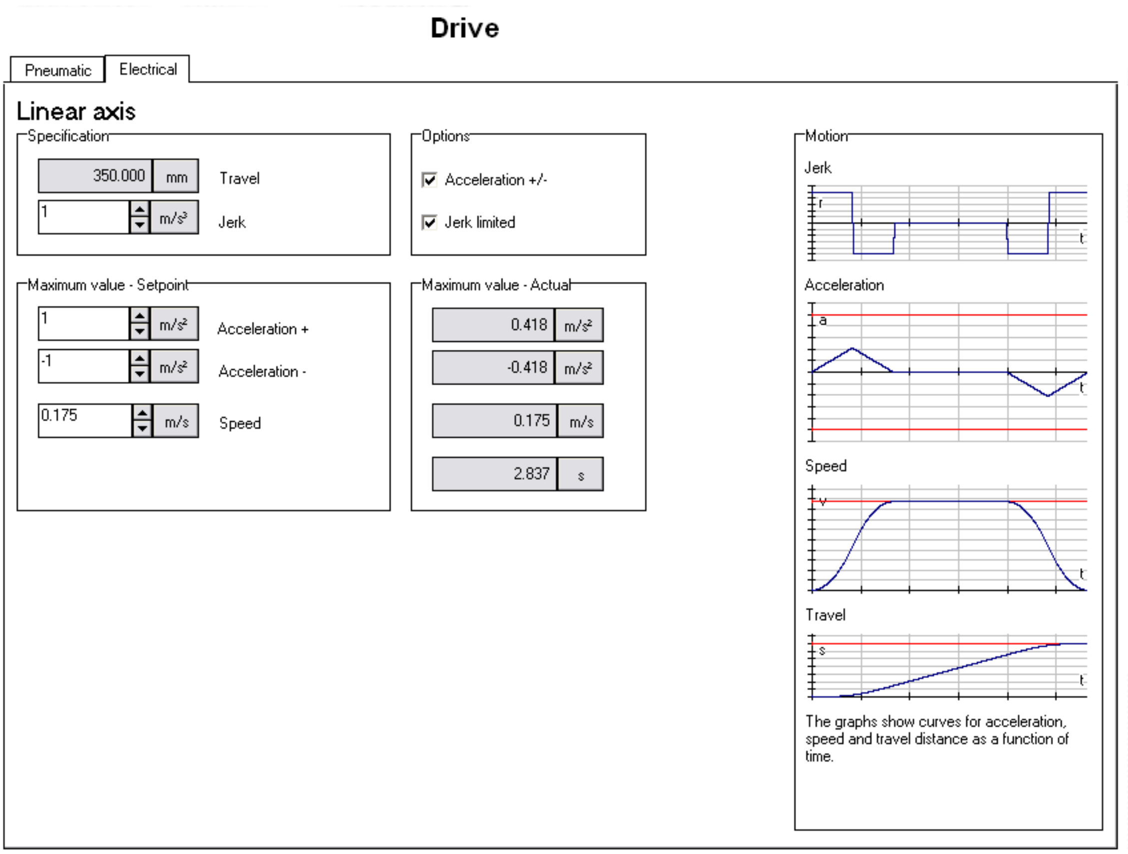

Figure 4.6: Velocity and Acceleration experienced by Gripper

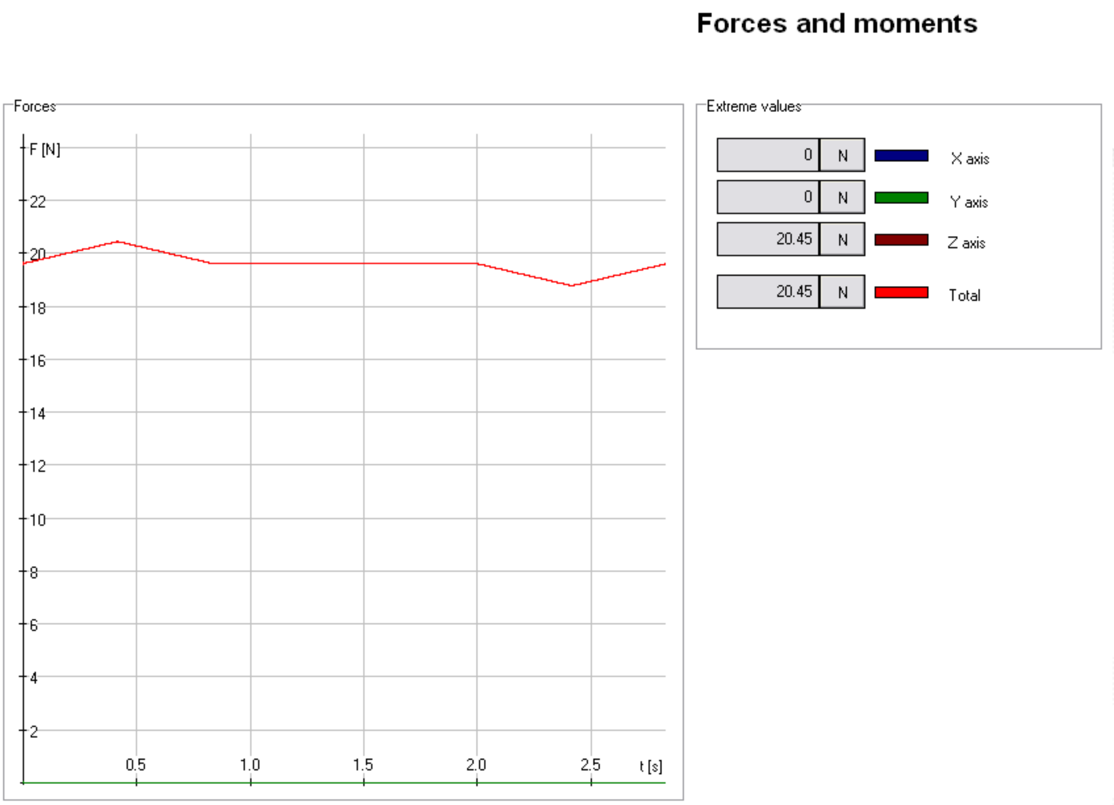

Figure 4.7: Force and moments experienced by Gripper

Figure 4.8: Suction Gripper

Feature	Data/description
Min. workpiece radius	40 - 330 mm
Suction cup diameter	50 mm
Suction cup volume	2.387 - 38.92 cm^3
Effective suction diameter	31.8 - 36.9 mm
Design structure	round, bellows 1.5 convolutions
	round, bellows 3.5 convolutions
	round, bell-shaped
	round, standard
	round, extra-deep
Operating medium	Atmospheric air
Corrosion resistance classification CRC	2
	1
Ambient temperature	-30 - 200 °C
Breakaway force at 70% vacuum	63.4 - 105.8 N
Shore hardness	50 ± 5
	60 ± 5
	72
Materials information for screw-in stud	Heat-treatment steel
Materials note	Copper and Teflon-free
Materials information for suction cup	VMQ (silicon)
	PUR
	NBR
	FPM

Table 4.6: Suction Gripper: Datasheet

Figure 4.9: Push-in Y connector

Figure 4.10: Socket Connector Cable

Feature	Data/description
Size	Standard
Nominal Size	3 mm
Design Structure	Push/Pull Principle
Operating Pressure	0 - 10 bar
Operating Medium	Compressed air, filtered, unlubricated Filtered, Lubricated air
Corrosion resistance classification CRC	1
Ambient temperature	0 - 60° C
Pneumatic connection	for tubing, 4 mm outside diameter

Table 4.7: Push-in Y connector: Datasheet

Feature	Data/description
Assembly position	Any
Switching position indicator	LED
Nominal operating voltage DC	24 V
Protection class	IP65
	to IEC 60529
Ambient temperature	-20 - 80 °C
Product weight	125 g
Wire ends	Wire end ferrule
Electrical connection	Plug socket
Round design	Design C
Cable structure	3 x 0.5 mm^2
Cable diameter	5.2 mm
Cable length	2.5 m
Protective earth connection	Available
Mounting type	On solenoid valve with M2.5 central screw
Materials information, housing	PA
	POM
Materials information, cable sheaths	PVC
Materials information, plug	Bronze

Table 4.8: Socket Connector Cable: Datasheet

Chapter 5

Second Arm

The second arm of the assembly is the transferring arm. In the final mechanism, this arm was chosen to be a 3 DOF jointed arm. To design the arm, we need to simultaneously analyze the motion and torque characteristics as these play a major role in the selection of actuators. Since this arm is a cantilever beam, the choice of actuators also determines the loads that will act on the arm. We assume that the motors used weigh 2.8 kg and their dimensions were chosen according to those stated by the manufacturer, Srijan Control Drives.

The paths that have to be traced should preferably be traversed by employing trajectories that ensure that accelerations experienced are minimum possible. Also, it has to be planned so that no jerks are experienced. This ensures that electromagnets do not lose control over the plate. Also, avoiding jerks will reduce the incidence of high stresses in the components. A gradual build up of velocity and gradual slow down has to be planned for a given path. The simplest type of trajectory which satisfies these conditions is a polynomial function. The displacement of the end effector is a polynomial function of time. The following constraints are

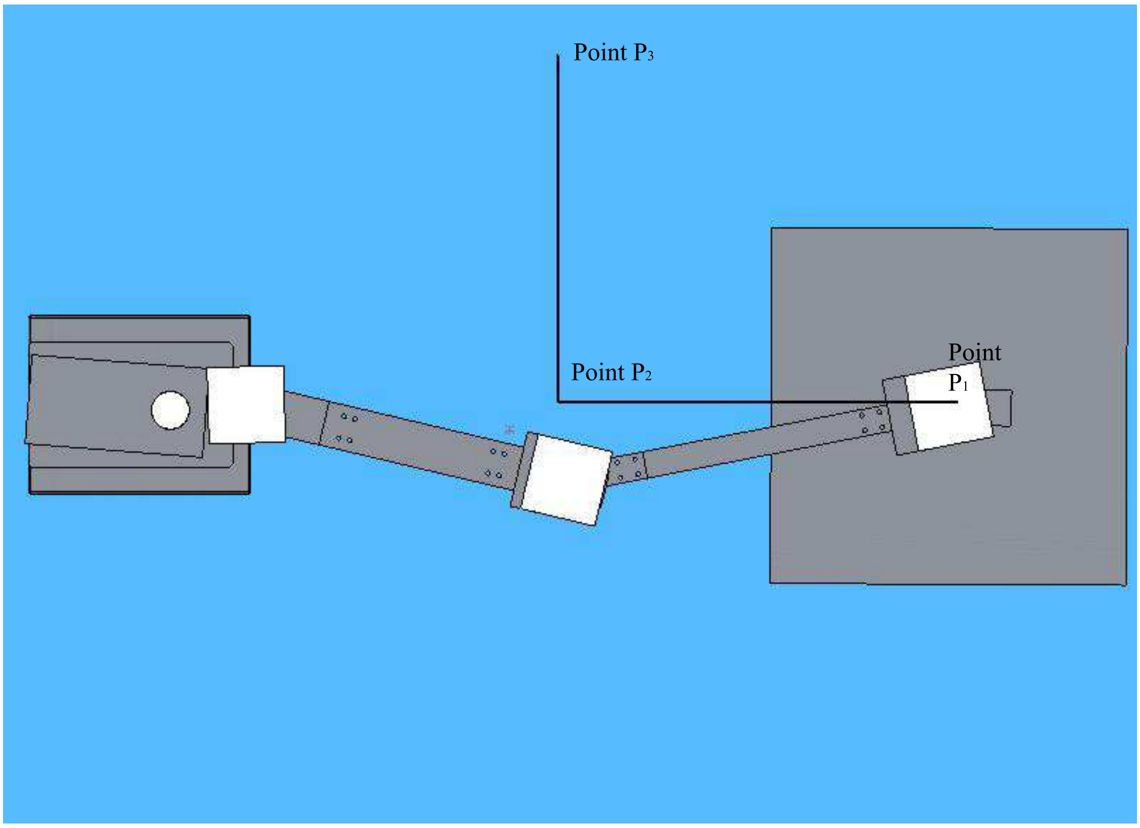

Figure 5.1: The start point P_1, intermediate point P_2 and the end point P_3 of motion

imposed on this polynomial function:

- Initial displacement, velocity and acceleration are zero
- Final displacement is the end point of the path
- Final velocity and acceleration are zero
- Initial and final values of jerk are zero

If $f(t)$ is the function of time which represents the percentage of path traveled then, the above conditions translate to the following equations:

$$\left.\begin{array}{ll} f(0) = 0\ ; & \mathrm{f(t}_f) = 1 \\ \frac{df}{dt}(0) = 0; & \frac{df}{dt}(t_f) = 0 \\ \frac{d^2f}{dt^2}(0) = 0; & \frac{d^2f}{dt^2}(t_f) = 0 \\ \frac{d^3f}{dt^3}(0) = 0 & \frac{d^3f}{dt^3}(t_f) = 0 \end{array}\right\} \text{where } t_f \text{ is time required for motion} \tag{5.1}$$

Setting these eight conditions on a polynomial will give us a system of eight simple linear equations in eight unknowns (the coefficients of a seventh degree polynomial) and can be easily solved to get polynomial function. The polynomial describes the percentage of the path traveled until time t. This polynomial is calculated for each section of the path shown in Fig. 5.1, ie the section P_1 to P_2 and the next section from P_2 to P_3. Using this information about the trajectory, we can then use the method of inverse kinematics to obtain the variation of joint angles with respect to time. This plot will then help us determine the velocities and accelerations that are to be generated by the actuator and by using the Newton-Euler Formulation [10] we can determine joint torques. The co-ordinates of points P_1, P_2 and P_3 are not fixed and hence these calculations are done for the extremities of motion.

The Newton-Euler Formulation can be described as such:
We use the following notations pertaining to the links and their respective

co-ordinate frames:

$a_{c,i}$ = the acceleration of the center of mass of link i

$a_{e,i}$ = the acceleration of the end of link i

ω_i = the angular velocity of frame i w.r.t frame 0 i

α_i = the angular acceleration of frame i w.r.t frame 0 i

f_i = the force exerted by the link $i-1$ on link i

τ_i = the torque exerted by the link $i-1$ on link i

R^i_{i+1} = the rotation matrix from frame $i+1$ to frame i

m_i = the mass of link i

I_i = the inertia matrix of link i about a frame parallel to frame i whose origin is at the center of mass of link i

$r_{i,ci}$ = the vector from o_i to the center of mass of link i

$r_{i+1,ci}$ = the vector from o_{i+1} to the center of mass of link i

$r_{i,i+1}$ = the vector from o_i to o_{i+1}

1. Start with the initial conditions

$$\omega_0 = 0 \ , \ \alpha_0 = 0 \ , \ a_{c,0} = 0 \ , \ a_{e,0} = 0 \tag{5.2}$$

and solve the following equations in order to compute link velocities, link accelerations with respect to the base frame.

$$\omega_i = (R_i^{i-1})^T \omega_{i-1} + b_i \dot{q}_i \tag{5.3}$$

where

$$b_i = (R_i^0)^T \begin{bmatrix} 0 & 0 & 1 \end{bmatrix}^T \tag{5.4}$$

$$\alpha_i = (R_i^{i-1})^T \alpha_{i-1} + b_i \ddot{q}_i + \omega_i \times b_i \dot{q}_i \tag{5.5}$$

Solving recursively will give us the angular velocities and accelerations of all links.

2. Start with the terminal conditions:

$$f_{n+1} = 0, \tau_{n+1} = 0 \tag{5.6}$$

and solve the following equations to get the joint forces and torques.

$$f_i = R^i_{i+1} f_{i+1} + m_i a_{c,i} \tag{5.7}$$

$$\tau_i = R^i_{i+1} \tau_{i+1} - f_i \times r_{i,ci} + (R^i_{i+1} f_{i+1}) \times r_{i+1,ci} + I_i \alpha_i + \omega_i \times (I_i \omega_i) \tag{5.8}$$

5.1 Prototype 1

In our first attempt, we chose the arm links to have the following lengths: $a_1 = 400$ mm, $a_2 = 450$ mm, $a_3 = 100$ mm. Based on these basic lengths we designed the links, brackets and bearings, and other components.

5.1.1 Components and Design

The motor is held in a bracket and another bracket holds the magnets on to which the plate will be held. This motor bracket is bolted to a solid block of M.S., which in turn is bolted to the Tee sections that make up the majority of the link. The other links are also designed in the same way: a bracket to hold the motor, a solid block to which the bracket is attached and which in turn is bolted to the Tee section. This design (Fig 5.2) was done by separately considering the components under the action of various forces and analyzing it using the software COSMOS EXPRESS.

5.1.2 Design Analysis

We first perform the motion analysis in order to allow for the actuator selection. We start by first setting up the mathematical model of the robot arm, using the DH convention [10]. The link length (a_i), link twist (α_i), link offset (d_i) and joint angle (θ_i) for each link are as follows:

Link 1

The basic lengths of the link, needed to define the mathematical model are:

$$a_1 = 0.400; \alpha_1 = 0; d_1 = 0; \theta_1 = 0 \tag{5.9}$$

The mass properties and interia properties are as described below:

Mass = 3.87331 kilograms

Volume = 0.00048 meters^3

Center of mass: (meters)

X = 0.17899

Y = 0.00000

Z = -0.00032

Principal axes of inertia and principal moments of inertia: (kilograms$\times$ meters^2) Taken at the center of mass:

Ix = (1.00000, 0.00000, 0.00304) Px = 0.00395

Iy = (-0.00304, 0.00000, 1.00000) Py = 0.05309

Iz = (0.00000, -1.00000, 0.00000) Pz = 0.05560

Moments of inertia: (kilograms$\times$ meters^2)

Taken at the center of mass and aligned with the output coordinate system.

Lxx = 0.00395 Lxy = 0.00000 Lxz = 0.00015

Lyx = 0.00000 Lyy = 0.05560 Lyz = 0.00000

Lzx = 0.00015 Lzy = 0.00000 Lzz = 0.05309

Link 2

The basic lengths of the link, needed to define the mathematical model are:

$$a_2 = 0.450; \alpha_2 = 0; d_2 = 0; \theta_2 = 0 \tag{5.10}$$

The mass properties and interia properties are as described below:

Mass = 1.45837 kilograms

Volume = 0.00018 cubic meters

Center of mass: (meters)

X = 0.22271

Y = 0.00390

Z = 0.00000

Principal axes of inertia and principal moments of inertia: (kilograms× meters^2)

Taken at the center of mass.

Ix = (-0.99999, -0.00516, 0.00000)	Px = 0.00159
Iy = (0.00516, -0.99999, 0.00000)	Py = 0.02737
Iz = (0.00000, 0.00000, 1.00000)	Pz = 0.02879

Moments of inertia: (kilograms× meters^2)

Taken at the center of mass and aligned with the output coordinate system.

Lxx = 0.00160	Lxy = 0.00013	Lxz = 0.00000
Lyx = 0.00013	Lyy = 0.02737	Lyz = 0.00000
Lzx = 0.00000	Lzy = 0.00000	Lzz = 0.02879

Link 3

The basic lengths of the link, needed to define the mathematical model are:

$$a_3 = 0; \alpha_3 = 0; d_3 = -0.080; \theta_3 = 0 \tag{5.11}$$

The mass properties and interia properties are as described below:

Center of mass: (meters)

X = 0.00

Y = 0.00

Z = -0.07

Moments of inertia: (kilograms$\times$ meters^2)

Taken at the center of mass and aligned with the output coordinate system.

Lxx = 0.03535	Lxy = 0.00000	Lxz = 0.00058
Lyx = 0.00000	Lyy = 0.03592	Lyz = 0.00000
Lzx = 0.00058	Lzy = 0.00000	Lzz = 0.06893

Note that the inertia matrix for the link 3 was calculated considering the metal sheet to be lifted as also a part of the link. It is assumed that the sheet centre coincides with the shaft axis of the third motor, which actuates the link 3.

Trajectory Planning and Dynamic Analysis

Based on the link properties, Eq. 5.9, Eq. 5.10 and Eq. 5.11, we can formulate the transformation matrices needed for the inverse kinematics calculations. The transformation matrix $\mathbf{A_{i-1,i}}$ is given by

$$\mathbf{A_{i-1,i}} = \begin{bmatrix} \cos\theta_i & -\sin\theta_i\cos\alpha_i & \sin\theta_i\sin\alpha_i & a_i\cos\theta_i \\ \sin\theta_i & \cos\theta_i\cos\alpha_i & -\cos\theta_i\sin\alpha_i & a_i\sin\theta_i \\ 0 & \sin\alpha_i & \cos\alpha_i & d_i \\ 0 & 0 & 0 & 1 \end{bmatrix} \tag{5.12}$$

The total transformation matrix $\mathbf{T}$ is given by

$$\mathbf{T} = \mathbf{A}_{0,1} \times \mathbf{A}_{1,2} \times \mathbf{A}_{2,3} \tag{5.13}$$

For the given links, the total transformation matrix becomes

$$\mathbf{T} = \begin{bmatrix} \cos(\theta_{1,2,3}) & -\sin(\theta_{1,2,3}) & 0 & 450\cos(\theta_{1,2}) + 400\cos\theta_1 \\ \sin(\theta_{1,2,3}) & \cos(\theta_{1,2,3}) & 0 & 450\sin(\theta_{1,2}) + 400\sin\theta_1 \\ 0 & 0 & 1 & -80 \\ 0 & 0 & 0 & 1 \end{bmatrix} \tag{5.14}$$

$$\text{where} \qquad \theta_{1,2,3} = \theta_1 + \theta_2 + \theta_3 \qquad \& \qquad \theta_{1,2} = \theta_1 + \theta_2$$

Now considering the link lengths, the press bed size and the location at which the arm base will be fixed, we set the following extremities of motion:

$$\begin{aligned} P_1 &= \begin{bmatrix} 700 & 0 & -80 \end{bmatrix} \\ P_3 &= \begin{bmatrix} 350 & 500 & -80 \end{bmatrix} \end{aligned} \tag{5.15}$$

Thus, $P_2 = [350 \quad 0 \quad -80]$, since motion is initially along X axis and then along Y axis. Setting these conditions, evaluating the trajectory polynomial and using this information to get end effector position matrix at each point of time allows us to perform the inverse kinematics at each point and get the variation of joint angles as shown in Fig. 5.3. Using the method of forward differences, we also plot the velocity (Fig. 5.4) and acceleration curves (Fig. 5.5) for the joint angles.

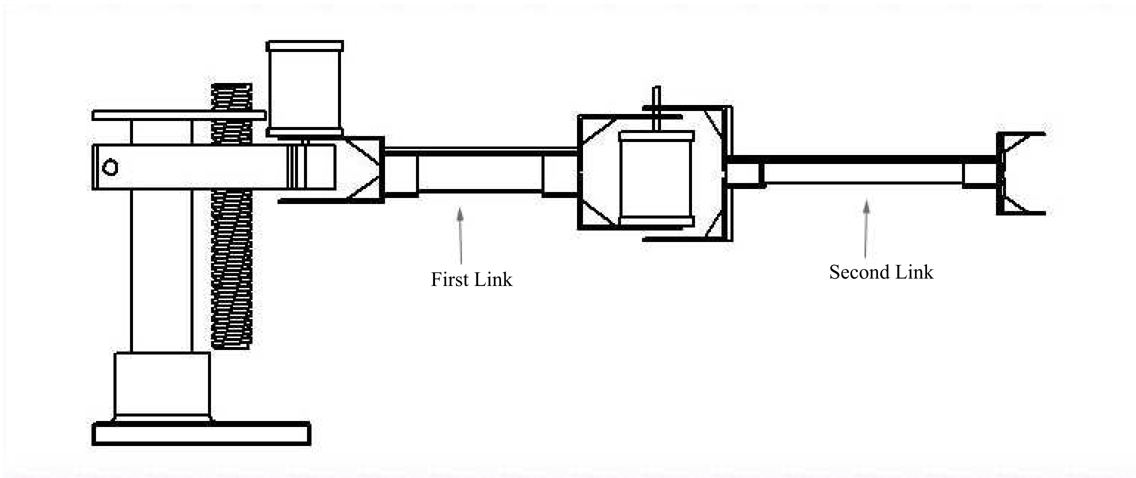

Figure 5.2: Transferring arm, first design

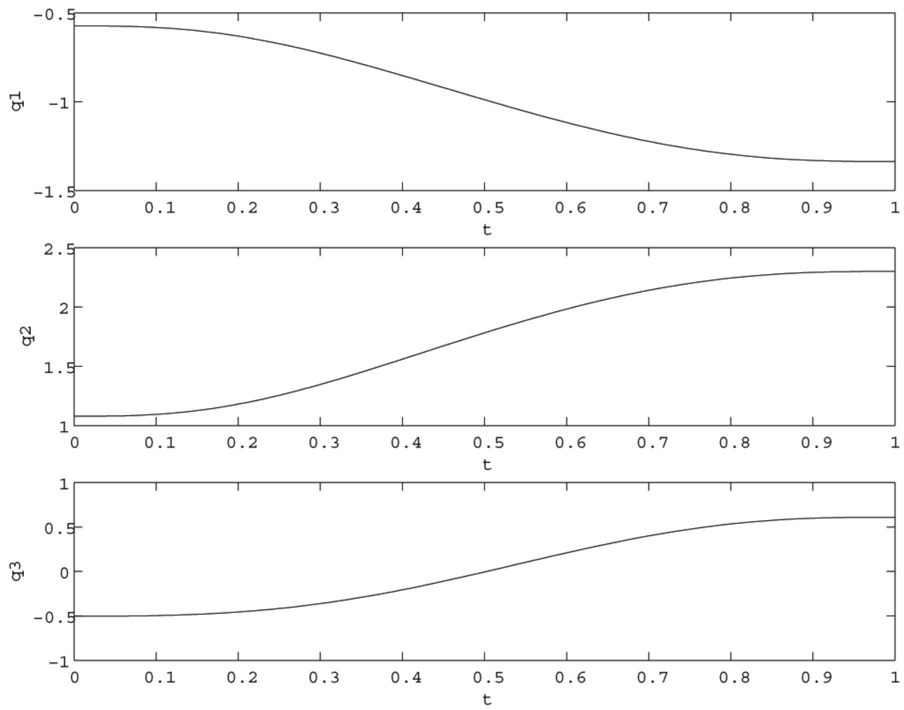

Figure 5.3: Joint displacements, for end effector motion from P_1 to P_2

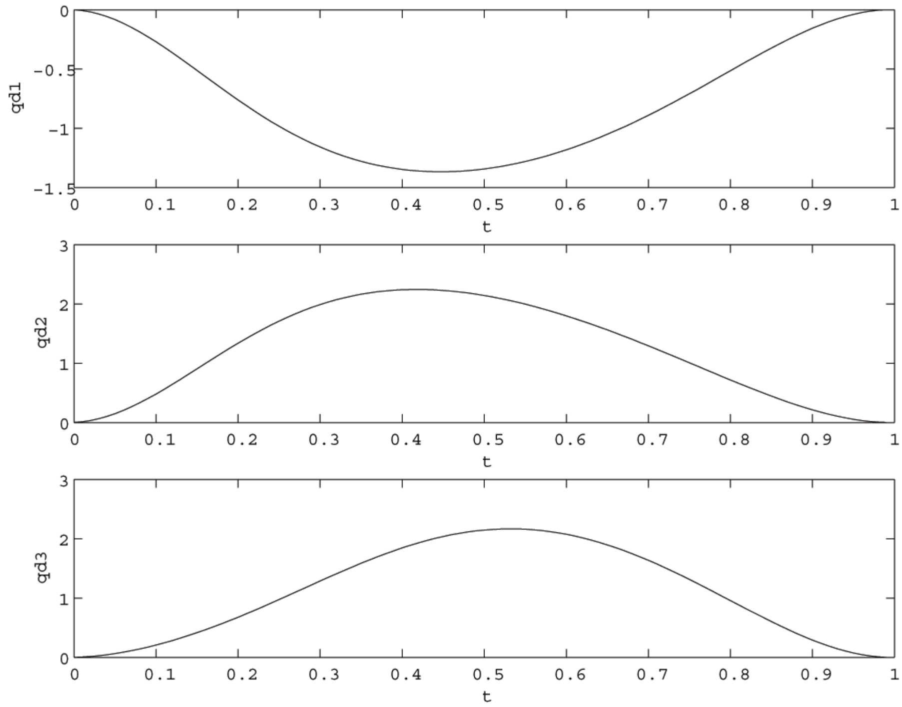

Figure 5.4: Joint Velocities

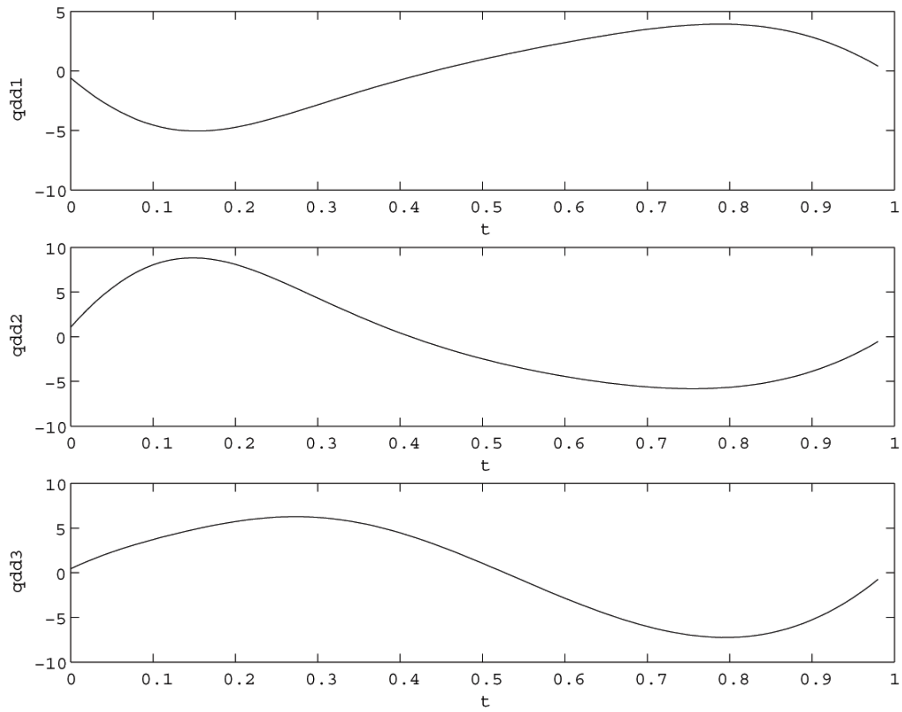

Figure 5.5: Joint Accelerations

For the dynamic analysis, using the inertia matrices and mass properties of links as descibed in the earlier sections we solve the Equations 5.3, 5.5, 5.7 and 5.8.

Design discussion

The design described here is technically fit for use. However, it presents many practical difficulties in its implementation. The brackets, which hold the motors, though safe in the static force aspect, may not sustain the effects of frequent loading and unloading cycles. These load cycles occur when the links accelerate and decelerate. Also, one other factor in the design of this bracket is the difficulty in assembly. The bracket must permit easy assembly and disassembly of bearings, motor and bushings needed to connect shaft to links. This becomes quite difficult in the current design.
The other factor that comes into play is the deflection. The links (Tee sections) were designed considering the stress criteria. However, these links will suffer from deflections which may hamper the accuracy of the arm. As a result, the links must be re-designed keeping the deflection criterion in mind. While most of the components designed in the above attempt are sufficient, it would be appropriate to redesign them. The detailed designs and link properties that overcome the major problems of this first attempt are described in the following section.

5.2 Prototype 2

In our second attempt (Fig 5.6), we chose the arm links to have the following lengths: $a_1 = 370$ mm, $a_2 = 434$ mm, $a_3 = 50$ mm & $d_3 = 65$. These length modifications are made in order to incorporate the necessary changes for

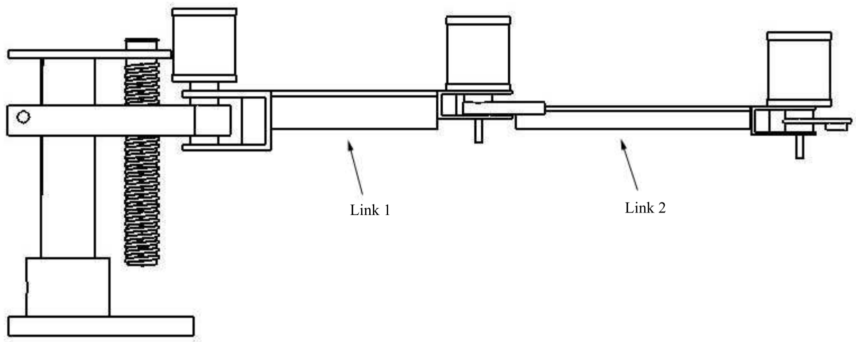

Figure 5.6: Transferring arm, final design

Components	**Specifications**
Actuator	3 DC Stepper Motors (one for each link) 14Kg-cm; 20Kg-cm; 40Kg-cm
Transmission Drive	1 Spur Gears Box (1:4) Lead Screw (Trapizoidal Thread; M40; P=7mm)
End Effector	2 Electromagnets (ϕ40 $\times$ 20mm) with P=5Kg. each
Configuration	Planar with 3 joints
Degree of Freedom	3 D.o.f.
Links	T sections (6$\times$50$\times$225mm) & (4$\times$30$\times$325mm)
Main Frame	Calibrated for fine adjustment for height
Sensing Elements	Proximity Sensors at each link for alignment
Controller	Atmel Microcontroller
Speed	3 to 4 seconds per cycle

Table 5.1: Transferring Arm - Specifications

creating a structurally safe robot arm.

The major changes in design were in the link lengths, the positioning of the motors and the bracket design. The end effector was also modified in order to achieve easy adjustments for the electromagnets. The various parts were checked for safety against bending loads, and the deformations were also calculated, as enlisted in the following sections.

5.2.1 Components and Design

Tee Sections

The Tee sections in both the links are acted upon by cantilever loads. Thus, we design both links against bending and check them for their deflections. For the Tee in the first link, the resultant load is equivalent to a mass of 10 kg acting in the downward direction.

Tee - Link 1

Principal moment of Inertia of the Tee section at centroid of the area:
I_x = 62277 mm^4
I_y = 131098 mm^4

The deflection at the end for a beam is given by

$$\delta = \frac{Pl^3}{3EI_y} \tag{5.16}$$

As length of the beam l = 240 mm, Young's modulus for steel E = 210 GPa and the load P = 100 N, we get
$\delta = 0.02$ mm

Tee - Link 2

Principal moments of inertiaof the Tee section at centroid of the area:

I_x = 8596.76 mm^4

I_y = 18524.60 mm^4

The length of this tee l = 320 mm, and the load acting P = 60 N. Thus, we get

$\delta = 0.15$ mm

Brackets

The brackets on which the motors are mounted are under a load of approximately 160 N and a bending moment of 160 Nm. The design for the bracket was checked by performing its strength analysis on Ansys. The meshing was auto-generated, as shown in Fig. 5.7.

We apply the boundary conditions that are encountered in the system, with the force and bending moments due to the cantilever action of the Tee links, the motors and the plate acting on the weld, and the constraints due to bearings. These are shown in Fig 5.8.

The displacement and stress results for this loading are given in Table 5.2 and Table 5.3. The solution is graphically shown in Fig. 5.9

5.2.2 Design Analysis

Link 1

The basic lengths of the link, needed to define the mathematical model are:

$$a_1 = 0.370; \alpha_1 = 0; d_1 = -0.016; \theta_1 = 0 \tag{5.17}$$

The mass properties and interia properties are as described below:

Mass = 5.455139 kilograms

Volume = 0.000910 $meters^3$

Center of mass: (meters)

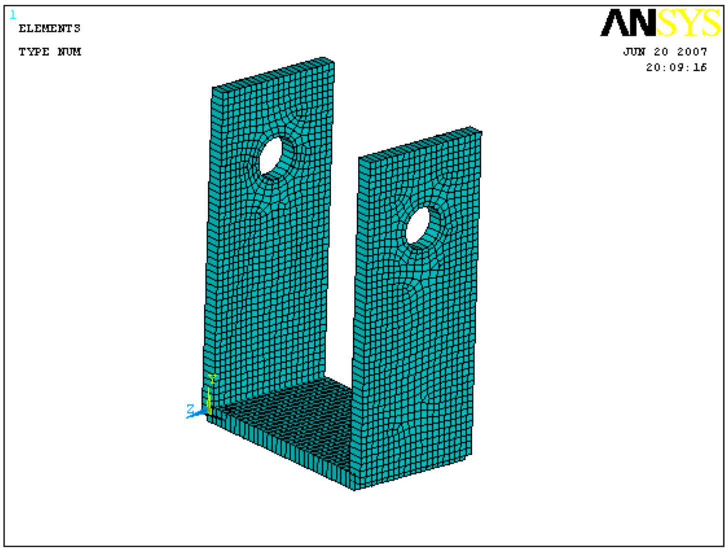

Figure 5.7: Meshing for Bracket

	X	**Y**	**Z**	**Vector Sum**
Maximum	0.08924	0.01009	6.94e-005	0.08924

Table 5.2: Maximum nodal displacement, in mm

	Stress Intensity	**Equivalent Stress**
Minimum	0	0
Maximum	35.03	30.77

Table 5.3: Stress Intensity & Equivalent Stress

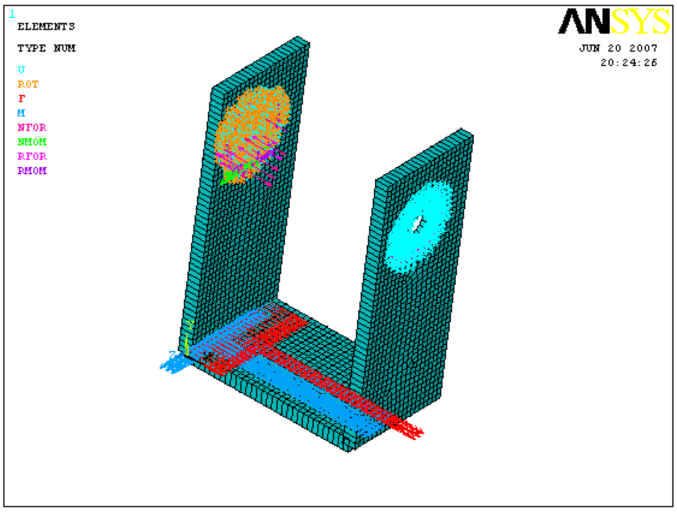

Figure 5.8: Boundary conditions for bracket analysis

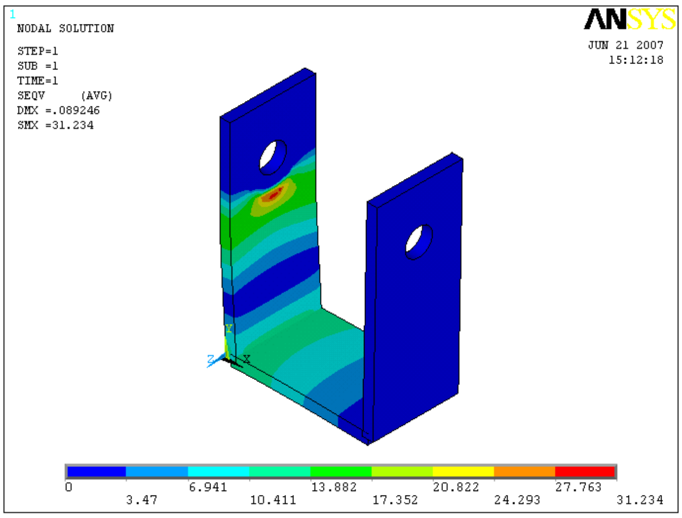

Figure 5.9: Stress Distribution in Bracket

X = 0.280974

Y = 0.000000

Z = 0.009909

Principal axes of inertia and principal moments of inertia: (kilograms× meters^2) Taken at the center of mass.

Ix = (0.973025, 0.000000, 0.230698) Px = 0.009578

Iy = (0.230698, 0.000000, -0.973025) Py = 0.100102 Moments of inertia: (kilograms× meters^2)

Iz = (0.000000, 1.000000, 0.000000) Pz = 0.105610

Taken at the center of mass and aligned with the output coordinate system.

Lxx = 0.014396 Lxy = 0.000000 Lxz = 0.020321

Lyx = 0.000000 Lyy = 0.105610 Lyz = 0.000000

Lzx = 0.020321 Lzy = 0.000000 Lzz = 0.095285

Link 2

The basic lengths of the link, needed to define the mathematical model are:

$$a_2 = 0.435; \alpha_2 = 0; d_2 = -.022; \theta_2 = 0 \tag{5.18}$$

The mass properties and interia properties are as described below:

Mass = 4.04526 kilograms

Volume = 0.00073 meters^3

Center of mass: (meters)

X = 0.36410

Y = -0.00048

Z = 0.02181

Principal axes of inertia and principal moments of inertia: (kilograms× meters^2)

Taken at the center of mass.
Ix = (-0.99086, -0.00893, -0.13462) Px = 0.00667

Iy = (0.13456, 0.00784, -0.99088) Py = 0.07524

Iz = (0.00990, -0.99993, -0.00657) Pz = 0.07874
Moments of inertia: (kilograms$\times$ meters^2)

Taken at the center of mass and aligned with the output coordinate system.

Lxx = 0.00792	Lxy = 0.00064	Lxz = 0.00915
Lyx = 0.00064	Lyy = 0.07873	Lyz = 0.00006
Lzx = 0.00915	Lzy = 0.00006	Lzz = 0.07400

Link 3

The basic lengths of the link, needed to define the mathematical model are:

$$a_3 = 0.0625; \alpha_3 = 0; d_3 = -0.0650; \theta_3 = 0 \tag{5.19}$$

The mass properties and interia properties are as described below:

Mass = 2.94654 kilograms

Volume = 0.00037 meters^3

Center of mass: (meters)

X = -0.01409

Y = -0.04553

Z = -0.00358
Principal axes of inertia and principal moments of inertia: (kilograms$\times$ meters^2)

Taken at the center of mass.
Ix = (0.99986, -0.01665, 0.00000) Px = 0.03559

Iy = (0.00000, 0.00000, -1.00000) Py = 0.03578

Iz = (0.01665, 0.99986, 0.00000) Pz = 0.06899
Moments of inertia: (kilograms$\times$ meters^2)

Description	Value
Start point of motion P_1	[700 0 -103] (in mm)
Intermediate point P_2	[350 0 -103] (in mm)
End point of motion P_3	[350 500 -103] (in mm)
Time to reach P_2	1 sec
Time to reach P_3	2 sec

Table 5.4: Design Constraints for motion

Taken at the center of mass and aligned with the output coordinate system.

Lxx = 0.03560	Lxy = -0.00056	Lxz = 0.00000
Lyx = -0.00056	Lyy = 0.06898	Lyz = 0.00000
Lzx = 0.00000	Lzy = 0.00000	Lzz = 0.03578

Dynamic Analysis

Using similar assumptions as in Sec. 5.1.2 and applying the same analysis, the results obtained regarding displacement, speed, acceleration and torque characteristics are as shown in Fig 5.10, Fig. 5.11, Fig. 5.12 and Fig 5.13. The list of assumptions is given in Table 5.4

Accordingly, stepper motors chosen are: a 4.0 Nm motor for joint 1, a 2 Nm motor coupled to a 1:4 speed reduction gearbox for joint 2 and a 1.4 Nm motor for joint 3.

Matlab Programs

The section enlists the Matlab Programs written to perform the trajectory planning and dynamic analysis described in the above sections.

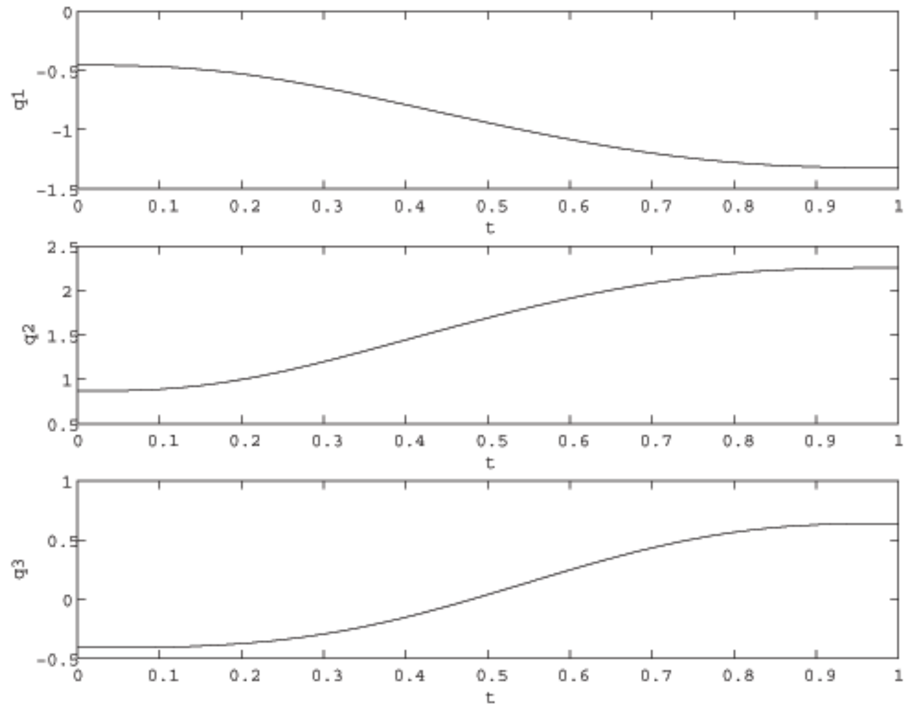

Figure 5.10: Joint displacements, for end effector motion from P_1 to P_2

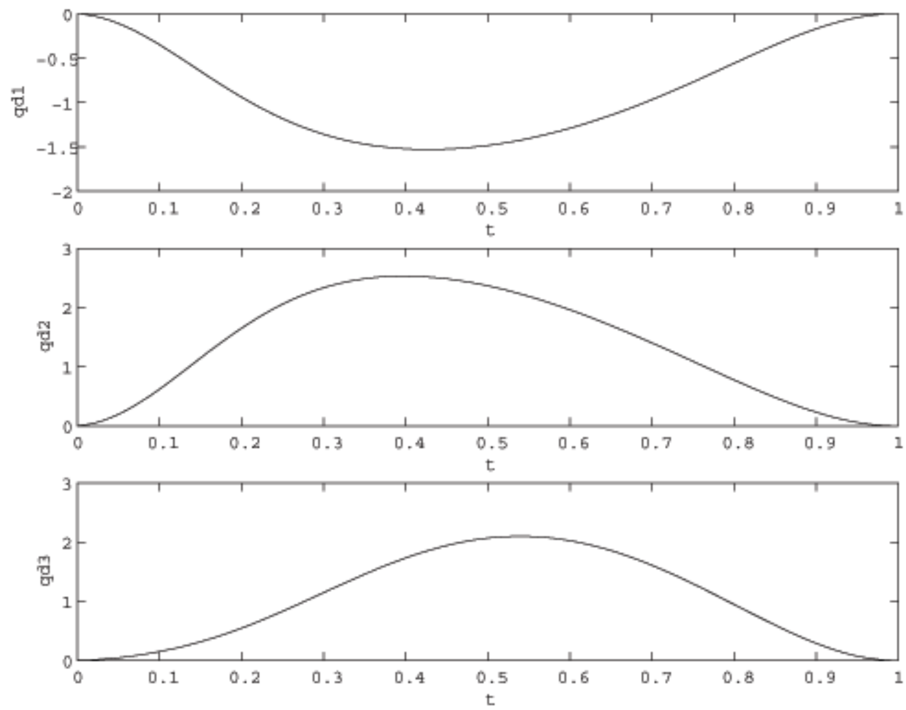

Figure 5.11: Joint Velocities

Program one.m (to calculate the joint displacements)

```
a1 = 370;
L1 = link([0 a1 0 -16 0]);
a2 = 434;
L2 = link([0 a2 0 -22 0]);
d3 = 65;
a3 = 50;
L3 = link([0 a3 0 -d3 0]);

r = robot({L1, L2, L3});
ox1 = 750;
oy1 = 10; ;
oz1 = -(16+22+65);;
o1 = [ox1 oy1 oz1]'
phi1 = 0;
R1 = rotz(phi1);
T0 = transl(o1);
T1 = T0*R1;
ox2 = 350;
oy2 = 10;
oz2 = oz1;

o2 = [ox2 oy2 oz2]'
phi2 = pi/2;

R2 = rotz(phi2);
T2 = transl(o2)*R2;
```

```
step = input('enter number of steps to calculate');
accu = 1/step;
t =[0:accu:1];
r1=jtraj(0, 1, t);
Tc1=ctraj(T1,T2,r1);

q = [0 0 0];

for i = 1:1:(step+1)
    T = [Tc1(1,1,i) Tc1(1,2,i) Tc1(1,3,i) Tc1(1,4,i);
        Tc1(2,1,i) Tc1(2,2,i) Tc1(2,3,i) Tc1(2,4,i);
        Tc1(3,1,i) Tc1(3,2,i) Tc1(3,3,i) Tc1(3,4,i);
        Tc1(4,1,i) Tc1(4,2,i) Tc1(4,3,i) Tc1(4,4,i)];

    phi = acos( T(1,1)/(T(1,1)^2 + T(1,2)^2));
    b1 = T(1,4) - 20*cos(phi);
    b2 = T(2,4) - 20*sin(phi);
    C = [b1; b2; 0];
    c = norm(C);
    chat = C/c;
    E = ((a1^2 - a2^2 + c^2)/(2*c));
    B1 = E*chat +sqrt(a1^2- E^2)*cross(chat, [0 0 1]');
    B2 = C - B1;
    theta1 = atan(B1(2)/B1(1));
    theta12 = atan(B2(2)/B2(1));
    theta2 = theta12-theta1;
    theta3 = phi - theta12;
```

```
    q = [q; theta1 theta2 theta3];

end
q(1,:) = [];
```

Program differences.m (to create the difference matrices necessary for velocity and acceleration calculations)

```
points= step+1;
op=eye(points,(points-1));
op1=eye(points,points);
op=[zeros(points,1) op];

traveltime = input('Enter time for intended motion');

op=(op1-op)/(-(traveltime/step));
opp=eye((points-1),(points-2));
opp1=eye((points-1),(points-1));
opp=[zeros((points-1),1) opp];
opp=(opp1-opp)/(-(traveltime/step));
```

Program getcurves.m (to get the plots for displacement, velocity and acceleration)

```
q1=q*[1 0 0 ]';
q2=q*[0 1 0 ]';
q3=q*[0 0 1 ]';
steptime = traveltime/step;
time1=[0:steptime:traveltime]';
time2=[0:steptime:traveltime]';
time3=[0:steptime:traveltime]';
```

```
qd1 = (op*q1)'; qd2 = (op*q2)'; qd3 = (op*q3)';
qd1(points)=[];  qd2(points)=[]; qd3(points)=[];
time2(points)=[];
qd1=qd1'; qd2=qd2'; qd3=qd3';
qdd1 = (opp*qd1)'; qdd2 = (opp*qd2)'; qdd3 = (opp*qd3)';
qdd1((points-1))=[]; qdd2((points-1))=[];
qdd3((points-1))=[]; time3(points)=[];time3((points-1))=[];
qdd1=qdd1';
qdd2=qdd2';
qdd3=qdd3';
figure
subplot(3,3,1);  plot(time1,q1)
xlabel('t')
ylabel('q1')
subplot(3,3,2); plot(time1,q2)
xlabel('t')
ylabel('q2')
subplot(3,3,3); plot(time1,q3)
xlabel('t')
ylabel('q3')
subplot(3,3,4); plot(time2,qd1)
xlabel('t')
ylabel('qd1')
subplot(3,3,5); plot(time2,qd2)
xlabel('t')
ylabel('qd2')
subplot(3,3,6); plot(time2,qd3)
xlabel('t')
```

```
ylabel('qd3')
subplot(3,3,7); plot(time3,qdd1)
xlabel('t')
ylabel('qdd1')
subplot(3,3,8); plot(time3,qdd2)
xlabel('t')
ylabel('qdd2')
subplot(3,3,9); plot(time3,qdd3)
xlabel('t')
ylabel('qdd3')
```

Program: dynamics.m (to calculate the motor torques)

```
tau = [0 0 0 0];
for i = 1:1:(step-1)
th1 = q1(i);
th2 = q2(i);
th3 = q3(i);
th4 = q4(i);
dq1 = qd1(i);
ddq1 = qdd1(i);
dq2 = qd2(i);
ddq2 = qdd2(i);
dq3 = qd3(i);
ddq3 = qdd3(i);
dq4 = qd4(i);
ddq4 = qdd4(i);
Rot10 = [cos(th1)   sin(-th1)    0;
        sin(th1)    cos(th1)     0;
         0             0        1];
```

```
Rot21 = [cos(th2)   sin(-th2)    0;
        sin(th2)    cos(th2)     0;
          0              0       1];
Rot32 = [cos(th3)   sin(-th3)     0;
        sin(th3)    cos(th3)      0;
          0              0        1];

w1 = (Rot10'*[0 0 1]')*dq1;
alpha1 = (Rot10'*[0 0 1]')*ddq1 + cross(w1,((Rot10'*[0 0 1]')*dq1));
com1 = (1/1000)*[280.67 0.00 10.0]';
end1 = (1/1000)*[a1 0.00 -16.00]';
lc1 = com1(1);
ac1 = Rot10'*[0 0 0]' + cross(alpha1,com1) +
         cross(w1,cross(w1,com1));
ae1 = Rot10'*[0 0 0]' + cross(alpha1,end1) +
          cross(w1,cross(w1,end1));
w2 = [0 0 dq1+dq2]';
alpha2 = [0 0 (ddq1+ddq2)]';
com2 = (1/1000)*[364.61 -0.49 21.86]';
end2 = (1/1000)*[434 0 -22]';
ac2 = Rot21'*ae1 + cross(alpha2,com2) +
         cross(w2, (cross(w2,com2)));
ae2 = Rot21'*ae1 + cross(alpha2,end2) +
         cross(w2, (cross(w2,end2)));
w3 = [0 0 dq1+dq2+dq3]';
alpha3 = [0 0 ddq1+ddq2+ddq3]';
com3 = (1/1000)*[-14.1 -45.5 -03.5]';
ac3 = Rot32'*ae2 + cross(alpha3,com3) +
```

```
         cross(w3, (cross(w3,com3)));
ae3 = Rot32'*ae2 + cross(alpha3,end3) +
          cross(w3, (cross(w3,end3)));

I1 = [0.014396           0              0.020321;
         0              0.10561         0;
      0.020321           0              0.095285];
I2 = [0.00792       0.00064      0.00915;
      0.00064        0.07873      0.00006;
      0.00915        0.00006      0.07400];
I3 = [0.03560       -0.00056         0;
      0.00056        0.06898         0;
      0                  0          0.03578];

f4 = 0;
tau4 = 0;
f3 = 2.9*ac3;
tau3 = -cross(f3,com3)+ I3*alpha3+cross(w3,(I3*w3));
f2 = Rot32*f3+4.4*ac2;
tau2 = Rot32*tau3-cross(f2,com2)+cross((Rot32*f3),(com2-end2))+
           I2*alpha2+cross(w2,(I2*w2));
f1 = Rot21*f2+5.36*ac1;
tau1 = Rot21*tau2-cross(f1,com1)+cross((Rot21*f2),com1-end1)+
          I1*alpha1+cross(w1,(I1*w1));
t1 = (tau1'*tau1)^(0.5);
t2 = (tau2'*tau2)^(0.5);
t3 = (tau3'*tau3)^(0.5);
t4 = (tau4'*tau4)^(0.5);
```

```
tau =[tau; t1 t2 t3 t4];
end

torque1 = tau*[1 0 0 0]';
torque2 = tau*[0 1 0 0]';
torque3 = tau*[0 0 1 0]';

[size1 size2]=size(t);
if size2==(step+1)
    t(size2)=[];
end
figure
subplot(3,1,1);
plot(t,torque1)
hold on
plot(t,-qd1,'--r')
hold off
legend('Torque','Joint Velocity');
title('Joint 1')
subplot(3,1,2);
plot(t,torque2)
hold on
plot(t,qd2,'--r')
hold off
legend('Torque','Joint Velocity');
title('Joint 2')
subplot(3,1,3);
plot(t,torque3)
```

```
hold on
plot(t,qd3,'--r')
hold off
legend('Torque','Joint Velocity');
title('Joint 3')
```

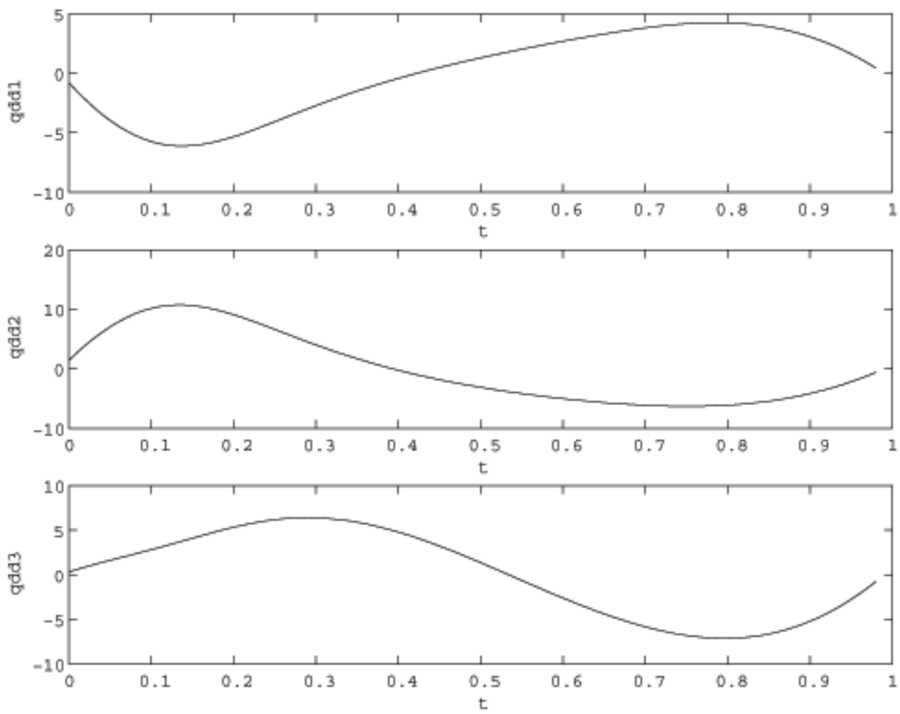

Figure 5.12: Joint Accelerations

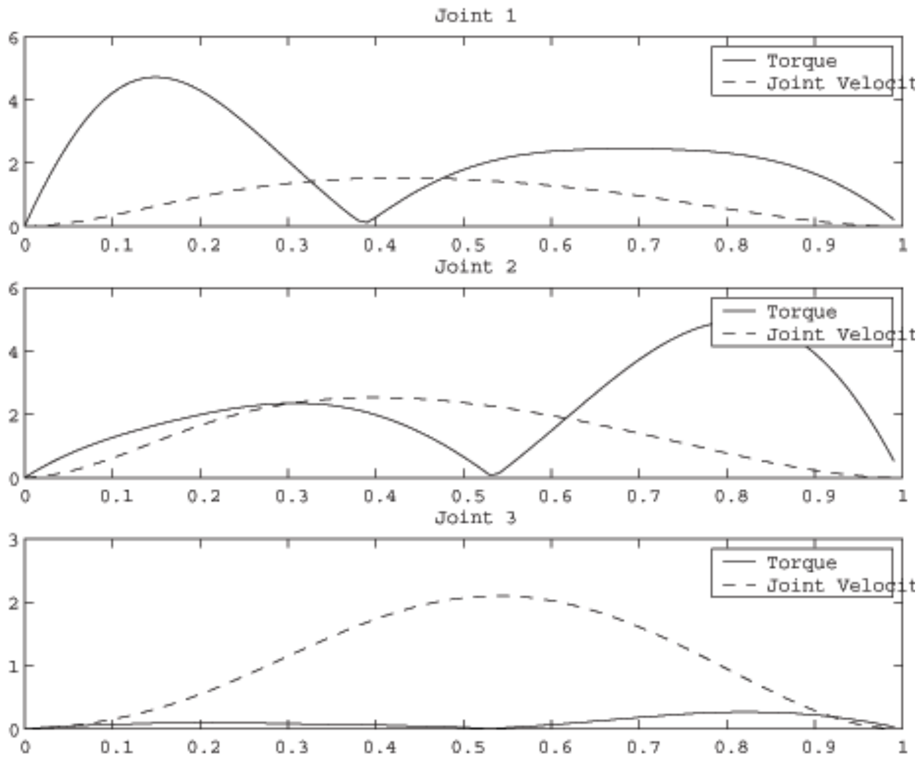

Figure 5.13: Joint Torques & Velocity

Chapter 6

Third Arm

6.1 Initial Proposals

For unloading, having the same assembly as that used for loading was not required because there was a need for neither precise pick up nor precise placement of the job after removal. The only need was of lifting the job by maximum 10mm out of the locating pins and placing it outside the press bed area. In order to achieve a mechanism with minimum number of linkages, a number of ideas were proposed.

The position of the finished job is always the die center. Also, the final location of the job is also fixed ie. outside the press bed area. As a result, the path endpoints of the third arm are fairly fixed. Hence, we proposed using a four-bar mechanism that would follow a set path repetitively. An analysis for this was done using Coupler-Curve synthesis [9] and a mechanism was synthesised. However, the link lengths needed for the intended motion were quite large and bulky. It was also proposed that we use a scaled down mechanism in conjuction with a pantograph, which would suitable amplify the motions and give the same end results with smaller links. However, the number of links in this mechanism was quite large, increasing the chances of failure and also increasing the overall complexity of the mechanism. This proposal also made it difficult to factor in small variations in path arising due to variations in the job shapes that might be encountered.

The simplest solution proposed was of using a angular rocker link controlled by a motor. When the motor would rotate the rocker into the die area, the link holding the gripper would move down and lift the plate by about 3 to 5mm. However, this was not sufficient for precisely the same conditions that the transferring arm had encountered. The presence of guide posts makes it impossible to have rotary motion without interference. This arm would then need to be fitted with another motor, thus making it similar to the transferring arm. As a result, this mechanism too, was rejected.

6.2 Final Mechanism

The final mechanism selected for the unloading arm uses two actuators: a pneumatic double acting cylinder and a permanent magnet DC motor. The electromagnetic end-effector is mounted onto a vertical rack. The rack & pinion arrangement is driven by the DC motor. This DC motor is attached on an arm which moves horizontally into and out of the bed. This actuation is provided by the cylinder. Thus, the assembly has 2 degrees of freedom: horizontal linear motion (to pull the finished product out of the bed area) and vertical linear motion (to vertically lift the product out of the locating pins).

The motion of the rack is limited by proximity switches which sense the position of the job. The pneumatic cylinder is actuated by a 5/2 solenoid DC valve. The synchronization of the motions is achieved by means of magnetic proximity sensors which are directly mounted on the cylinder body. These two sensors, one mounted on each end, sense the completion of stroke and send a signal to the DC motor and electromagnets attached on the end-effector. The start of this entire operation occurs when the ram of the press has completed its upward vertical stroke. The pneumatic circuit for this arm is shown in Fig 6.2

6.3 Components Design and Actuator Selection

Using data from the manufacturer's catalogues [4], we selected the following components for the third arm.

Pneumatic Cylinder - DSNU-16-200-PPV-A - Q

The DSNU standard modular system (Fig 6.3) is an expansion of existing standard cylinders DSN/ESN and DSNU/ESNU. The expansion is 2-dimensional:

- Additional sizes including 32, 40, 50 and 63 mm diameters
- Modular system expansion with 3 additional cap types and innumerable additional variants
- The existing ESNU/DSNU represents the basic cylinder to which the variant characteristics are added. Basic cylinder types ESNU/DSNU with 8 to 25 mm diameters are in compliance with ISO 6432. Diameters 32 to 63 mm, the cap variants and additional variants are closely comparable to standard cylinders which correspond with the engineering design of the basic cylinder.

Variants and functions:

Components	**Specifications**
Actuators	Permanent Magnet DC Motor 10rpm; 6Kg-cm Pneumatic Double Acting Cylinder (with end cap sensors)
Transmission Drive	Angular Rocker Link
End Effector	2 Electormagnets ($\phi 50 \times 20$mm)
Degree of Freedom	2 D.o.f.
Mounting	Adjustable table mounted
Sensing Elements	2 Proximity Sensors

Table 6.1: Third arm specifications - initial proposal

Components	**Specifications**
Actuators	Permanent Magnet DC Motor 5rpm; 20Kg-cm Pneumatic Double Acting Cylinder (with end cap sensors)
Transmission Drive	Rack and Pinion (m=1; z_g = 11)
End Effector	2 Electormagnets ($\phi 50 \times 20$mm)
Degree of Freedom	2 D.o.f.
Mounting	Adjustable table mounted
Sensing Elements	2 Proximity Sensors

Table 6.2: Third Arm - Final Design Specifications

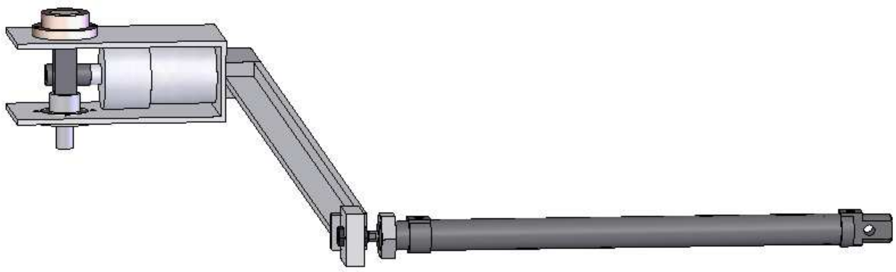

Figure 6.1: Unloading Arm

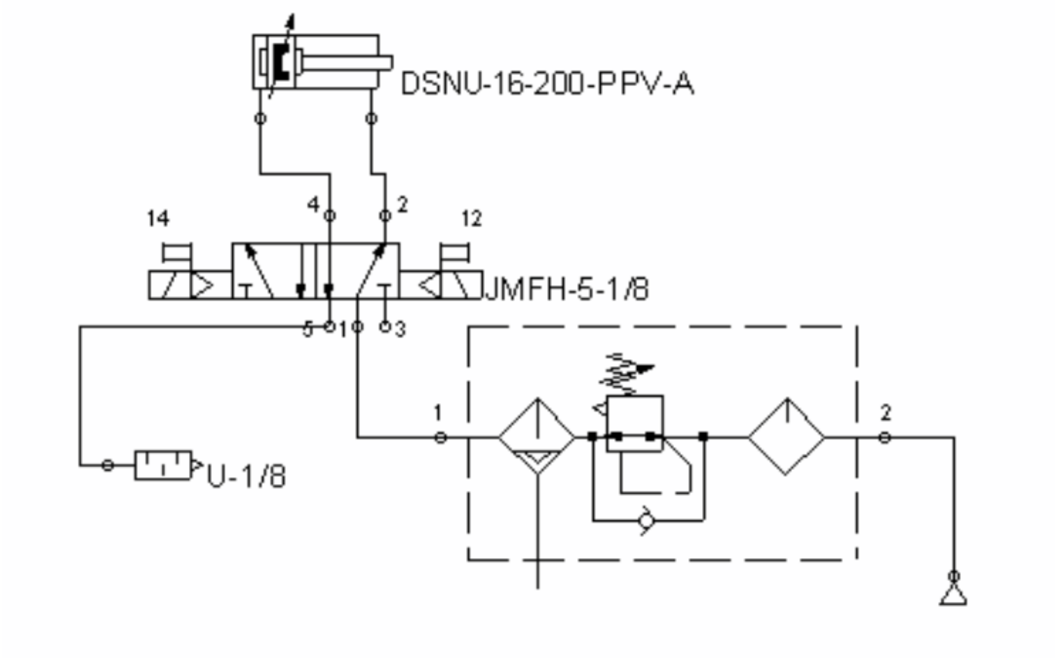

Figure 6.2: Pneumatic Circuit for Unloader

Figure 6.3: DSNU-16-200-PPV-A Standard Cylinder

- 8 to 63 mm diameters for double-acting cylinders
- 8 to 63 mm diameters for single-acting cylinders
- Double-acting P, P-A, PPV , PPV-A
- Single-acting pushing P, P-A
- Standard stroke lengths, double-acting: 10 to 500 mm, X strokes from 10 to 500 mm
- DSNU-... basic cylinder: bearing cap LD with flange thread, end cap AD with threaded pins and swivel bearing

Additional variant:

- Q square piston rod

Solenoid valve - JMFH-5-1/8

Features

- Explosion protection
- In-line valves
- Electrically and pneumatically actuated valves
- With dominating signal at 14 (JMFDH)
- Manual override tool, non-detenting (standard), can be reconfigured to detenting and blocked
- With or without auxiliary pilot air connection
- Durable poppet valve concept
- G1/8, G1/4, G1/2 and G3/4 pipe connector threads

- Optimised response times with patented U-ring and servo control
- Manifold mounting to P manifold strip or PRS manifold block for 2 to 6 valve positions with hollow bolt
- Separate pressure level for individual valves via hollow bolts with threaded connection

Solenoid coil - MSFG-12DC

Solenoid coils are fastened to the armature tube of solenoid valves. The solenoid coils are in compliance with VDE regulation 0580, insulation class F. They can be replaced without interrupting the pneumatic circuit.

Foot mounting HBN-12/16x2

Foot mounting (Fig 6.6) for standard cylinders per ISO 6432 and round cylinders. Sizes 8 to 25 per ISO 6432

- HBN-...-x1: standard
- HBN-...-x1-A: large clearances
- CRHBN-..-x1: corrosion and acid resistant

Scope of delivery: 1 foot

- HBN-...-x2: standard
- HBN-...-x2-A: large clearances
- CRHBN-...-x2: corrosion and acid resistant

Scope of delivery: 2 feet and 1 hex nut

Feature	Data/description
Nominal size	5 mm
Exhaust-air function	throttleable
Type of actuation	electrical
Sealing principle	soft
Assembly position	Any
Manual override	detenting
Design structure	Poppet seat
Type of piloting	Piloted
Flow direction	non reversible
Valve function	5/2
Operating pressure	1.5 - 8 bar
Control pressure characteristics (diagram)	Diagram
Standard nominal flow rate	600 l/min
Switching time reversal	10 ms
Operating medium	Dried compressed air, lubricated or unlubricated
Medium temperature	-10 - 60 °C
Protection class	IP65
Ambient temperature	-5 - 40 °C
Product weight	425 g
Electrical connection	Via F coil, must be ordered separately
Mounting type	Optional, with through hole, On PR manifold

Pilot exhaust port 82	M5
Pilot exhaust port 84	M5
Pneumatic connection, port 1	G1/8
Pneumatic connection, port 2	G1/8
Pneumatic connection, port 3	G1/8
Pneumatic connection, port 4	G1/8
Pneumatic connection, port 5	G1/8
Materials information for seals	NBR
Materials information, housing	Aluminium die cast, Anodised
Authorisation	UL - Recognized (OL)

Table 6.3: Solenoid Valve: Datasheet

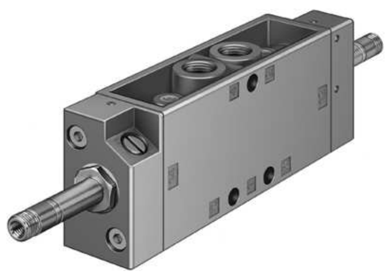

Figure 6.4: Solenoid Valve

Figure 6.5: Solenoid Coil

Feature	Data/description
Assembly position	Any
Min. pickup time	10 ms
Duty cycle	100%
Characteristic coil data	12V DC: 4.1W
Permissible voltage fluctuation	± 10 %
Medium temperature	-10 - 60 °C
Protection class	IP65
Ambient temperature	-5 - 40 °C
Product weight	65 g
Electrical connection	Plug vanes for MSSD-F; 3-pin
Mounting type	With knurled nut
Materials information, housing	PA
Materials information, plug	Steel
Material information, coil	Copper

Table 6.4: Solenoid Coil: Datasheet

Figure 6.6: Foot mounting

Figure 6.7: Mounting Kit

Figure 6.8: Proximity Sensors

Proximity Sensor SMEO-4U-K-LED-24

Festo's proximity sensors are position sensors (Fig 6.8) specially adapted and optimised for use with Festo drives. These sensors are mounted on cylinders either directly or by means of mounting kits. The proximity sensor only functions after a permanent magnet has been attached to the drive piston. Proximity sensors are adjusted mechanically on the cylinder and locked into the desired position. As soon as the cylinder piston returns to this position, the status of the switching signal changes. Switching status is indicated by means of an LED

Features:

- Compact design
- Simple installation and initial start-up
- Attachment by means of mounting component
- Corrosion and acid resistant design (CRSMEO)

Function: Contact-type cylinder sensors SME consist of a reed switch whose contacts close when a magnetic field approaches, thus generating a switching signal. SME proximity sensors are used mainly in applications where it is necessary to switch high load currents (e.g. for the direct control of electrical consuming devices). In applications involving large capacitive loads or long cable lengths (7.5 m), a protective circuit must be provided.

Feature	Data/description
Design	Round
Assembly position	Any
Short circuit strength	No
Measuring principle	Reed magnetic
Switching element function	Normally open contact
Polarity protected	No
Operating status display	Yellow LED
Switch-off time	0.03 ms
Switch-on time	$\leqslant$ 0.5 ms
Operating voltage AC	12 - 27 V
Operating voltage DC	12 - 27 V
Max. output current	500 mA
Max. switching output voltage AC	27 V
Max. switching output voltage DC	27 V
Max. contact rating DC	10 W
Switch output	with contact, bipolar
CE Symbol	In compliance with EU directive 89/336/EWG (EMV)
Protection class	IP67
Ambient temperature	-5 - 60 °C; -20 - 60 °C
Product weight	70 g
Reproducibility of switching value	$\pm$ 0.1 mm

Electrical connection	Cable; 3-core
Cable length	2.5 m
Mounting type	with accessories
Materials information, housing	PET
Materials information, cable sheaths	PVC

Table 6.5: Proximity sensors: Datasheet

Figure 6.9: Push-in Fitting

Mounting kit SMBR-16

Mounting kits (Fig 6.7) for attaching magnetic proximity sensors for position sensing in drive units
Variants
Proximity sensor for 8 mm sensor slot, SME/SMT-8

- SMBR-8-...: for round cylinders DSNU, ESNU, DSEU, ESEU, DSW, ESW
- SMB-8-FENG-...: for standard cylinders DNC with guide unit FENG

Push-in fitting

The stainless steel retaining ring inside the fitting (Fig 6.9) holds the tubing securely without damaging its surface. Vibration and pressure surges are safely absorbed. The tubing can be detached easily by pressing down the blue release ring. For convenience, the appropriate outside tubing diameter is marked on the release ring. An NBR rubber sealing ring guarantees a perfect seal between standard OD tubing and the body of the fitting. Standard tubing is suitable for use with compressed air and vacuum. All of the brass components included with Festo's push-in fittings are nickel plated, and are thus highly resistant to corrosion.

Performance of Pneumatic Cylinder

We simulated the performance of the cylinder using the software ProPneu (Version 4.2.10.2004) provided by Festo Controls Ltd. The input details (system parameters) are:

Required stroke	320 mm	Direction of movement	Extend
Alignment angle	0 deg	Air supply pressure	4 bar
Number of cylinders in parallel	1	Moving Mass	10 kg

Calculated results are:

Total positioning time	0.35 s	Impact speed	1.71 m/s
Kinetic impact energy	14.99 J	Maximum air consumption	0.5285 l
Average Speed	0.89 m/s	Maximum speed	1.72 m/s
Mean Flow Speed	45.37 m/s	PPV settings	20 %

Gear Design

Since we are using a rack and pinion arrangement, the gear ratio is 1:1. For the design of the pinion, we use the procedure and equations enlisted in Section 4.2.2. The material properties of the gear used here are same as those enlisted there. The results are as follows:

Z_p = 11, with module m = 1 mm

Torque acting on the pinion = 5 kg-cm.

F_t = 81.75 N

F_b = 520.33 N

F_w = 406.275 N

F_d = 9.705 N

F_{eff} = 324.44 N

Thus, the effective factor of safety is N_f = 1.25. Since the load assumed itself is twice the actual load, we get that the gear used is safe.

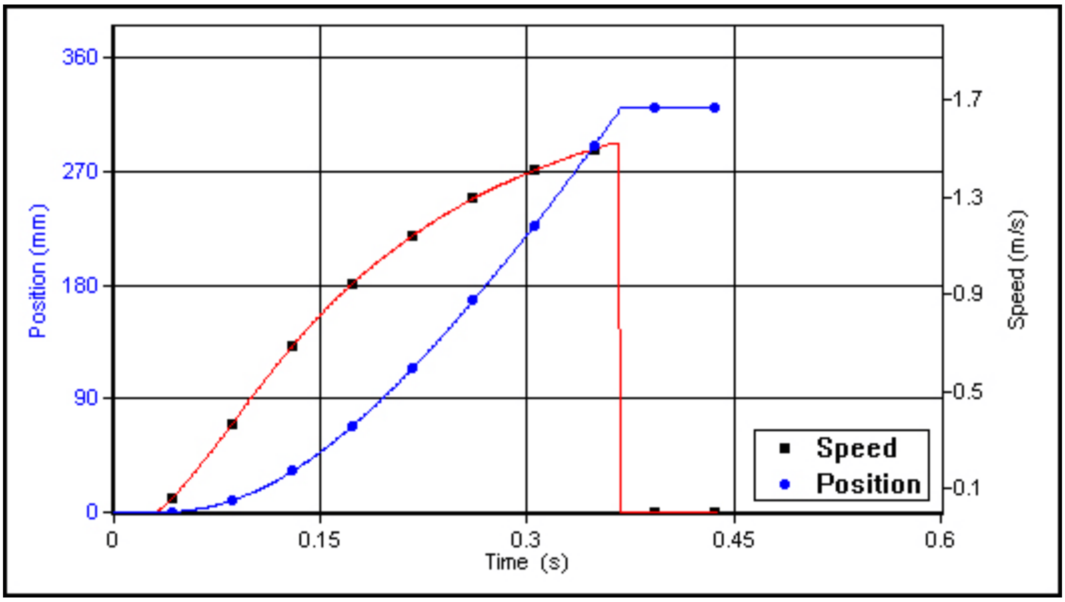

Figure 6.10: Cylinder speed/position Vs Time

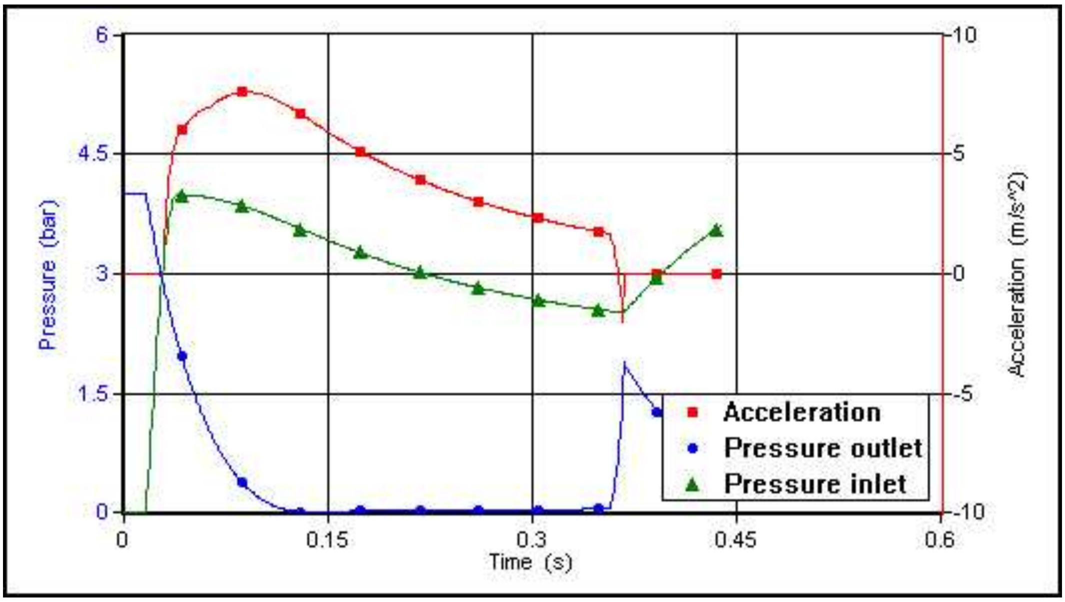

Figure 6.11: Cylinder acceleration/pressure Vs Time

Chapter 7

Electronics and Control

One of the main factors in reduction in costs was the use of a microcontroller to control all the actions of the robots. The microcontroller used is an Atmel ATMEGA16L. Some of its major features include - 16K Bytes of In-System Self Programmable Flash with and an endurance of 10,000 Write / Erase cycles, 512 Bytes EEPROM (Endurance: 1,00,000 Write / Erase cycles), 1K Byte of internal SRAM, programming through JTAG interface, two 8-bit Timer/Counters with separate prescalers and compare modes, one 18-bit Timer/Counter with separate prescalers, compare mode and capture mode, Real Time counter with separate oscillator, Byte oriented 2-wire serial interface, programmable serial USART, Master/Slave SPI serial interface, Programmable Watch-dog Timer with separate on-chip oscillator, On-chip analog comparator, Power-on Reset and programmable Brown-out detection, internal calibrated RC oscillator, external and internal interrupt sources and an operating voltage of 2.7-5.5V.

The microcontroller gives the control signals to the LCD and the motors. To step the motors through the appropriate angles in the correct direction, the logic sequence is generated by the logic sequence generator IC L298.

The microcontroller gets the V_{cc} from 7805 directly. Since stepper motors require high value of driving current we use Power MOSFETS to drive the motors. Power MOSFETS require very less driving current but provide a high value of drain current in order drive stepper motors. Power MOSFETS also have very high switching speed therefore bit sequence for rotation of motor can be fed very fast in order to achieve high r.p.m. Microcontroller output pins give a maximum output of 5 V when in high state. But this voltage is not enough to for a stepper motor. Stepper motors require at least 12 V DC to work. Therefore, a separate power supply was designed to provide required voltage.

Sensors are needed to account for various types of feedback. While the system is not a closed loop, the timing of all the various actions is synchronised by sensing the start or completion of intended actions. Thus, a number of proximity switches have been used. As the entire robotic assembly is metallic, all sensors except those mounted on the pneumatic cylinder are not magnet. Optical, inductive or capacitive sensors have been used. The transferring arm contains switches only to indicate the basic position. These sensors are utilized only when the robot is switched on and are needed to align all the links of the arm. The entire operation of the robot from here on does not use these switches.

The lifting arm, or the loader, contains two switches. The switch mounted on the bracket is used to sense the presence of a plate. This switch is used to stop the central beam of the lifter in its downward motion. The switch mounted on the side plate is used to fix the vertical limit of travel. Similarly, two switches are mounted on the end effector of the unloader, two fix the two ends of travel of the rack.

The unloader and lifter have a purely hard-wired circuit, with minimal control from the microcontroller. Only the start of each cycle is indicated and each arm performs its own operation. The arms provide signals, indicating the status of its action, to the microcontroller, thus ensuring synchronization of operations. The arms, and the ram “wait” for each other in case there is a mismatch in timing.

All these components listed above are standard parts with few complications. The most difficult part is that of motor control, and that too is solved by the use of an efficient power supply, power MOSFETS and the use of micro-stepping. The electromagnets that have been used need a 230 V AC supply and are equipped with their own power source. As a result, these magnets need to be provided only with the control signal to actuate them.

Chapter 8

Manufacturing Drawings & Process Sheets

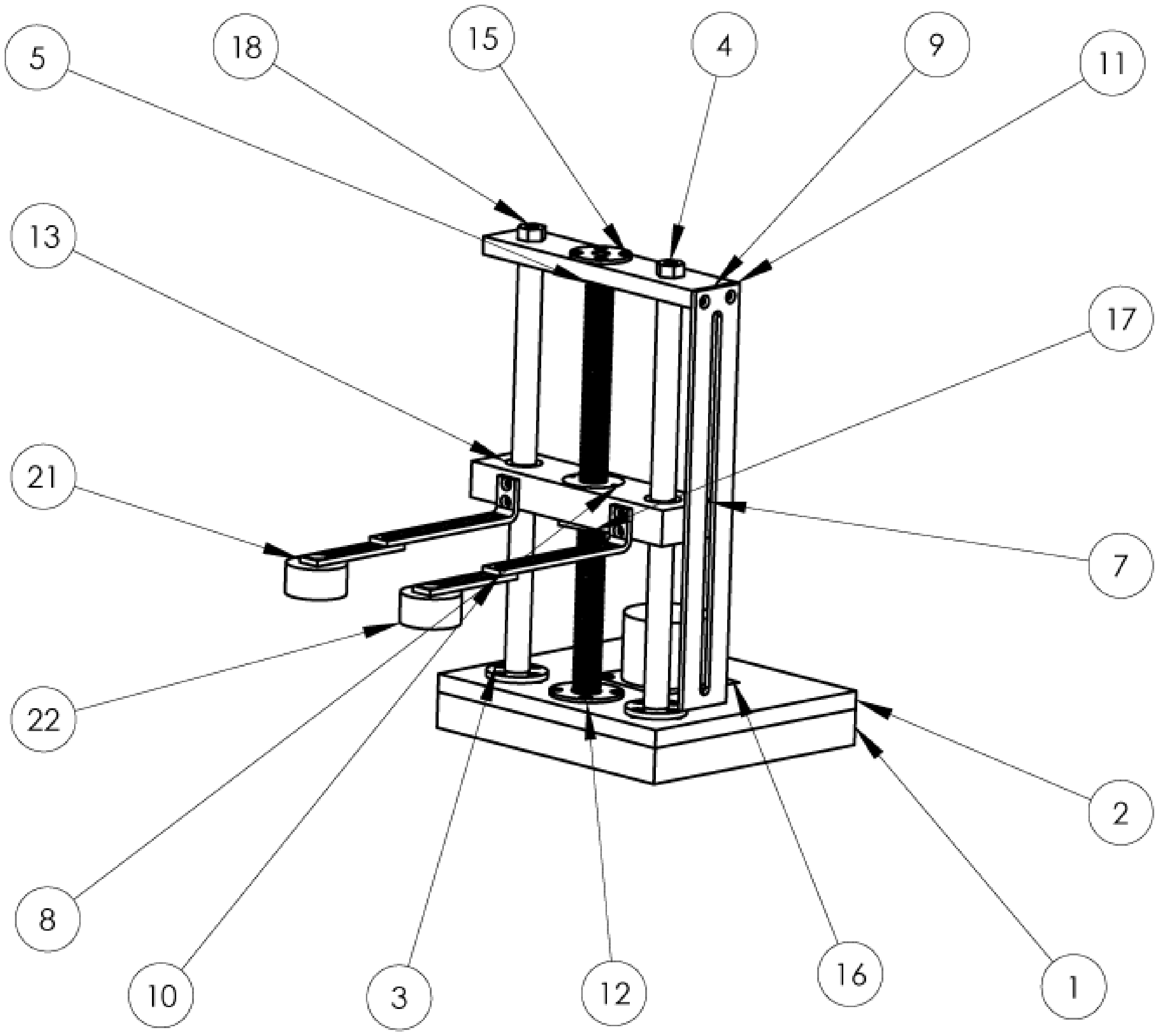

Figure 8.1: First Arm

ITEM NO.	PART NAME	QTY.
1	frame	1
2	base	1
3	bush of support	2
4	support	2
5	lead screw	1
6	bottom bearing	1
7	nut-holder	1
8	new nut	1
9	top plate	1
10	bracket	2
11	Sensor mount	1
12	bearing cap2	1
13	linear bearing	2
14	top bearing	1
15	top bearing cap	1
16	motor	1
17	hex lock nut	1
18	hex nut	2
19	pinion	1
20	gear	1
21	extension	2
22	gripper	2

Figure 8.2: First Arm - Part List

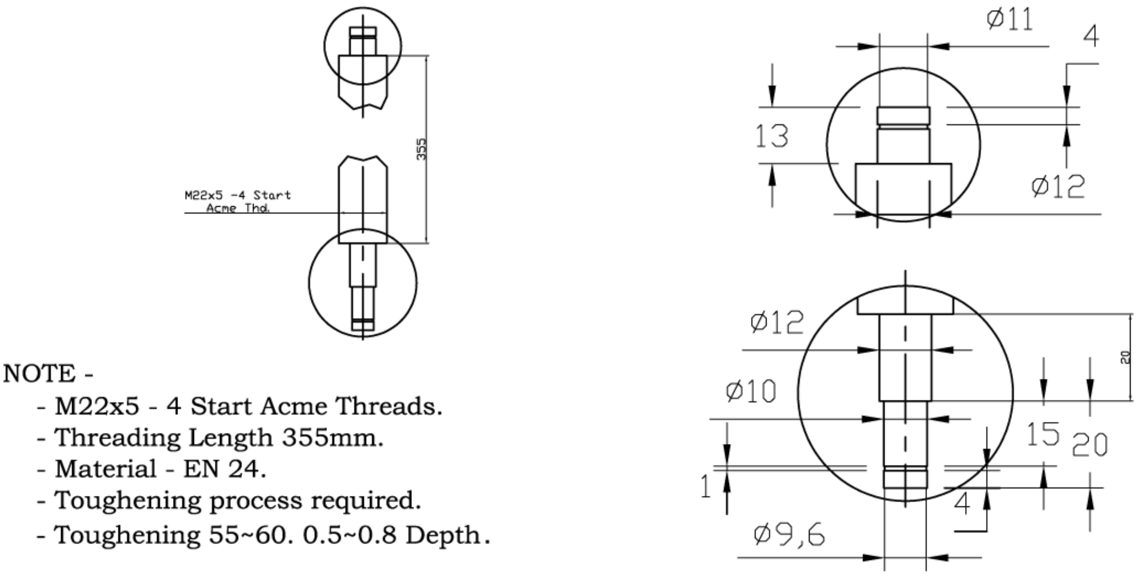

Figure 8.3: Lead Screw for First Arm

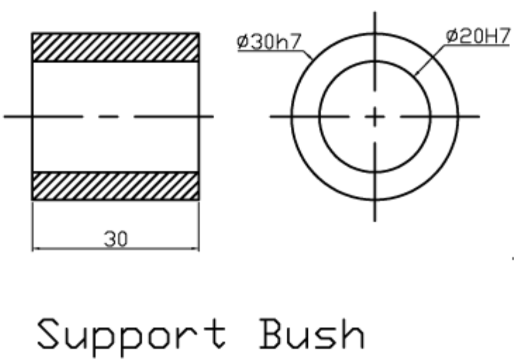

Figure 8.4: Support Bush for First Arm

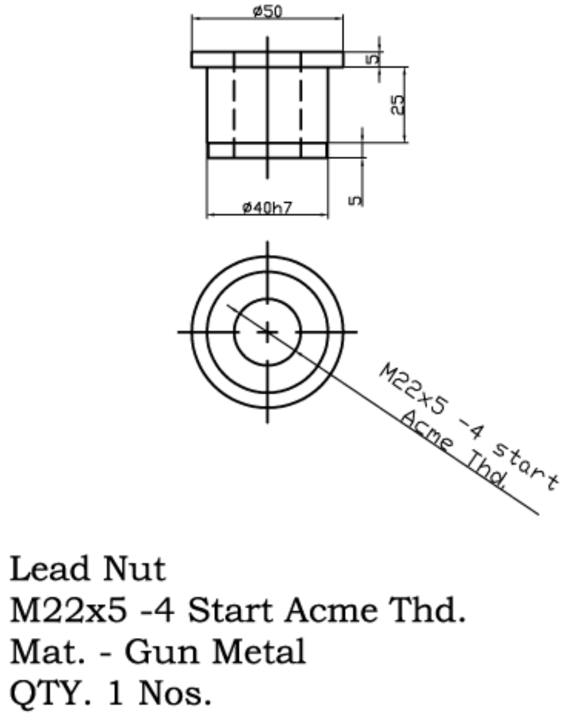

Figure 8.5: Nut for Lead Screw of First Arm

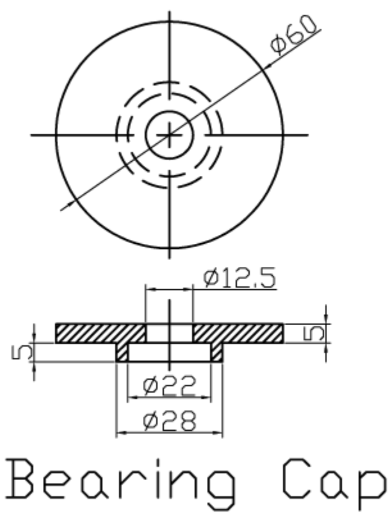

Figure 8.6: Bearing Cap for First Arm

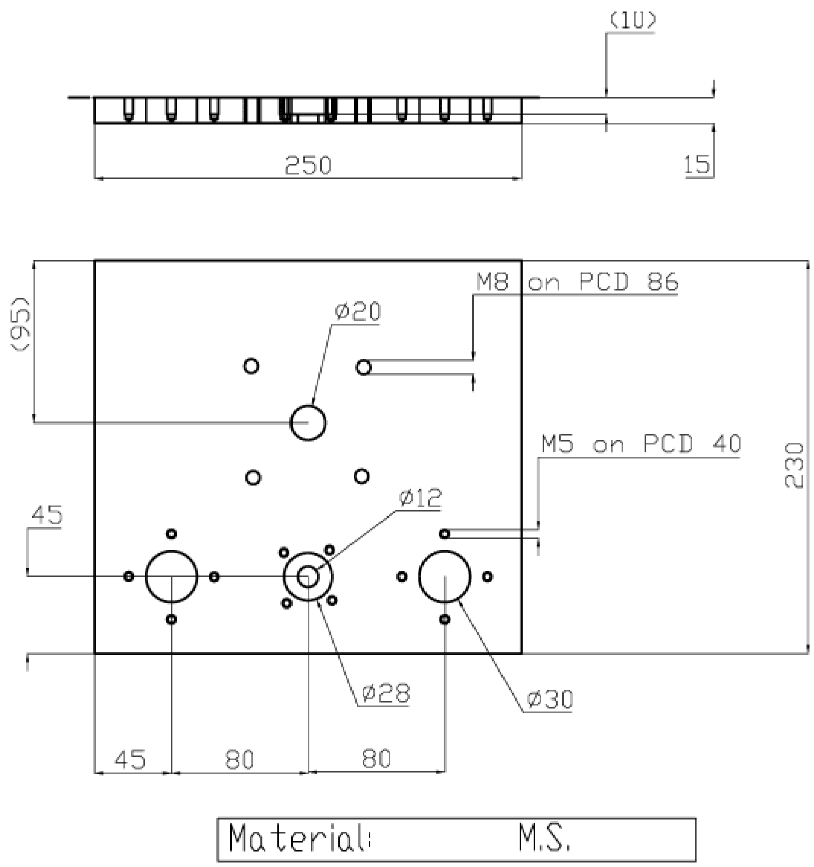

Figure 8.7: Base for First Arm

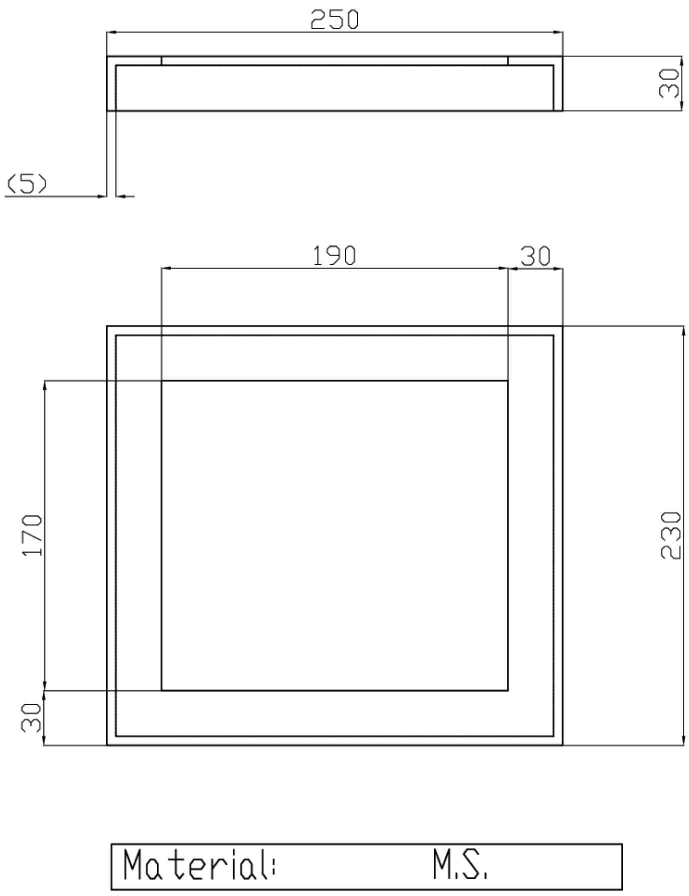

Figure 8.8: Base Frame of First Arm

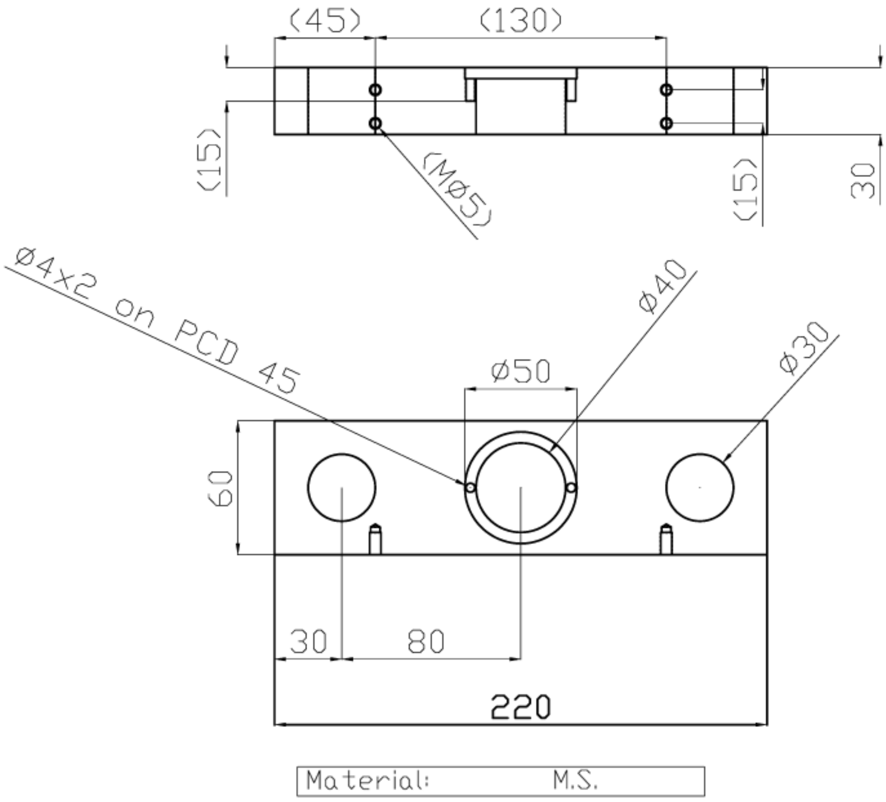

Figure 8.9: Translating Beam of First Arm

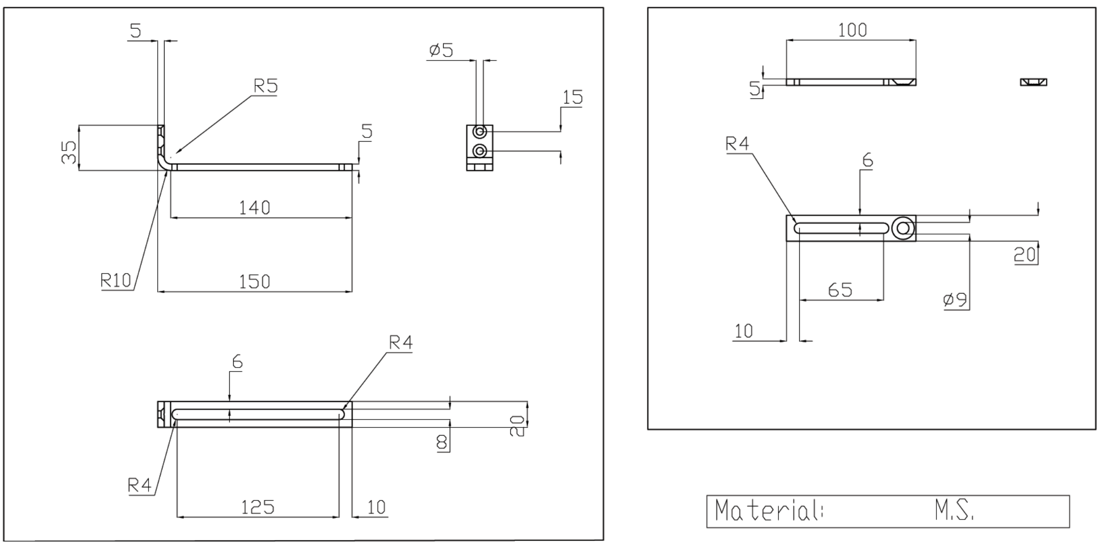

Figure 8.10: Suction Cup holder of First Arm

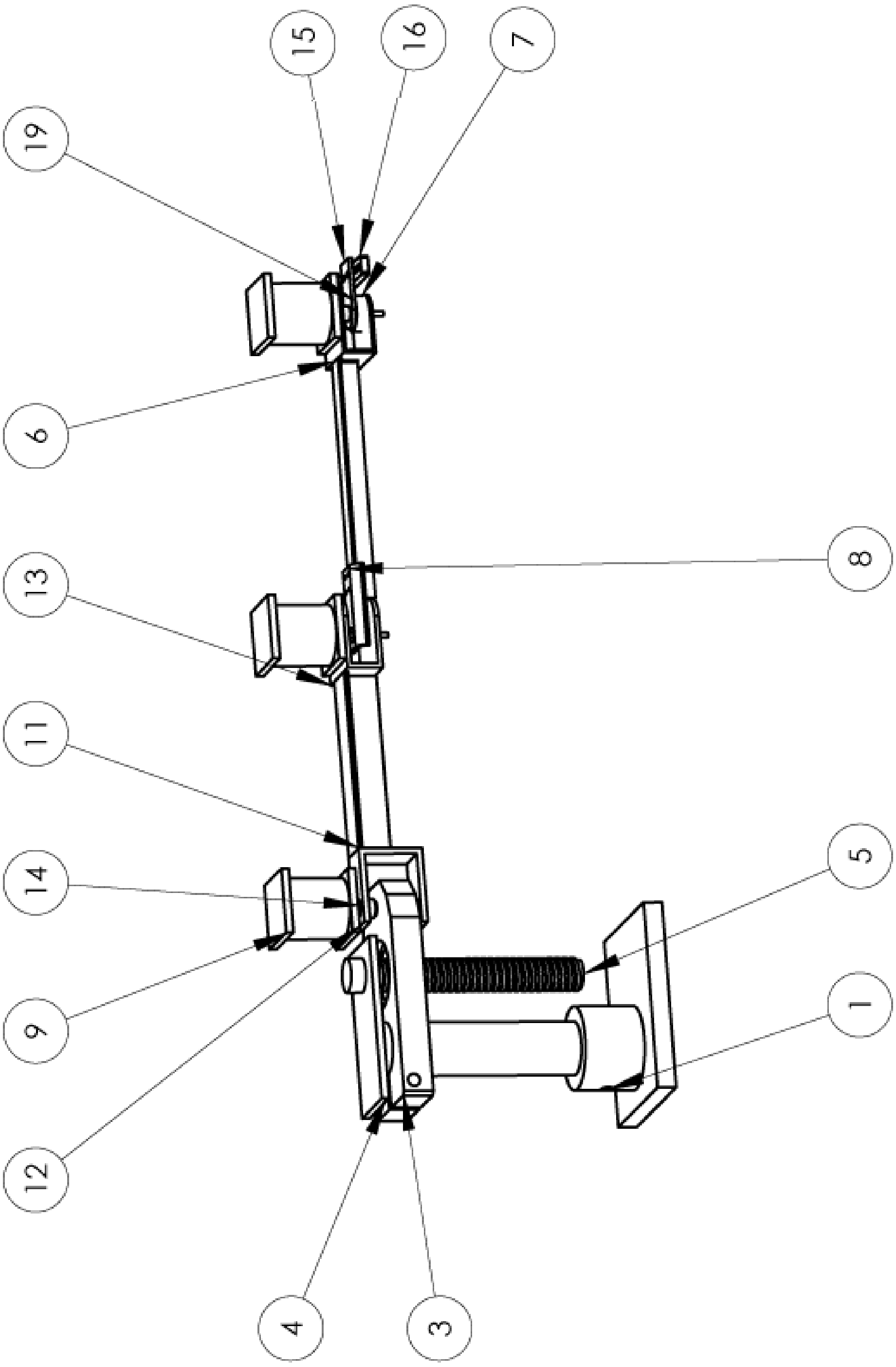

Figure 8.11: Second Arm

ITEM NO.	Part Name	QTY.
1	base plate and bush	1
2	support rod	1
3	arm platform	1
4	top plate	1
5	lead screw	1
6	T link	1
7	U BracketB	1
8	clamping plate	1
9	motor1	3
10	weldment	1
11	weldment	1
12	bushing for clamping plate	1
13	T link	1
14	bracket	1
15	U bracket A	1
16	bushing	2
17	weldment	1
18	weldment	1
19	plate for magnet holder	1
20	magnet holder	1
21	bushing	1
23	bearings	7

Figure 8.12: Part list for Second Arm

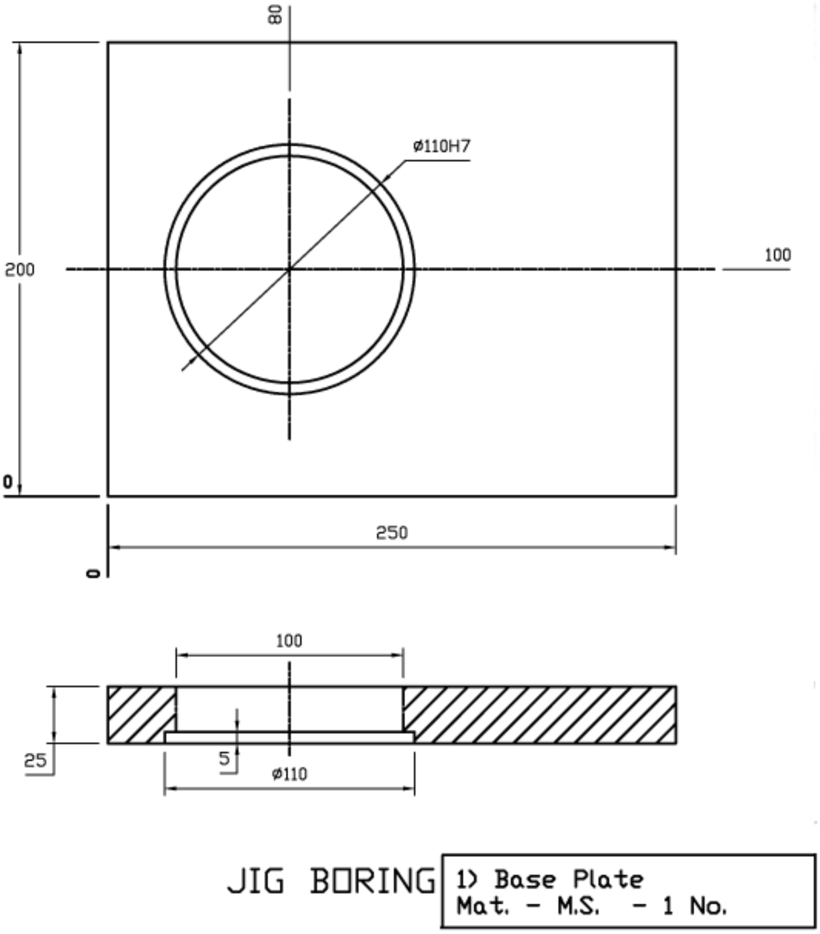

Figure 8.13: Base Plate of Second Arm

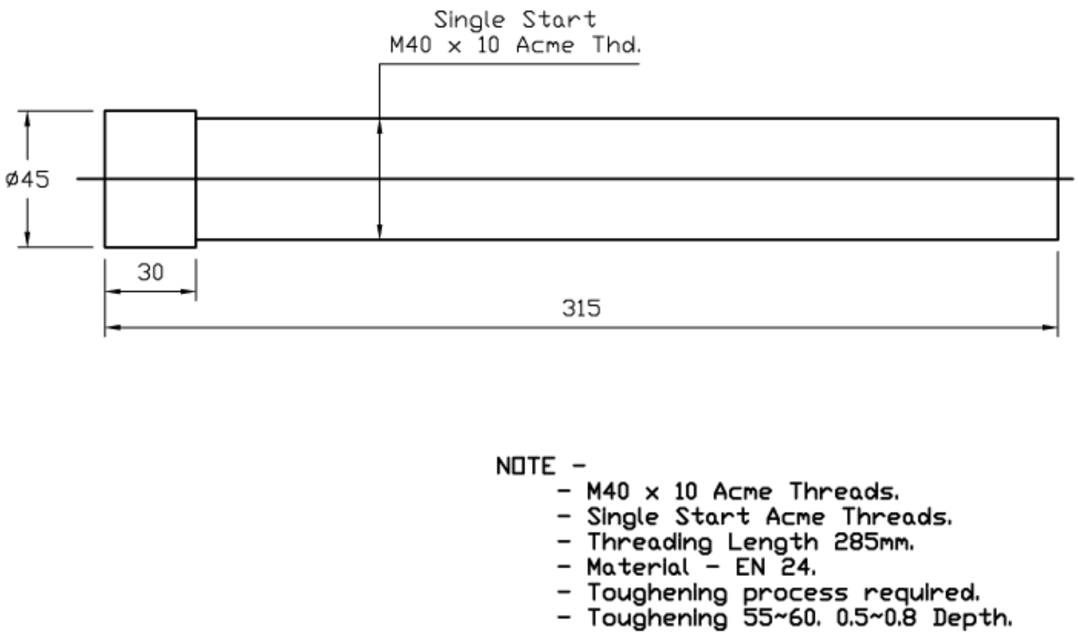

Figure 8.14: Lead Screw of Second Arm

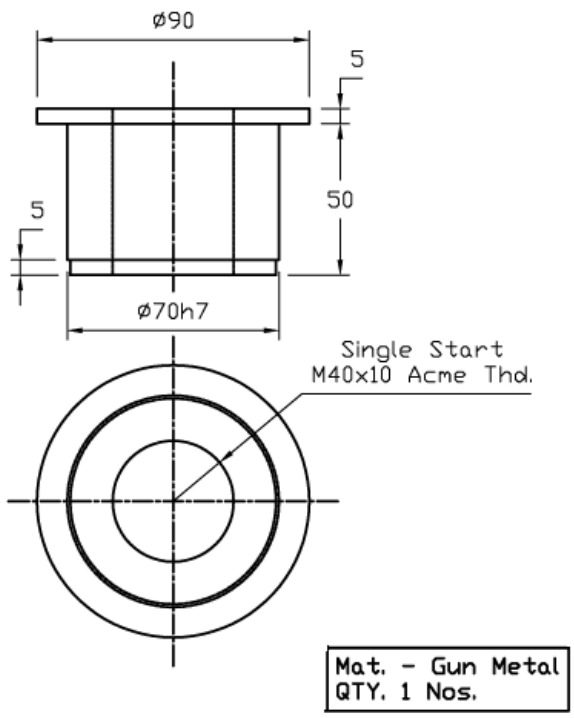

Figure 8.15: Nut for Lead Screw of Second Arm

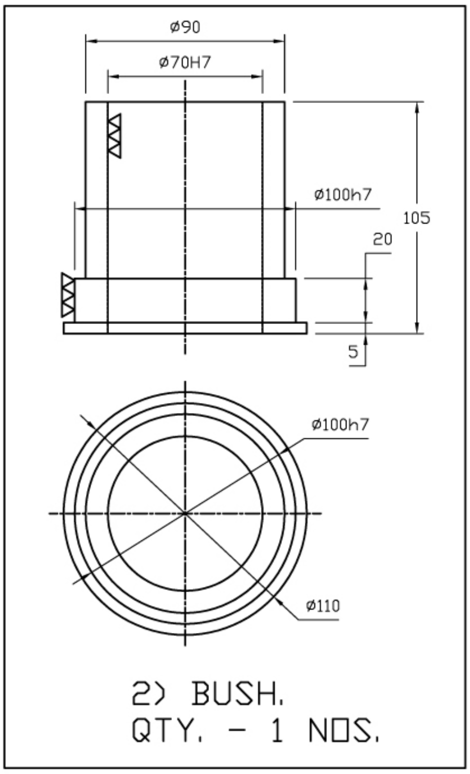

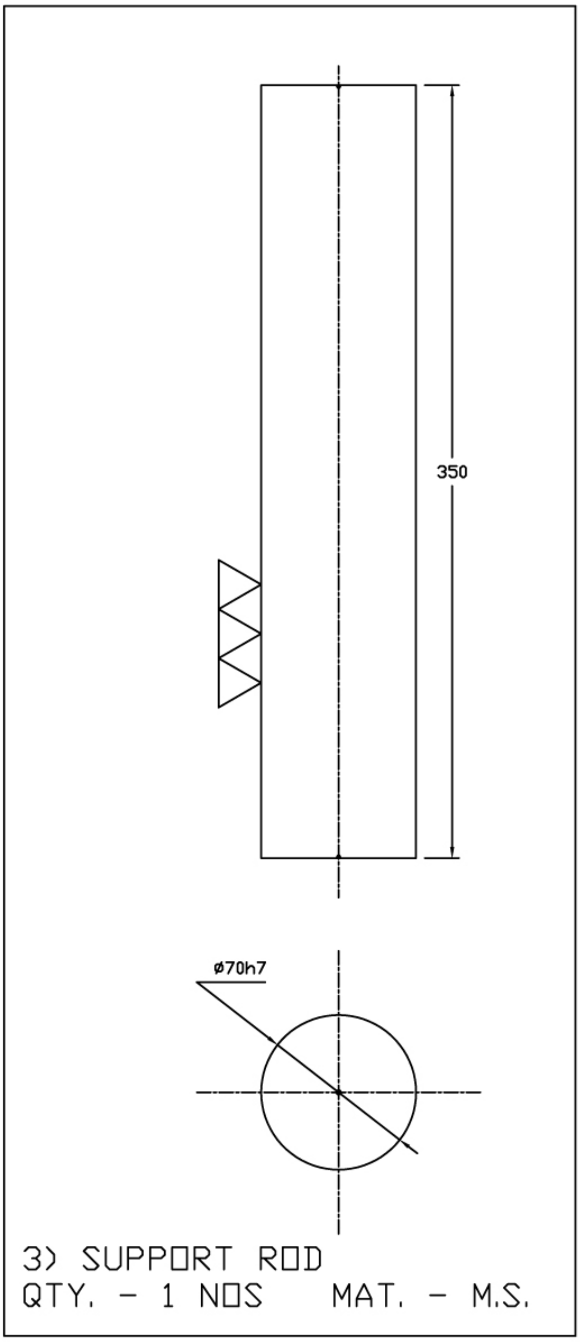

Figure 8.16: Support Rod & Bush of Second Arm

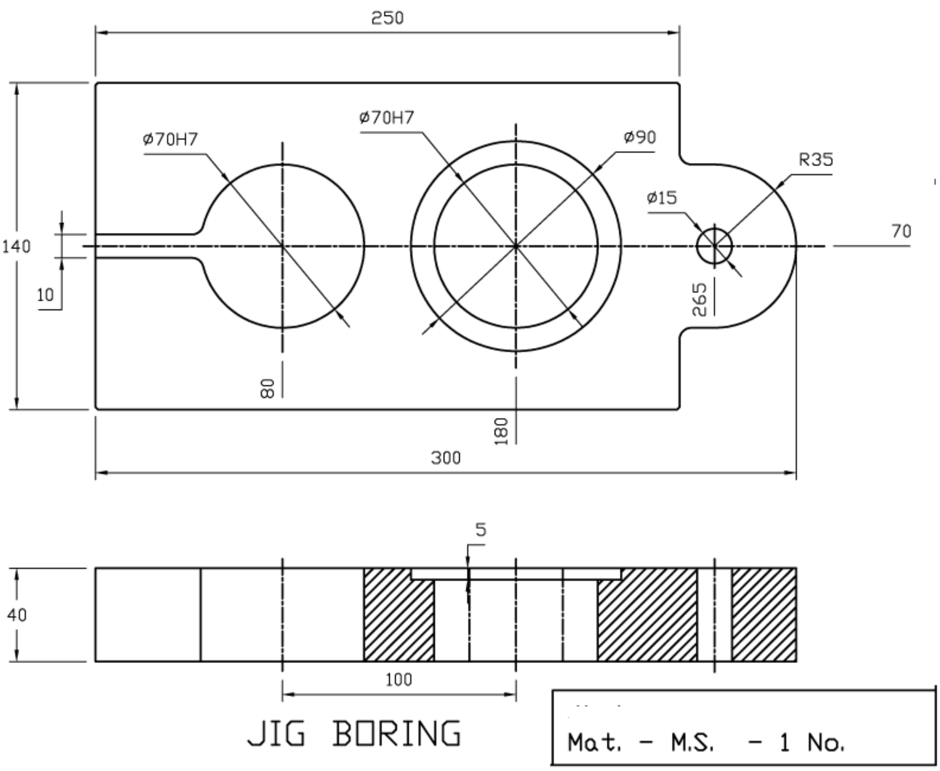

Figure 8.17: Arm Platform of Second Arm

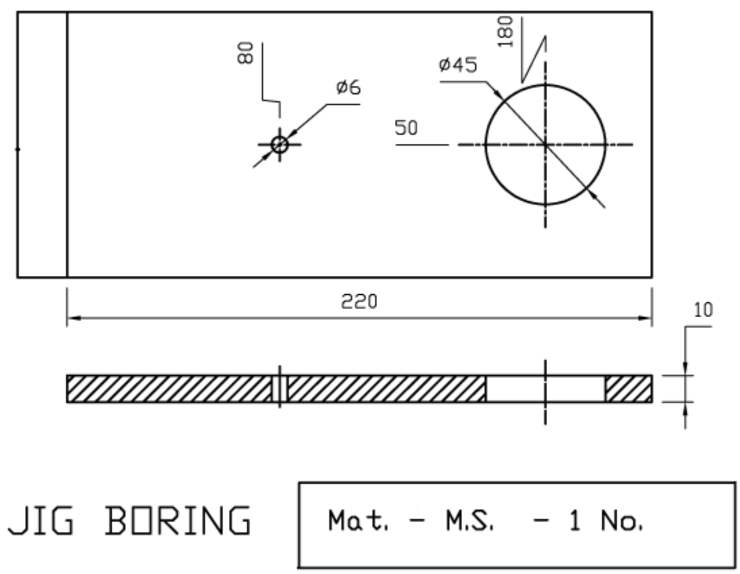

Figure 8.18: Top Plate of Second Arm

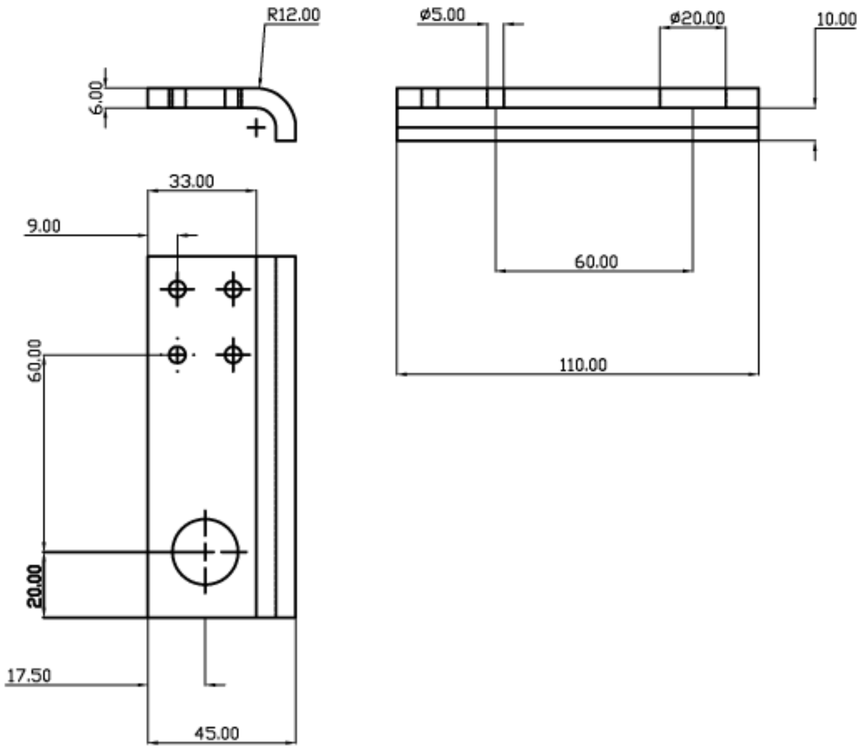

Figure 8.19: Bracket for motor in Second Arm

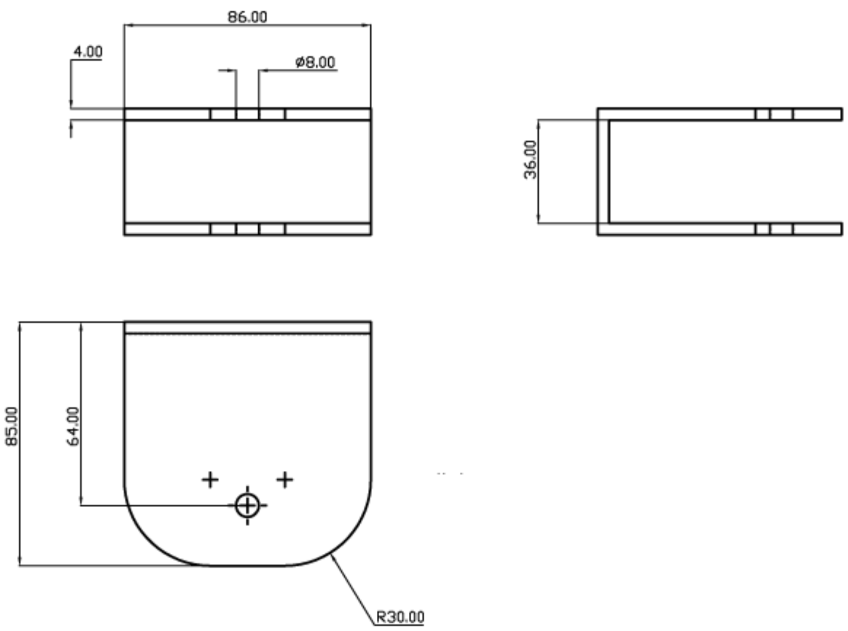

Figure 8.20: Bracket for motor of Second Arm

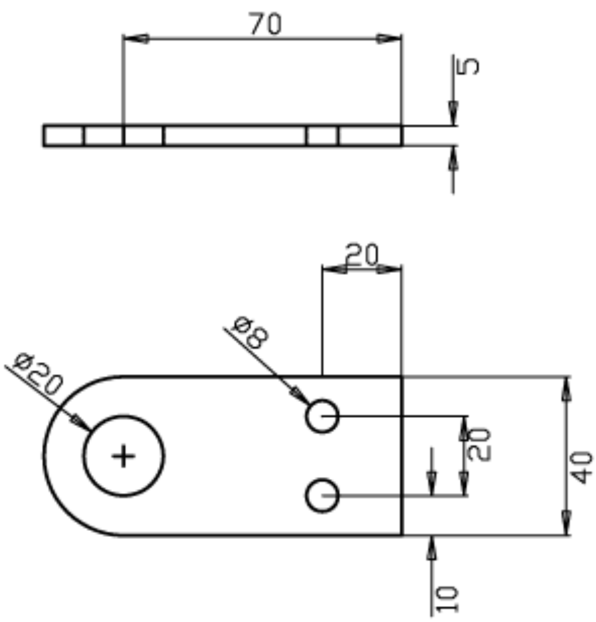

Figure 8.21: Clamp for magnet holder of Second Arm

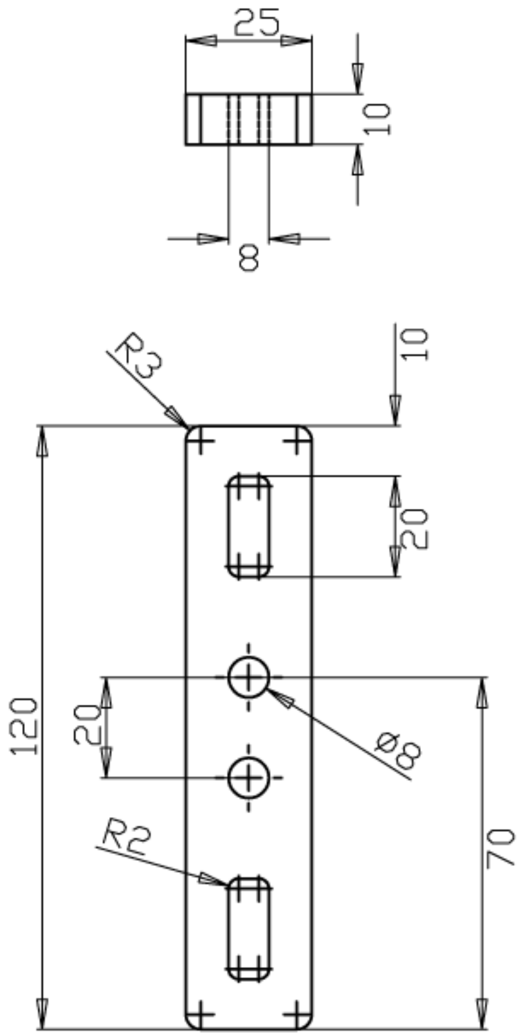

Figure 8.22: Magnet holder of Second Arm

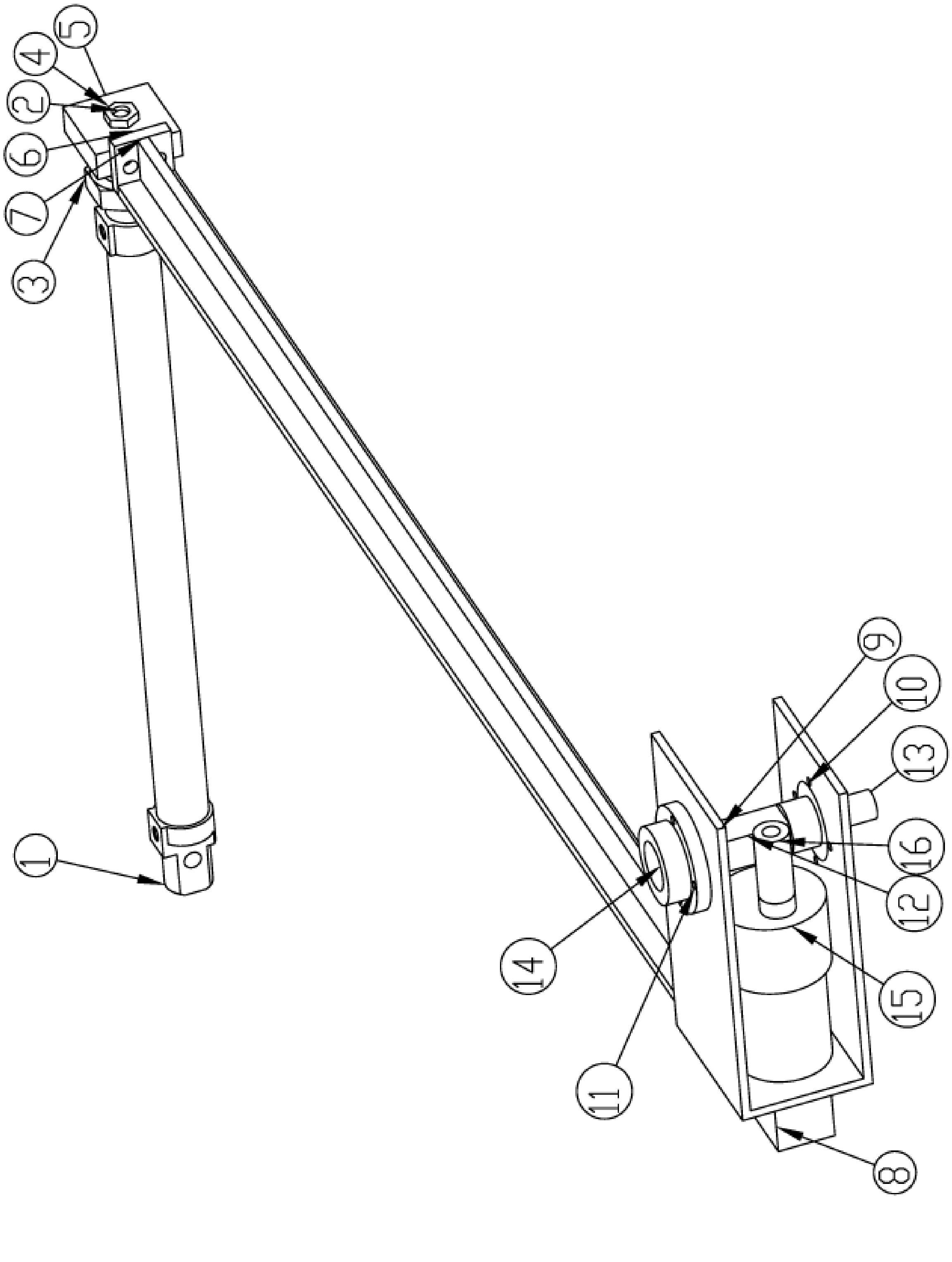

Figure 8.23: Third Arm

ITEM NO.	PART NAME	QTY.
1	cylinder-body	1
2	cyl-piston	1
3	cyl-nut	1
4	hex nut	2
5	square nut	1
6	fixing plate	1
7	trod	1
8	block	1
9	c-plate	1
10	bottom bush	1
11	top bush	1
12	rack-1	1
13	rack bottom	1
14	rack-top	1
15	motor	1
16	pinion	1

Figure 8.24: Part List for Third Arm

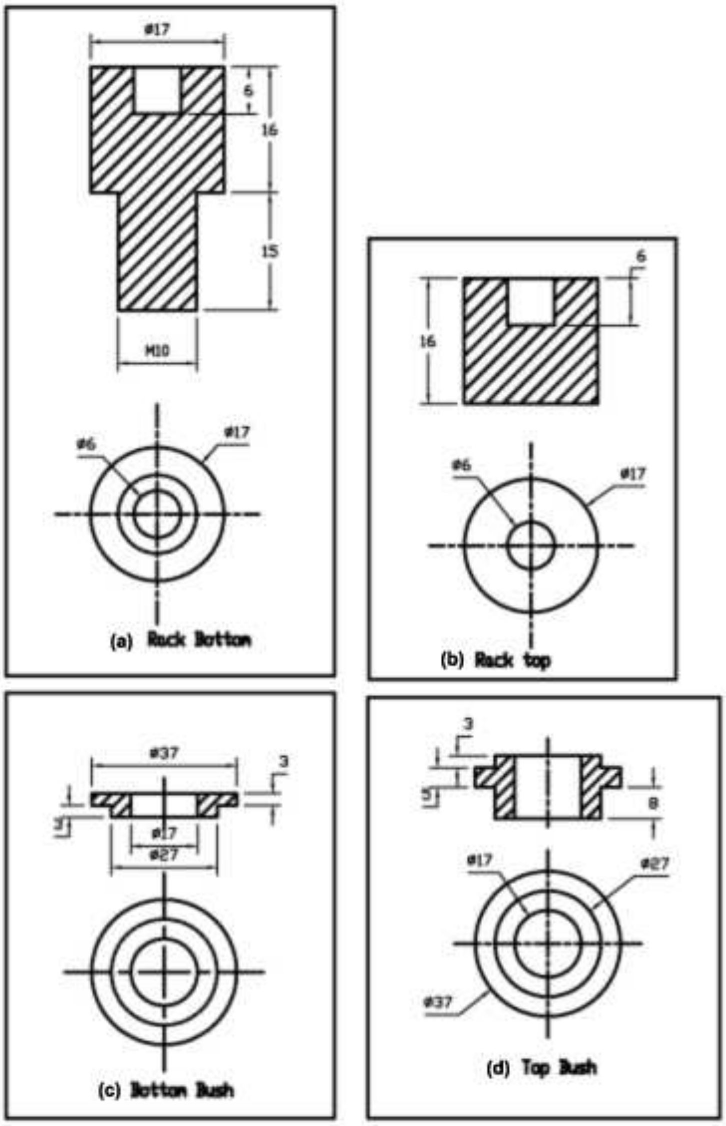

Figure 8.25: Lifter Assembly of Third Arm

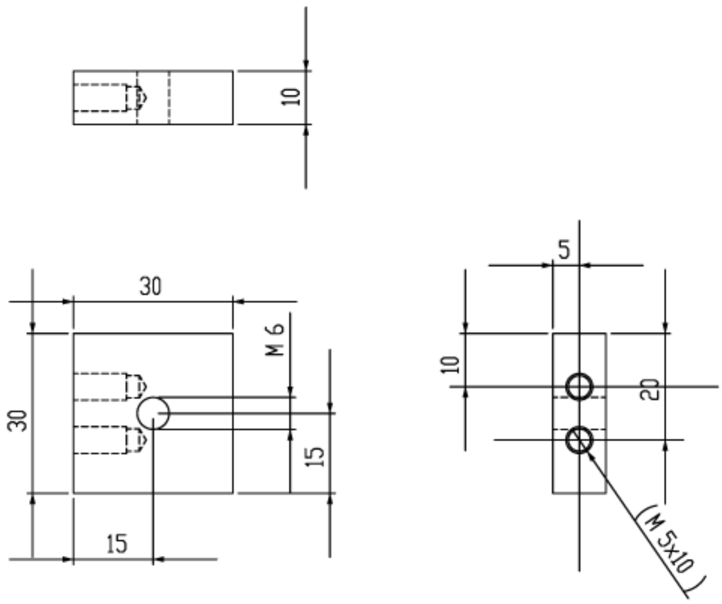

Figure 8.26: Square Nut of Third Arm

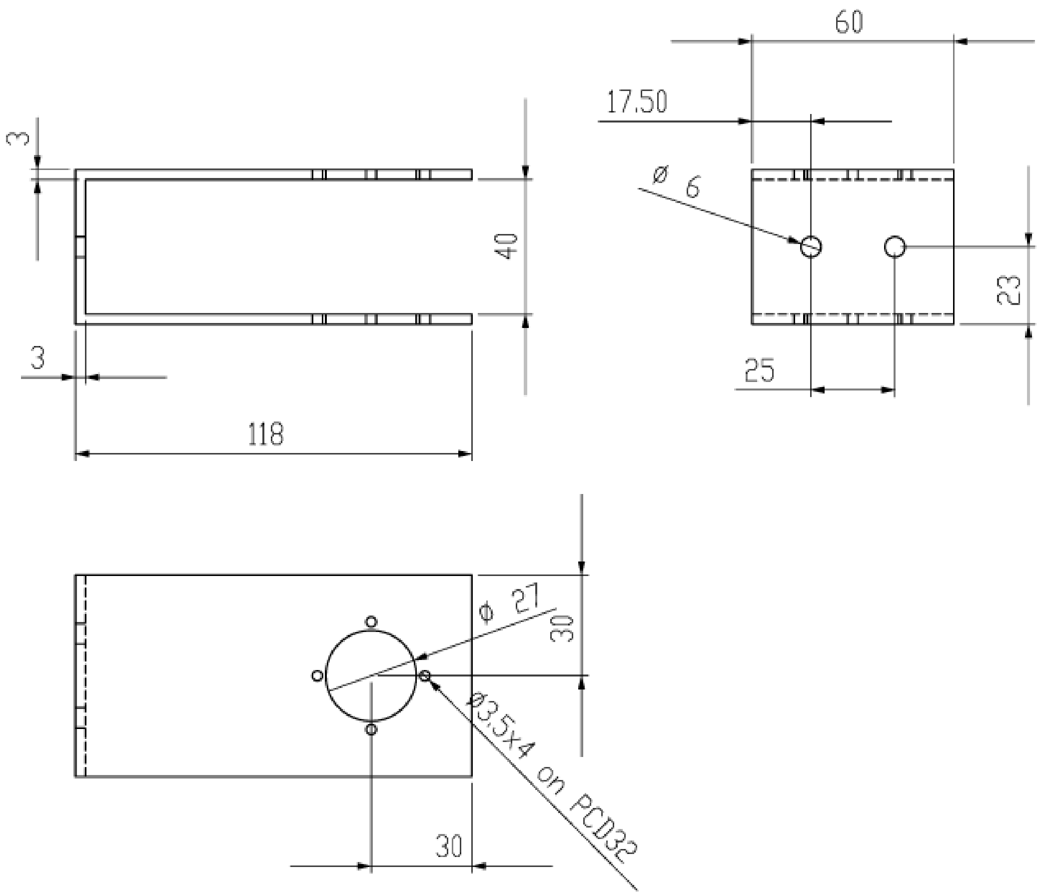

Figure 8.27: C plate of Third Arm

Process Sheets

First Arm

Sr. No.	**Part Name**	**Raw Material (mm)**	**Material**	**Qty.**	**Operations**
1.	Frame	Angle $5 \times 30 \times 1000$	M.S.	1	Milling Welding
2.	Base Plate	$18 \times 255 \times 235$	M.S.	1	Milling Grinding Jig Boring Drilling Tapping
3.	Holder	$6 \times 20 \times 200$	Bright Plate	2	Bending Drilling
4.	Holder	$6 \times 20 \times 105$	Bright Plate	2	Bending Drilling
5.	Beam	$18 \times 65 \times 225$	M.S.	1	Milling Grinding Jig Boring Drilling Tapping
6.	Support Rods	$\phi\ 22 \times 420$	M.S.	2	Turning Hardening Grinding Tapping

Sr. No.	**Part Name**	**Raw Material(mm)**	**Material**	**Qty.**	**Operations**
7.	Bush	ϕ 32 × 35	OHNS	2	Turning Hardening Grinding
8.	Top Plate	18 × 55 × 245	M.S.	1	Milling Grinding Jig Boring Drilling Tapping
9.	Lead Screw	ϕ 25 × 415	EN24	1	Turning Milling
10.	Nut	ϕ 55 × 40	Gun Metal	1	Turning
11.	Sensor Mount	6 × 50 × 355	Bright Plate	1	Milling Drilling
12.	Support Bush	ϕ 55 × 55	OHNS	2	Turning Hardening Grinding Drilling
13.	Bearing Cap	ϕ 65× 15	OHNS	2	Turning Hardening Grinding Drilling

Second Arm

Sr. No.	Part Name	Raw Material(mm)	Material	Qty.	Operations
1.	Base Plate	$30 \times 205 \times 255$	M.S.	1	Milling Grinding Jig Boring
2.	Bush	ϕ 105×110	M.S.	1	Turning Drilling Hardening Grinding
3.	Support Rod	ϕ 72×355	M.S.	1	Turning Drilling Tapping Grinding
4.	Arm Platform	$45 \times 145 \times 305$	M.S.	1	Gas Cutting Milling Grinding Jig Boring Drilling
5.	Top Plate	$15 \times 105 \times 255$	M.S.	1	Milling Grinding Jig Boring Drilling

Sr. No.	**Part Name**	**Raw Material(mm)**	**Material**	**Qty.**	**Operations**
6.	Bracket	8 × 125 × 55 × 80	M.S.	1	Bending Welding Drilling
7.	U' Bracket - A	5 × 105 × 90 × 40	M.S.	1	Bending Welding Drilling
8.	'T' Plate - A	6 × 50× 225	M.S.	1	Drilling Welding
9.	Clamping Plate	6 × 45 × 120	M.S.	1	Bending Welding Drilling
10.	'T' Plate - B	4 × 30 × 325	M.S.	1	Drilling Welding
11.	U' Bracket - B	5 × 90 × 95 × 40	M.S.	1	Bending Welding Drilling
12.	Plate	6 × 40 × 100	M.S.	1	Drilling
13.	Magnet Holder	15 × 30 × 125	M.S.	1	Milling Grinding
14.	Lead Screw	ϕ 50 × 320	EN24	1	Turning
15.	Nut	ϕ 90 × 45	Gun Metal	1	Turning

Third Arm

Sr. No.	Part Name	Raw Material(mm)	Material	Qty.	Operations
1.	Square Nut	15×35×35	M.S.	1	Milling Drilling Tapping
2.	Fixing Plate	6×25×25	M.S.	1	Drilling
3.	'T' Plate	4×20×560	M.S.	1	Welding
4.	Block	25×55×55	M.S.	1	Milling Drilling Tapping
5.	C' Plate	4×60×280	M.S.	1	Bending Drilling
6.	Bottom Bush	ϕ 40 × 10	M.S.	1	Turning Grinding Drilling Tapping
7.	Top Bush	ϕ 40 × 20	M.S.	1	Turning Grinding Drilling Tapping
8.	Rack Bottom	ϕ 20 × 35	M.S.	1	Turning Grinding Drilling
9.	Rack Top	ϕ 20 × 20	M.S.	1	Turning Grinding Drilling

Part IV

Discussion & Conclusions

Most robots in use in the industry cost upwards of Rs. 5 lakhs. In most of these state-of-art robots, actuators like servo motors, and linear motors, control systems based on PLC, mechanisms employing re-circulating ball screws, harmonic drives are used. End-effectors have intelligent grippers, with additional DOF or sensing capabilities to account for load variations. Vision capabilities are also frequently a part of the system. However, these robots are expensive for small scale industries. If the major problem of high initial cost is addressed, a robot can be introduced in any industry to bring in automation,

Our design uses extremely simple ideas and mechanisms to achieve a complex set of actions and is intended to imitate the actions of the operators. The simplistic design ensures that the motors we choose are not bulky. The comparatively low torque and low motor speed requirements permit us to use stepper motors instead of servo motors. The accuracy lost in this is not a major problem for our purposes. Also, the stepper motor can be micro-stepped to compensate for this accuracy. As these stepper motors are not heavily loaded, we can keep the robot control system open loop. This greatly reduces the cost of the drive circuit. The mechanical links and parts that have been fabricated are extremely simple.

Cost Analysis

A brief outline of the manufacturing and fabrication costs incurred are provided in this section. The costs have been listed with respect to each arm.

Sr. No.	Material	Qty.	Amount (in Rs.
1	Base Plate 16x65x225. -M.S Beam 16x65x225 -M.S Top plate 16x55x245 -M.S. Base plate 30x205x255 -M.S Top plate 15x105x255 -M.S	1 No. Each	1954
2	Arm Platform 45x145x305 -M.S.	1No.	865
3	Support Rod Dia.22x425 -M.S. Support Bush Dia.55x55 -OHNS Bush Dia.105x110	1 No. Each	1057.5
4	Support Rod Dia.75x355	1 No.	572
5	Lead Screw - Dia.25x415 - EN 24 Bush - Dia.32x35 - OHNS Bearing Cap Dia.65x15 - OHNS Lead Screw	1No. 2 No. 2 No. . 1No.	784.
6	Square Nut - 15x35x35 - M.S. Block - 25x55x55 - M.S.	1 No Each	43
7	Bottom Bush - Dia. 40x10 -M.S. Top Bush Dia.40x20 - M.S. Rack Bottom - Dia. 20x35 - M.S. Rack Top Dia. 20x20 - M.S.	1 No Each	97

Table 8.1: Cost of raw materials

Sr. No.	Material Machining	Qty.	Amount in Rs.
1	Milling and grinding	6 Nos.	1630
2	Jig Boring	6 Nos.	2325
3	Turning - Support Rod, Support Bush, Bush, Support Rod	6 Nos.	640

Table 8.2: Costs of machining

Sr.No.	Product Name	Product Description	Unit Price	Qty	Amount
1.	Stepper Motor	Srijan Controls: STM 1101	2800	1	2800
2.	Gear	Albro Engineers: Spur Gear 2x30	300	1	300
3.	Gear	Spur Gear 2x150	1610	1	1610
4.	Bearing	SKF 6000	200	1	200
5.	Bearing	SKF 6002	200	1	200
6.	Vacuum Cups	Festo: ESG-50-BS-HD-QS	1838	2	3676
7.	Vacuum Generator	Festo: VADM-95	3815	1	3815
8.	Push in Fitting	Festo: QS-1/8-4	42	2	84
9.	Push in Y Connector	Festo: QSY-4	100	2	200

Table 8.3: Cost of standard components - First Arm

Sr. No.	Product Name	Product Description	Unit Price	Qty	Amount (in Rs)
1.	Stepper Motor	Srijan Controls: STM 982	2500	1	2500
2.	Stepper Motor	STM 983	3000	1	3000
3.	Stepper Motor	STM 985	4500	1	4500
4.	Electro Magnets	Armatech Associates: Crystal AA 317	3900	1	3900
5.	Gear Box	Revolution Engineers: Spur Gear Box 1:4	3200	1	3200
6.	Bearing	SKF 51204	700	4	2800
7.	Bearing	SKF 51205	700	3	2100
8.	Bearing	SKF 51209	700	1	700

Table 8.4: Cost of standard components - Second Arm

Sr. No.	Product Name	Product Description	Unit Price	Qty	Amount (in Rs.)
1.	Pneumatic Cylinder	Festo: DSNU-16-320-PPV-A-Q	3495	1	3495
2.	Solenoid DC-Valve	Festo: JMFH-5-1/8	1895	1	1895
3.	Solenoid Coil	Festo: MSFG-12DC	411	2	822
4.	Silencer	Festo: U-1/8	90	2	180
5.	Proximity Sensor	Festo: SMEO-4-K-LED-24-B	452	2	904
6.	Plastic Tubing	Festo: PUN-6x1-BL	28	5	140
7.	Push in Fitting	Festo: QSM-M5-6	57	2	114
8.	Push in Fitting	Festo: QS-1/8-6	44	2	88
9.	Mounting Kit	Festo: SMDR-16	64	2	128
10.	Foot Mounting	Festo: HBN-12/16x2	110	1	110
11.	DC PM Gear Motor	Servo Electronics: TG-38123000	384	1	384
12.	Rack	Albro Engineers: Spur Gear 1x300	550	1	550
13.	Gear	Spur Gear 1x11	200	1	200
14.	Electro Magnets	Armatech Associates: Crystal AA 317	3900	1	3900

Table 8.5: Cost of standard components - Third Arm

Total Cost

Raw Material cost	=	Rs. 5,363.5
Machining Cost	=	Rs. 4,595
Cost of Standard components	=	Rs. 48,495
Cost of Electronic components	=	Rs. 10,000
Prime cost	=	Raw Material Cost + Machining Cost + Cost of Standard Components
	=	5363.5 + 4595 + 48495 + 10000
	=	Rs 68,453.5

Taking overhead cost 10% of prime cost

Total Cost	=	Prime Cost + Overhead cost
	=	68453.5 + 6845.3
∴ **Total Cost**	=	**Rs. 75298.3**

Performance Analysis

Activity	Average Time taken (in sec)
Load sheet onto die	7
Press operation	2
Unload finished product	6

Table 8.6: Time study for manual loading and unloading of press

In the current scenario, where the robot is intended to be installed, a job is produced every 15 seconds. The speed of the robot can be deduced by referring to the various design constraint imposed on the individual parts. The lifting arm (Sec. 4.2.1, page 55) is designed with a beam is driven at 0.175 m/s by a 4 start lead screw with pitch of 5 mm rotating at 100 rpm. Thus, it will take 2 seconds to travel the maximum lift of 350 mm. By referring to Table 5.4 (page 91, we note that the second arm takes a maximum of 4 seconds to complete its motion. The performance analysis of pnuematic cylinder, described in Sec. 6.3 (page 119), shows that the unloading action takes about 3 seconds.

Activity	Maximum Expected Time (in sec)
Load sheet onto die	4
Press operation	2
Unload finished product	3

Table 8.7: Expected robot times for loading and unloading of press

The lifting and transferring action are performed simulatenously, while the unloading action takes place after the press ram has moved up. When unloading action takes place, the planar transfer motion is stopped. Thus, the maximum total time for a cycle is given by 9 seconds. We can thus expect a job to be produced 2 times faster than the current situation.
This robotic assembly is in the final stages of installation and the results of the final testing will be available in the first week of July.

Bibliography

[1] V. V. Athani. *Stepper Motors: Fundamentals, Applications and Design*. New Age International Publishers, 1997.

[2] V. B. Bhandari. *Design of Machine Elements*. Tata McGraw-Hill Publishing Company Limited, 1994.

[3] P.I. Corke. A robotics toolbox for MATLAB. *IEEE Robotics and Automation Magazine*, 3(1):24–32, March 1996.

[4] Festo Controls Ltd. *Pneumatic catalogue*, 2005.

[5] M. P. Groover, M. Weiss, R. N. Nagel, and N. G. Odrey. *Industrial Robotics: Technology, Programming and Applications*. McGraw-Hill, 1986.

[6] Mandar Harshe, Colin Menezes, Bhushan Walzade, and K. H. Munde. Design and control of a multi-DOF robotic arm assembly using low cost alternatives. In *International Conference on Advances in Machine Design and Industry Automation*, 2007.

[7] S. R. Majumdar. *Pneumatic Systems - Principles and Maintenance*. Tata McGraw Hill Publishing Company Ltd., 1995.

[8] PSG College of Technology, Coimbatore. *Design Data - Data Book for Engineers*, 1978.

[9] J. Shigley and J. Uicker. *Theory of Machines and Mechanisms*, chapter Synthesis of Linkages, pages 353–358. Mcgraw-Hill International Editions, second edition, 1995.

[10] Mark W. Spong, Seth Hutchinson, and M. Vidyasagar. *Robot Modeling and Control*. John Wiley & Sons Inc., 2006.

Achievements

- Paper titled "Design and control of a multi-DOF autonomous robotic arm assembly using low cost alternatives" presented at the **International Conference on Advances in Machine Design and Industry Automation 2007** held in January 2007

- Won first prize at the state level paper presentation competition "Mechtrix 07" organised by the D.Y. Patil College of Engineering, Akurdi, Pune, held in February 2007.

- Project selected for exhibition at the "Technoquest 2007" organised by the Confederation of Indian Industries, Pune chapter.